

A209675

Environmental Measurements in the Beaufort Sea, Spring 1988

by
T. Wen
W.J. Felton
J.C. Luby
W.L.J. Fox
K.L. Kientz

Technical Report
APL-UW TR 8822
March 1989

**Applied Physics Laboratory University of Washington
Seattle, Washington 98105-6698**

Approved for Public Release: Distribution is Unlimited

Contract N00039-88-C-0054

Acknowledgments

This work was supported by the Office of Naval Technology (ONT) with technical management provided by the Naval Ocean Research and Development Activity (NORDA). The authors wish to thank the Naval Surface Weapons Center and the Arctic Submarine Laboratory/Naval Ocean Systems Center for contributing their data to this report.



Accession For	
NTIS CRA&I	<input checked="" type="checkbox"/>
DTIC TAB	<input type="checkbox"/>
Unannounced	<input type="checkbox"/>
Justification	
By _____	
Distribution / _____	
Availability Codes	
Dist	Avail and/or Special
A-1	

ABSTRACT

This report summarizes environmental data obtained in March and April 1988 at an ice camp in the Beaufort Sea 350 km north of Prudhoe Bay, Alaska. The measurements include weather, floe drift, CTD profiles, ice properties, and underwater noise.

TABLE OF CONTENTS

	<i>Page</i>
I. INTRODUCTION.....	1
II. THE ICE CAMP FLOE	2
III. THE CAMP.....	5
IV. WEATHER	8
V. FLOE MOVEMENT.....	8
VI. CTD MEASUREMENTS	14
VII. WATER SAMPLES.....	20
VIII. CURRENTS.....	21
IX. PROPERTIES OF ICE	22
X. UNDER-ICE AMBIENT NOISE	28
XI. REFERENCES	33
APPENDIX A. Listing of ice camp positions obtained from NAVSAT system	A-1
APPENDIX B. Comparison of NAVSAT and GPS fixes at various times.....	B-1
APPENDIX C. CTD profiles at APLIS 88	C-1
APPENDIX D. Listing of sound speed profiles	D-1
APPENDIX E. Water clarity measurements by NSWC.....	E-1
APPENDIX F. Plots of under-ice ambient noise spectra	F-1
APPENDIX G. Noise level vs distance from the camp	G-1

LIST OF FIGURES

	<i>Page</i>
Figure 1. A view of APLIS 88, looking north	3
Figure 2. Under-ice undulation.....	4
Figure 3. Layout of the camp structures	6
Figure 4. Orientation of the XY coordinate system and the location of some sensors and hydroholes	7
Figure 5. Weather measurements at APLIS 88	9
Figure 6. Sky irradiance level at 457 nm wavelength	10
Figure 7. Drift track of APLIS 88.....	11
Figure 8. Drift speed and direction of APLIS 88.....	12
Figure 9. Comparison of daily drift speed and wind speed	13
Figure 10. Rotation of the floe and declination	13
Figure 11. Temperature profile from an XBT cast	16
Figure 12. Daily thermocline depth	17
Figure 13. Comparison of successive pairs of salinity profiles showing mixing ..	18
Figure 14. Ray trace with source depth near a thermocline (CTD cast No. 6).....	19
Figure 15. Ray trace with source away from a thermocline (CTD cast No. 32)...	19
Figure 16. Vertical current profile relative to the floe during high wind.....	22
Figure 17. Absolute current relative to Earth	23
Figure 18. Measured and computed properties of ice cores	26
Figure 19. Block diagram of ambient noise measurement setup.....	28
Figure 20. Daily ambient noise at 1, 5, and 20 kHz vs wind speed.....	30
Figure 21. Ambient noise at 1 kHz vs wind speed	30
Figure 22. Ambient noise at 5 kHz vs wind speed	31
Figure 23. Ambient noise at 20 kHz vs wind speed	31
Figure 24. Maximum and minimum noise spectra at APLIS 88	32

LIST OF TABLES

	<i>Page</i>
Table 1. List of CTD casts at APLIS 88	15
Table 2. Comparison of water sample analysis results and CTD readings	20
Table 3. Measured ice core temperatures	24
Table 4. Measured and computed ice core properties	25

I. INTRODUCTION

This report presents environmental data taken in the spring of 1988 at ice camp APLIS in the Beaufort Sea. The camp was established and maintained by personnel from the Applied Physics Laboratory, University of Washington, to support the Navy-sponsored research and test activities conducted by the many organizations participating in ICEX 1-88. The environmental data — weather, floe drift, CTD profiles, ice properties, and underwater noise — were gathered by APL-UW personnel, primarily to support the analysis of acoustic data obtained by ICEX 1-88 participants.

The camp was established on a multiyear floe approximately 350 km north of Prudhoe Bay, Alaska. The floe, which was first sighted on 1 March, was occupied for seven weeks and evacuated on 25 April upon the successful completion of test and research objectives. During the period, the floe drifted westward 155 km, driven mainly by the wind. A small amount of rotation accompanied the drift.

The camp was established at the edge of a refrozen lead, which was essential for building a runway for aircraft, the only means of transportation to and from APLIS 88. The finished runway was used almost daily by a Twin Otter and a CASA 212-200. It was made long enough to handle the landing and takeoff of a Lockheed Hercules (stretch version) that was used twice for delivery of fuel in drums. Multiyear pressure ridges and rubble fields surrounded the lead and the camp. All parts of the floe were easily accessible by snowmobile until, in the latter part of the exercise, one end of the runway was lost when high winds opened up a new lead.

Weather information on air temperature and pressure and on wind direction and speed was recorded several times daily. Relatively warm temperatures averaging about -18°C in the beginning were followed by a period of cold days averaging -30°C . In the latter days of the camp, the temperature was relatively high, generally around -5°C during the day and dropping to -20°C at night.

Many of the research activities at the ice camp involved underwater acoustic propagation. Knowledge of sound speed profiles was therefore essential for understanding the acoustic phenomena encountered. CTD casts were taken, usually early in the day, to determine the properties of the water column down to 300 m depth. Sound speed profiles were then obtained from the measured temperature and salinity. The real-time performance of acoustic equipment was predicted based on the profiles. The profiles were also used in later data analysis.

Underwater ambient noise affected the quality of the acoustic data gathered. Sources of the noise included thermal cracking of the ice, ridging, wind-generated waves at open leads, and biological organisms. A comprehensive measurement program was carried out to study the underwater ambient noise. Noise was received through an array

of four hydrophones placed 700 m from the camp and was recorded five minutes each hour for 30 days. A good correlation between the wind speed and the noise level was found. Noise levels 10 dB below that of sea state 0 in the open ocean were recorded. This report will present only a synopsis of the noise spectrum level measured daily. Detailed analysis will be presented in a later report.

All the data presented here are stored in digital format and available for further analysis.

II. THE ICE CAMP FLOE

Selection of an ice floe suitable for a two-month camp was based on several requirements. First, the floe area had to be at least 3×4 km to support planned tests. Second, it needed a refrozen lead long enough and thick enough (at least 1.2 m) to serve as a runway since transportation to and from the camp depended entirely on aircraft. Third, the floe needed to be over water with good acoustic propagation characteristics, i.e., minimal shadow zone and longest possible range. This last stipulation required the camp to be located north of 72° latitude where the warm subsurface intrusion layer (a remnant of the summer Alaskan Coastal Current that produces complex sound speed structure) is less pronounced. In addition, at those latitudes the water is deeper, which helps minimize the bottom acoustic interference.

On the first day of the search, reconnaissance flights out of the staging point at Prudhoe Bay located a floe that met all the criteria. It was approximately 350 km from Prudhoe Bay at $72^{\circ} 50'N$ and $141^{\circ} 44'W$ and over waters 3400 m deep. The floe was about 6×6 km, with a large expanse of refrozen lead in the middle (Figure 1). The lead was approximately 1.5 m thick with a snow cover of 15 cm. There were fissures several centimeters wide in the lead, but they were not wide enough to affect the operation of the runway. About two weeks after the camp was set up, a crack parallel to and north of the runway appeared, opening to a width of about 30 cm. A hydrophone deployed in the vicinity had to be recovered and redeployed on the camp side of the crack in order to avoid possible ridging or further widening that might damage the cable that ran from the hydrophone to the camp. The crack closed later without ridging. Small cracks such as this have been observed in the past and are common occurrences. Often they are hidden from view by snow cover.

The refrozen lead was surrounded on all sides by multiyear ice with hummocks as high as 6 m. Immediately north of the lead was a relatively fresh rubble field with large chunks of ice. The camp was established at the southern edge of the lead where the ice thickness ranged from 1.5 to 2.4 m.



Figure 1. A view of APLIS 88, looking north.

Observations of the surface beneath the flat lead during diving operations again revealed the undulating characteristics found in previous years.^{1,2} Some crude measurements of the under-ice undulation amplitude vs wavelength were taken by the divers, and the result is given in Figure 2 showing an amplitude of 3.7 cm and a wavelength of 8.5 m. The under-ice undulations were observed by the divers over a wide area of the refrozen lead with uniformity in wavelength and orientation. The undulations are thought to be caused by "sastrugi," or windrows, in the snow cover, resulting in varying freezing rates beneath. The snow cover was indeed uneven, but no measurements of amplitude and wavelength were carried out. Bottom roughness over a short distance was also examined during an acoustic experiment conducted at the lead. Cylindrical ice columns up to 84 cm in diameter were removed from the lead and the bottom roughness measured by laying an aluminum grid over the bottom and measuring the clearance between the ice and the grid at the grid points. The measured rms roughness ranged from 1 mm for a 27 cm diameter plug to 3 mm for an 84 cm one.

At different locations on the refrozen lead the divers also observed bubbles 6 mm and less in diameter entrained evenly within the skeletal layer. Unfortunately a quantitative estimate of the bubble density is not available. The mechanism for the formation of

the bubbles is currently not understood, nor is it known whether the bubbles were a rare event or are always present within a new skeletal layer, although we did also observe entrained bubbles in 1987.² The bubbles were not observed in the skeletal layer of the columns, mentioned above, that were removed from the water. Bubbles in the skeletal layer would play a significant role in the scattering of acoustic energy.

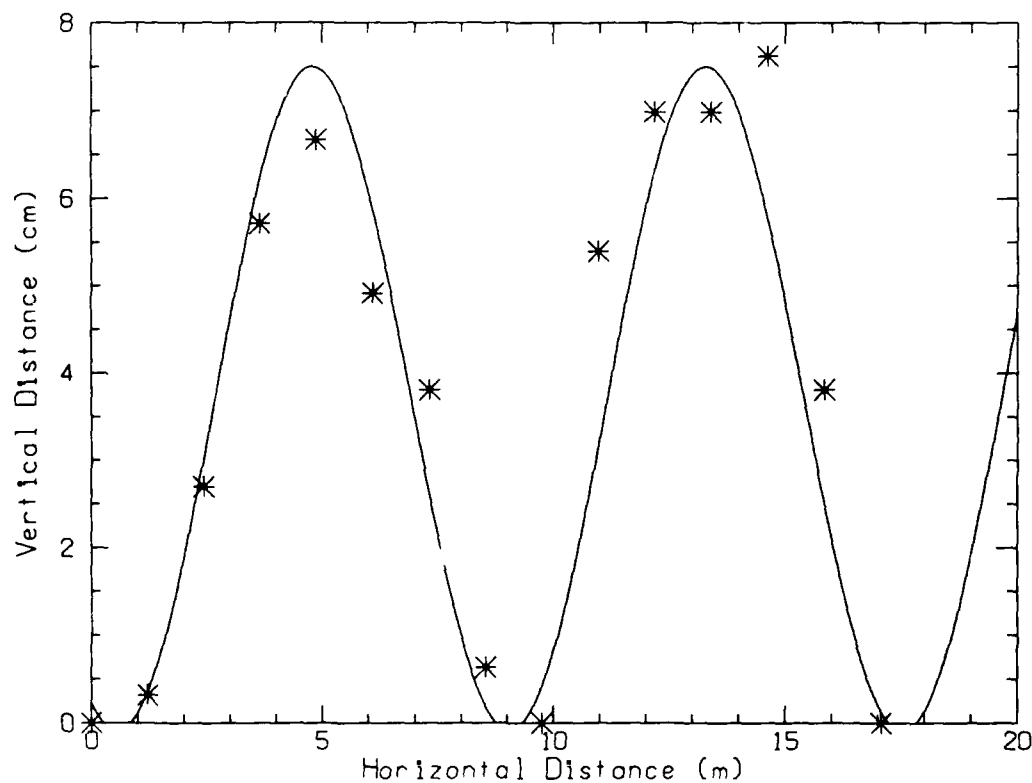


Figure 2. Under-ice undulation (least-squares-fitted sinusoid has amplitude of 3.7 cm and wavelength of 8.5 m).

Owing to the vertical temperature gradient in the ice at this time of year, the ice was still growing at a typical rate of about 0.5 cm per day under the flat ice of the refrozen lead. Ice cores removed from the lead at various times showed the new ice to be columnar.

Some relatively new keels a few months old were also investigated by the divers. These keels had not gone through melt-season changes and therefore still retained their original structure of randomly oriented blocks. No ice crystals were observed on the surfaces exposed to the water current. However, in protected areas such as pockets formed by the blocks, ice crystals were found on the block surfaces.

The surface and geometrical characteristics of the multiyear keels were totally different from those of the new keels. Divers reported that the multiyear keels generally had solid mass with polished surfaces, and some with the appearance of rotten ice, lacking recognizable signs of block structure. It was observed that when first formed the blocks within a keel were randomly stacked with inter-block spaces and pockets. In the course of melting and refreezing, the spaces were filled up, and the keel appeared as a solid mass without sharp features or deep pockets. Bubbles of slightly larger size and lower density than those in flat ice were observed within the surfaces of one keel selected for visual examination. No ice crystals were observed on the surface of the keel, indicating an apparent state of no growth, as contrasted to the fairly rapid growth of the flat ice in the refrozen lead.

During a period of high winds on 13 April, a lead developed to the west and to the north of the camp, rendering part of the runway unusable. Although this lead closed again, the resultant rough ice/rubble field rendered that area inaccessible. The remaining portion of the runway, however, was still more than adequate to handle the small aircraft used for transportation.

III. THE CAMP

The camp was established near the edge of the refrozen lead, at a location chosen for its relatively smooth surface. The thickness of the ice ranged from 1.5 m to 2.4 m, more than adequate to support the camp structures but not too thick for drilling hydroholes. A mixture of plywood buildings and tents was erected in stages, spreading out over an area of approximately 80 × 100 m. A layout and a photo of the camp structures are shown in Figure 3. The camp area was even larger if helopad, box piles, and fueling stations are taken into account (Figure 1).

The buildings can be separated into five categories by function: sleeping, mess, power, science, and logistics. Generally, sleeping quarters were 2.4 × 6.1 m, accommodating a maximum of six people. At the height of the activities, 62 people were billeted at the camp, though the camp averaged about 50 residents. In addition to the residents, there were usually a few transients who came to work during the day and did not stay overnight. The mess hall had a seating capacity of 54 which, in conjunction with cafeteria-style serving, was adequate for camp needs. Power generators and workshops were housed in three tents. During peak periods of power usage, a mix of five diesel generators provided up to 24 kW to power the scientific equipment. The majority of the scientific work was carried out in or directed from the control building, the ARL/PSU tents, and the oceanography hut, each with one or two hydroholes for deploying equipment into the water. The control building was shared by several organizations and also housed the communication equipment. Diving equipment was housed in the logistics building, where those involved in logistics and diving operations lived.

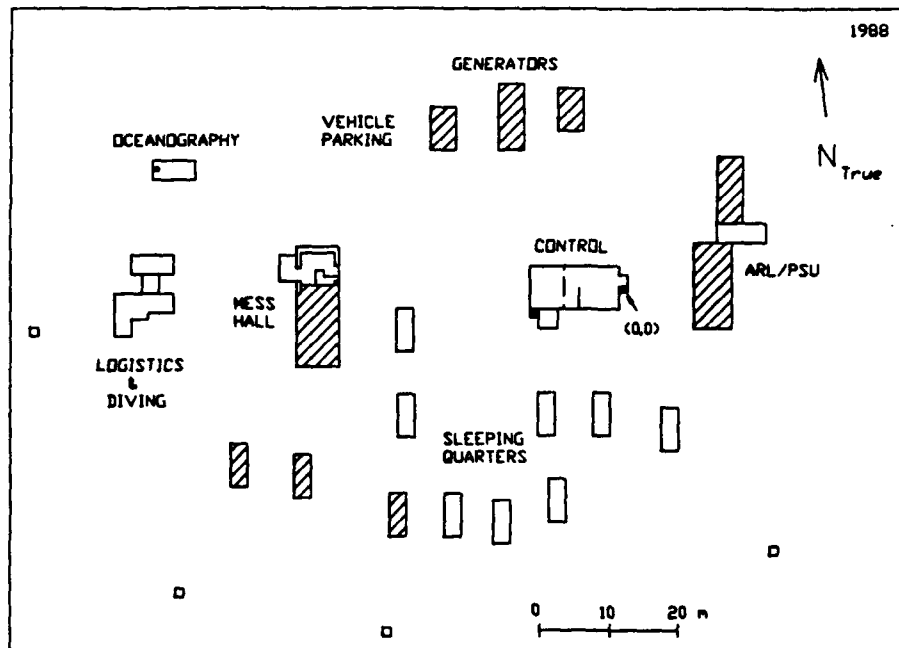


Figure 3. (a) Layout of the camp structures. Crosshatching denotes a tent; (0,0) indicates the origin of an XY coordinate system. Small circles represent 0.91 m diameter hydroholes. There was a 1.2 × 7.3 m hydrohole in the larger ARL/PSU tent. (b) Photograph of the camp corresponding to (a).

An XY coordinate system, with its origin at one of the hydroholes in the control building (where an acoustic scanner was deployed), was set up for tracking underwater vehicles and surveying hydroholes as shown in Figure 4. The XY axes were chosen to run parallel to the sides of the control building and in turn parallel to the axes on the tracking plotter so that a point on the plot could easily be visualized in the physical space on the ice.

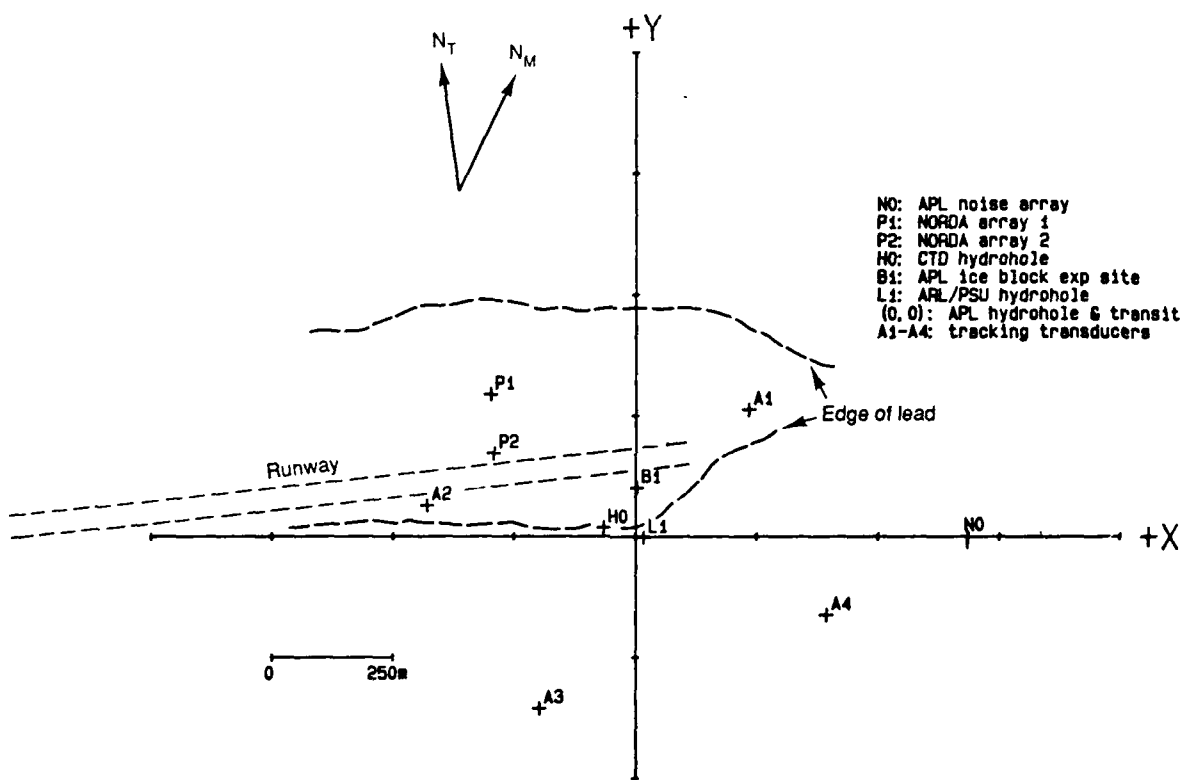


Figure 4. Orientation of the XY coordinate system and the location of some sensors and hydroholes.

An infrared ranging device and an engineer's transit were set up on the roof of the control building approximately over the (0,0) hydrohole to locate acoustically tracked or surveyed points beneath the ice. Given the range and bearing from (0,0) to the tracked point, the infrared device ranged on an optical target, which was hand-held and repositioned by trial and error, until a point on the ice was obtained that corresponded to the tracked point beneath.

IV. WEATHER

Air temperature, atmospheric pressure, wind speed, and wind direction were recorded daily at semiregular intervals during the camp occupancy. This information was used mainly for logistic operations, which did not require high accuracy. However, in analyzing acoustic data where correlation to weather parameters was apparent, the lack of accurate and frequent weather data proved to be a disadvantage.

While the camp was being set up, wind speed and direction were estimated or measured with a hand-held wind gauge, and the temperature was measured with a thermometer. After 16 March, an Ultimeter model 20 electronic weather station with an estimated accuracy of $\pm 2^{\circ}\text{C}$ in temperature, 2 mbar in pressure, and 0.5 m/s in wind speed was used. The anemometer was mounted on a pole 3 m high and 30 m northeast of the nearest camp structure. Figure 5 shows the weather measurements at APLIS 88. Because the data were manually logged, they suffer from a lack of consistency and regularity, with some days having very few or only one measurement. This is readily observed in the temperature data prior to 16 March, before a routine was established. The wind data, collected at 3 m height instead of the standard 10 m, may show lower speeds than actually existed because of the boundary layer effect. Furthermore, because the anemometer was northeast of a building, measurements of wind blowing from the general direction of southwest ($\sim 225^{\circ}$) may have been corrupted. A seasonal warming trend started in early April as shown in Figure 5. The temperature hovered around -5°C for several days, making outside work easier.

As part of an optical experiment, the intensity of the blue color in the spectrum of the sky irradiance was measured with a radiometer (United Detector Technology 360) during the period 19–28 March. The radiometer had a cosine diffuser and an interference filter with a centroid wavelength of 457 nm and effective bandwidth of 10.1 nm. The accuracy of the readings was about 10%. Figure 6 shows the insolation values measured. The sky was clear and sunny during the period except for three overcast/hazy days: 20, 21, and 24 March, as recorded in the weather log. The overcast resulted in lower intensities as expected. Note a generally increasing trend in the daily maximum radiation level that can be attributed to the progressively higher elevation angle of the sun in the sky.

V. FLOE MOVEMENT

Driven by the wind, the floe drifted 155 km westward during the camp occupancy, starting at a position 350 km northeast of Prudhoe Bay and ending at 300 km north. At the beginning of camp, the position was tracked by an Omega system on the logistic aircraft. After 8 March, a Transit Satellite Navigation System (NAVSAT) receiver (Furuno FSN-80) and a Global Positioning System (GPS) receiver/clock (Kinematics/Truetime GPS-DC) were set up at the camp. According to system specifications, the NAVSAT³ is

accurate to 100 m and the GPS⁴ is accurate to 25 m. The GPS receiver was a new piece of equipment being tested by APL, mainly as a clock to provide Coordinated Universal Time (UTC), and was consequently considered a backup system to the NAVSAT receiver.

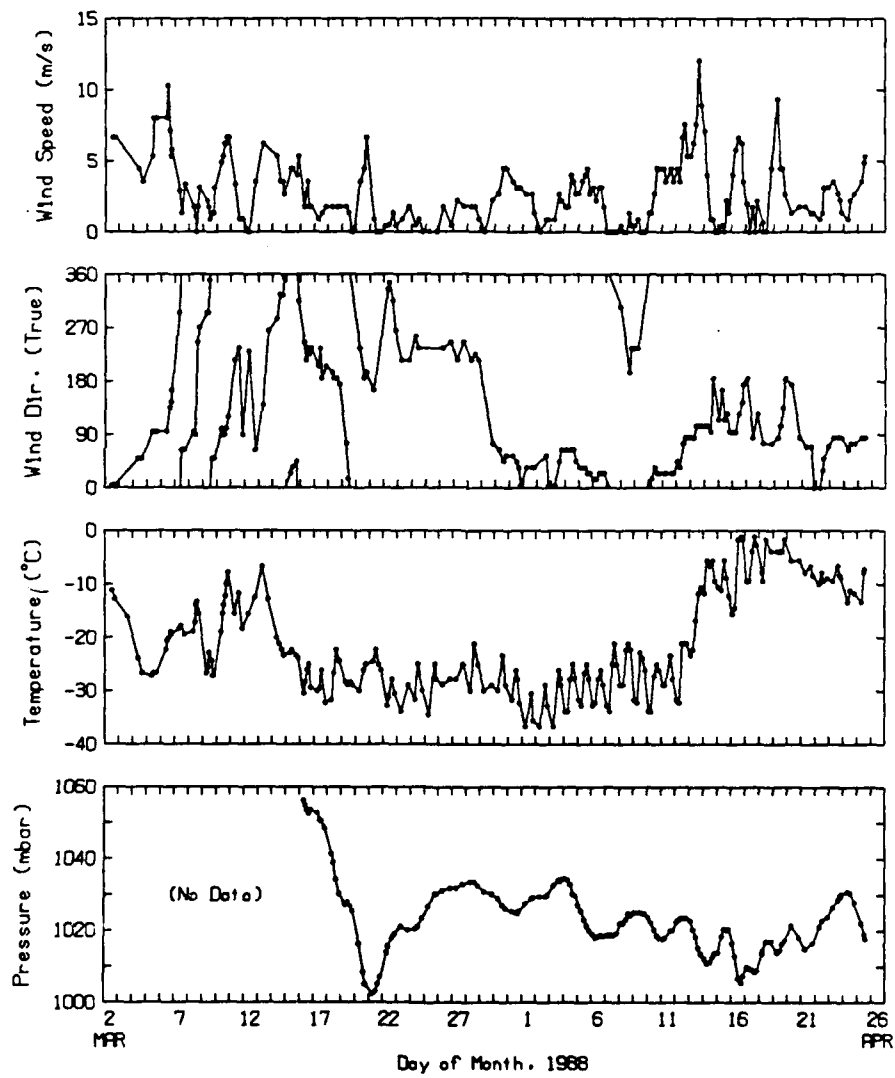


Figure 5. Weather measurements at APLIS 88.

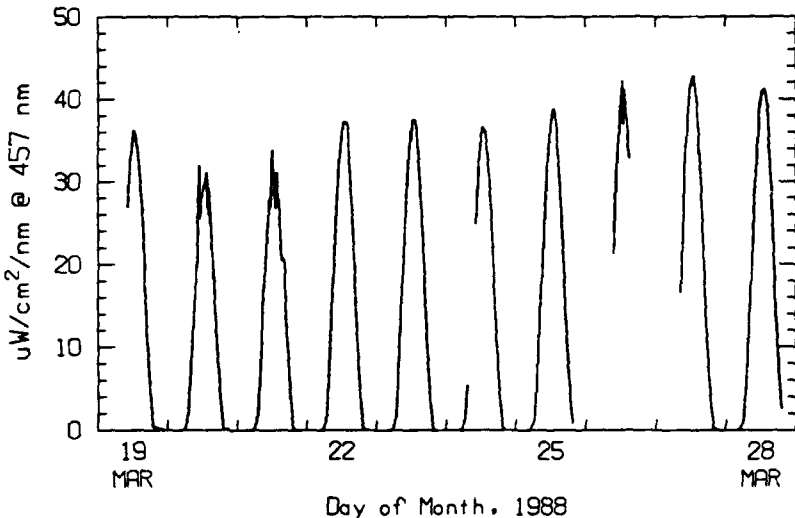


Figure 6. Sky irradiance level at 457 nm wavelength.

The NAVSAT fixes were automatically stored in the receiver for all satellite passes, which occurred at an average interval of 20 minutes. Every few hours, all accumulated sets of time, position, and elevation angle data were manually recalled and recorded in a log book.

For the GPS system, an HP85 computer was connected to the receiver via a GPIB interface and used as a data logger. GPS fixes were read from the receiver every 10 minutes and stored on a tape cartridge. Because of the limited number of GPS satellites currently in orbit, good position fixes, requiring a minimum of three satellites in view, were available less than half the time. Furthermore, problems with firmware/software for data I/O resulted in frequent periods of data loss.

The NAVSAT positions were processed using a 6-point unweighted running-average filter that yielded smoothed data points at roughly hourly intervals. Positions obtained from satellite elevation angles greater than 60° were discarded because they showed an offset in the longitude¹ relative to the ones with low elevation angles. Figure 7 shows a plot of the smoothed drift track of the floe. A listing of the floe position, drift speed, and direction is given in Appendix A. Note that the time of day of NAVSAT and GPS data is in UTC. For correlation to other data logged in local time (at Prudhoe Bay), the time offset was nine hours, i.e., 1200 Zulu = 0300 local, through 2 April. The offset became eight hours after 2 April because of the change to Daylight Savings Time.

To compare the fixes from the two satellite tracking systems, Appendix B gives some figures for several time periods when data from both systems were available. They show that the GPS system yielded better fixes, according to specification, and the NAVSAT positions, when smoothed, agreed well with the GPS ones.

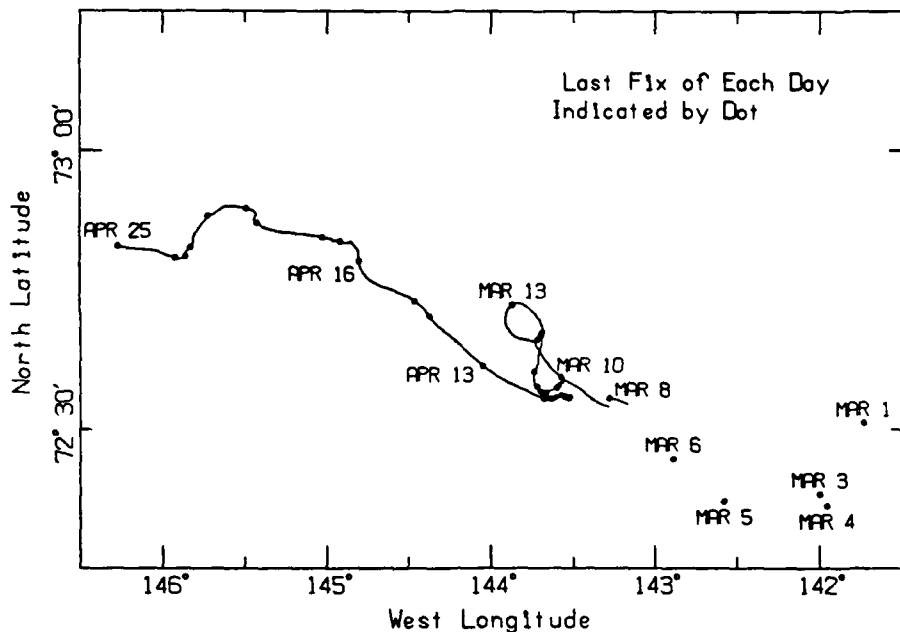


Figure 7. Drift track of APLIS 88.

The drift speed and direction of the floe are shown in Figure 8. The drift speed and the wind speed are shown together in Figure 9, where we see a good correlation between the wind and the drift speed. A rise in the wind speed above 5 m/s generally produced a corresponding increase in the drift speed of the floe. For example, see the correspondence for 10 March, and for 13, 16, and 19 April.

As the floe drifted, some rotation was generally expected due to unequal external forces acting on different parts of the floe. The amount of rotation was determined by measuring the true bearing of the +Y axis of the XY coordinate system. To obtain the true bearing of the +Y axis, the grid bearing of the Sun or the Moon was first read with a transit positioned atop the control building over the (0,0) hydrohole, while the 0° reference mark of the transit was oriented toward the +Y direction of the range. Then the true bearing of the Sun or the Moon at the time of the transit sighting was calculated using information from a nautical almanac. The difference between the true and grid bearings of the Sun or the Moon was the true bearing of the +Y axis.

The floe orientation was also checked by taking the magnetic bearing of the +Y axis on the transit compass and converting to true bearing by correcting for the magnetic declination (approximately 34°). The orientation of the +Y axis obtained by both methods is shown in Figure 10. The declination is also plotted and shown in the figure.

As in the past the floe generally rotated no more than 5° during camp occupancy. This could be attributed to the high overall ice concentration that restricted the rotation of individual floes.

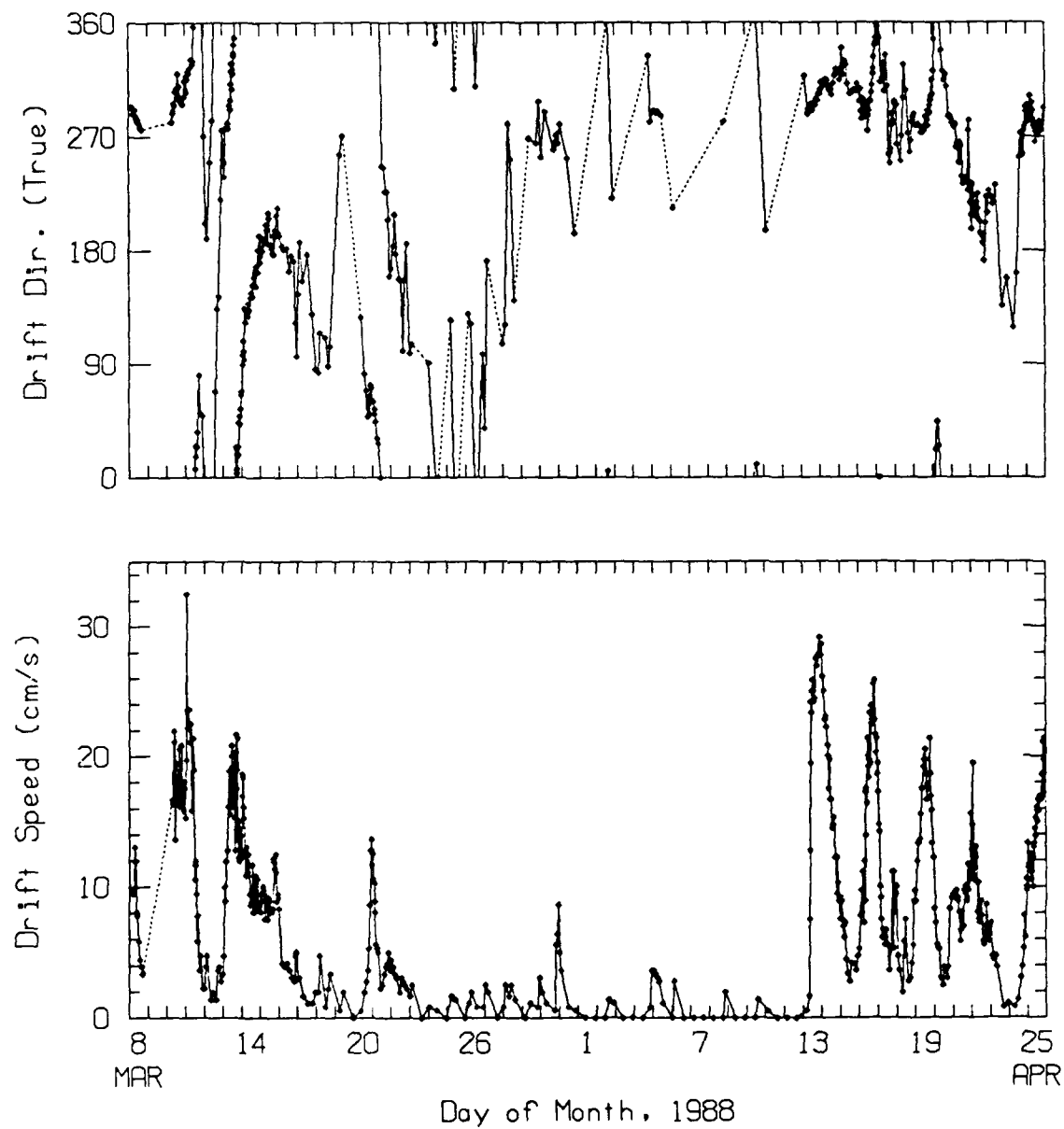


Figure 8. Drift speed and direction of APLIS 88. Time is in UTC.

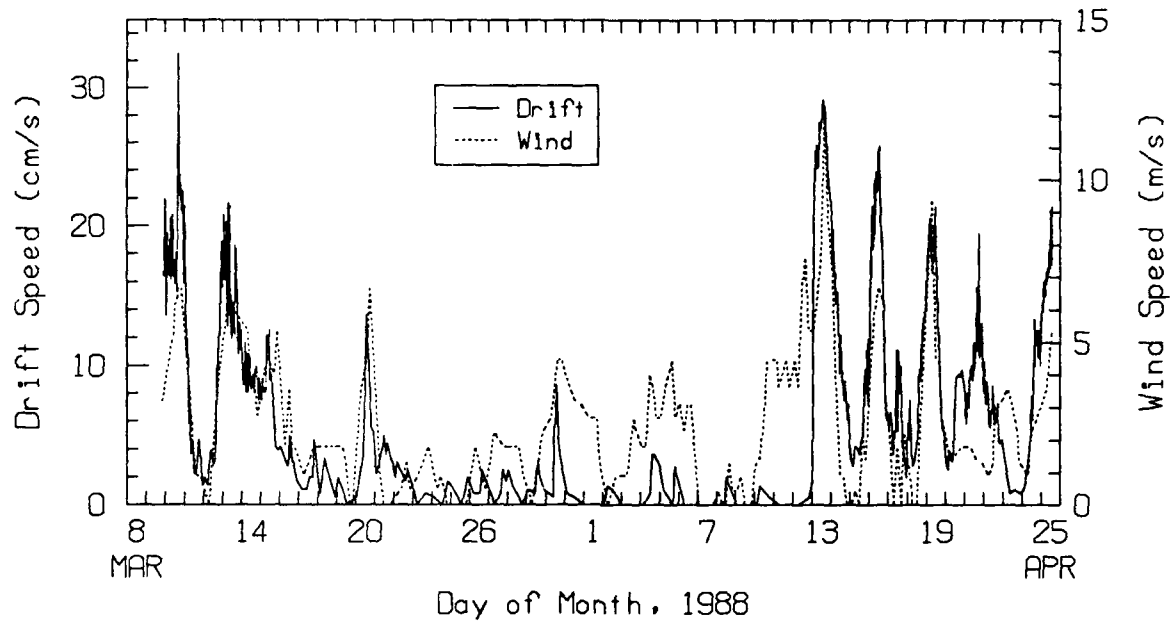


Figure 9. Comparison of daily drift speed and wind speed.

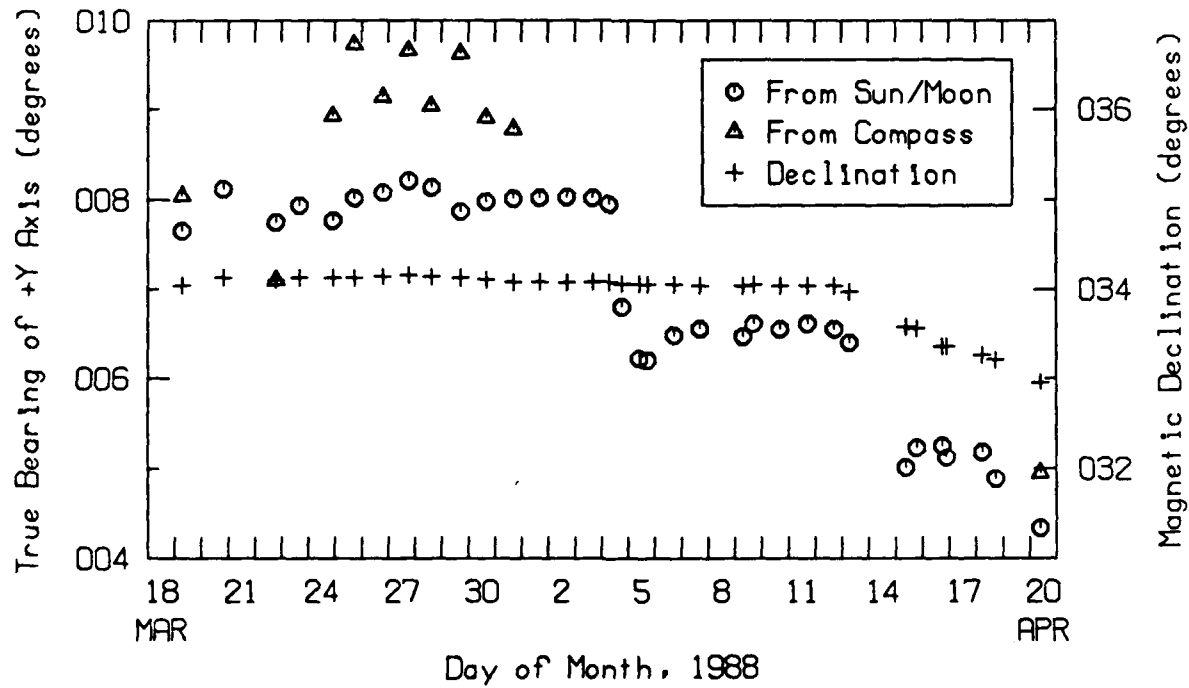


Figure 10. Rotation of the floe and declination.

As shown in Figure 10, there was a 1–2° difference between the two methods. The compass readings were more likely in error owing to the presence of ferromagnetic materials in the building below. The compass readings were therefore adequate for checking the floe rotation, but not for a good estimate of the true bearing of the +Y axis.

VI. CTD MEASUREMENTS

The CTD cast is the most important basic measurement for underwater acoustic studies. Understanding the nature of underwater sound propagation requires knowledge of the sound speed profile derived from the temperature and conductivity data obtained in a cast.

CTD casts were taken with a manual winch profiler mounted on a wall next to a hydrohole in the oceanography building. The winch drum contained recording electronics that were directly connected to sensors via a Kevlar-reinforced electrical cable. The sensor package consisted of a thermistor (Sea-Bird), a conductivity cell (Sea-Bird), a pressure sensor (Paroscientific Digiquartz), and a multiplexer. The sensors were manually winched into the water at a rate of about 1 m/s to a maximum depth of 300 m. Data were recorded on a cassette during the down cast. The sampling rate was 2.86 Hz, equivalent to one data point for every 0.35 m of depth. After the cast, the cassette was removed from the winch and inserted in a reader. The data were read out via a BCD bus to an HP Integral Personal Computer for processing and plotting.

Table 1 lists the casts made at the camp. The CTD profiles are shown in Appendix C. Listings of the corresponding sound speed profiles are given in Appendix D for the benefit of the reader who may want to do ray tracing. The points in the listing were obtained interactively on a computer by plotting each profile on a computer screen and then visually and manually selecting the features. The selection was made at small intervals where the change in the speed gradient is large and at larger intervals where the change is small. Because the sound speed profile structure varied daily, the number of points picked is different for each profile.

Figure 11 is a typical temperature profile obtained in a deep XBT cast⁵ in the vicinity of APLIS 88. Note the characteristic temperature profile of the Beaufort Sea: a well-mixed, very nearly isothermal upper layer that may extend down to 60 m (the figure shows fluctuations due to system noise), a warmer intrusion layer from the Bering Sea, a temperature minimum between 140 and 160 m, and Atlantic water below that increasing in temperature to a maximum of 0.5°C. The average temperature of the shallow layer was generally around –1.72°C, very close (0.01 – 0.04°C) to its freezing temperature. The water exhibited a high degree of clarity, as reported by divers and determined by optical transmission measurements carried out by personnel from the Naval Surface Weapons Center (NSWC) (see Appendix E).

Table 1. List of CTD casts at APLIS 88

Date	Local Time	Cast #	Comments
03-15-88	1705	1	installed sensors C16, T432, DQ1653
03-16-88	1950	2	
03-17-88	1950	3	noisy data
03-18-88	0630	4	noisy data
03-18-88	1845	5	
03-19-88	1010	6	
03-20-88	0750	7	
03-21-88	0620	8	
03-22-88	0620	9	
03-23-88	1240	10	
03-24-88	0610	11	
03-25-88	0610	12	
03-26-88	0620	13	
03-27-88	0620	14	CTD failed after 26 m
03-27-88	1240	15	
03-28-88	0620	16	
03-29-88	0625	17	
03-30-88	0620	18	partial data only
03-30-88	1150	19	
03-31-88	0615	20	
04-01-88	0625	21	
04-02-88	0625	22	
04-03-88	1330	23	
04-04-88	0900	24	
04-04-88	1020	25	installed sensors C3, T429, DQ1653 for comparison with #24
04-05-88	0630	26	installed sensors C16, T432, DQ1653
		*	no cast #27
04-06-88	0930	28	
04-07-88	0620	29	
04-08-88	0620	30	
04-09-88	0625	31	
04-10-88	0930	32	
04-11-88	0945	33	
04-12-88	0930	34	
04-13-88	0820	35	
04-14-88	0700	36	
04-14-88	2005	37	
04-15-88	0930	38	
04-16-88	0700	39	
04-17-88	0830	40	
04-18-88	0830	41	
04-19-88	0745	42	

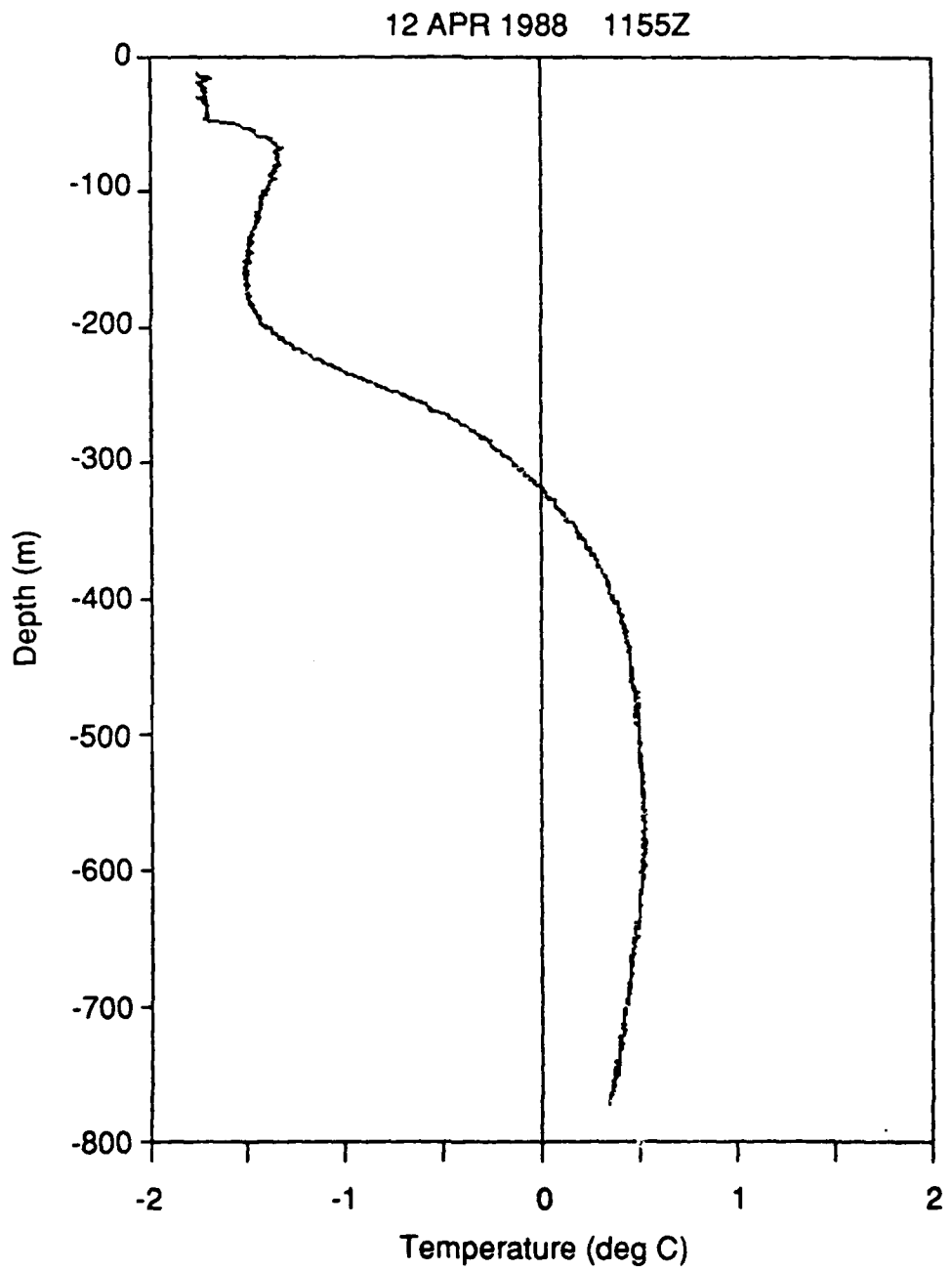


Figure 11. Temperature profile from an XBT cast.

Since sound speed is largely a function of the temperature, the depth of the thermocline is of great interest because it can have a major effect on sound propagation. Figure 12 shows the depth of the thermocline, which varied between 26 and 62 m during the camp period. The depths were estimated from the CTD profiles in Appendix C. A gradual deepening of the thermocline is observed from 1 April to 12 April. This may be attributed to mixing, as indicated by the changes; the salinity generally increases in the upper layer and decreases below it (see profiles, Figure 13). The mixing was not wind-driven since the wind and the drift were very small. Because freezing was still taking place, it was more likely caused by circulation set up by the sinking surface water that became denser owing to the brine ejected during the freezing process. The largest change in the thermocline depth, 20 m shallower than the previous day, occurred on 19 April. It might be attributed to the high wind and large drift that moved the floe over a different mass of water. Higher floe drift rates on 13 and 16 April, however, did not result in a significant change in the thermocline depth.

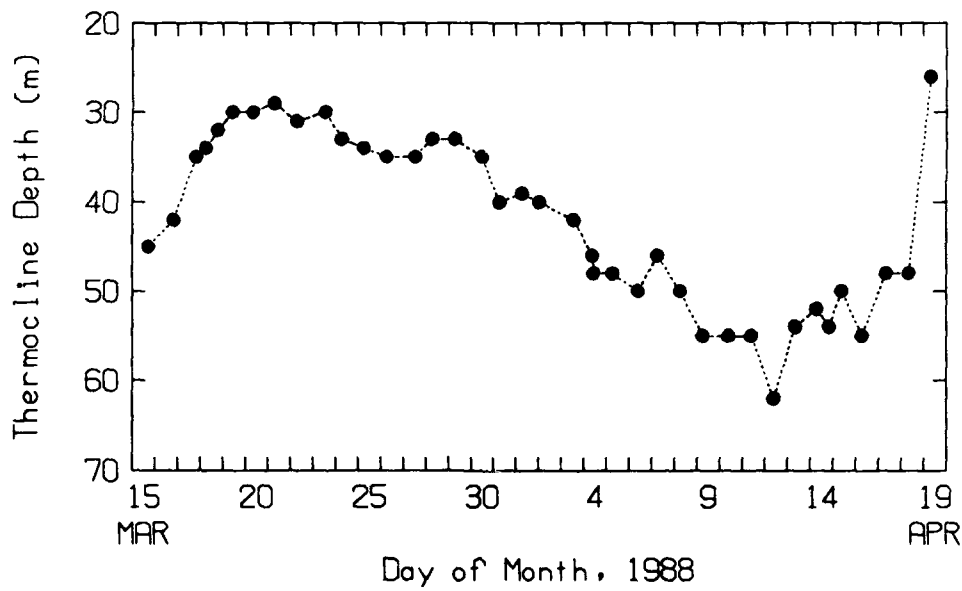


Figure 12. Daily thermocline depth.

Since the tracking hydrophones were deployed at a depth of 30.5 m, severe ray refraction (treating the hydrophone as the source) would have occurred when the thermocline was near that depth. This case is illustrated with a ray trace in Figure 14 for a thermocline of 30 m (cast #6). For comparison, a ray trace for a thermocline at 56 m (cast #32) is shown in Figure 15. The effect of the thermocline is greatest at medium ranges of 1000 – 5000 m and shallow depths of 0 – 60 m.

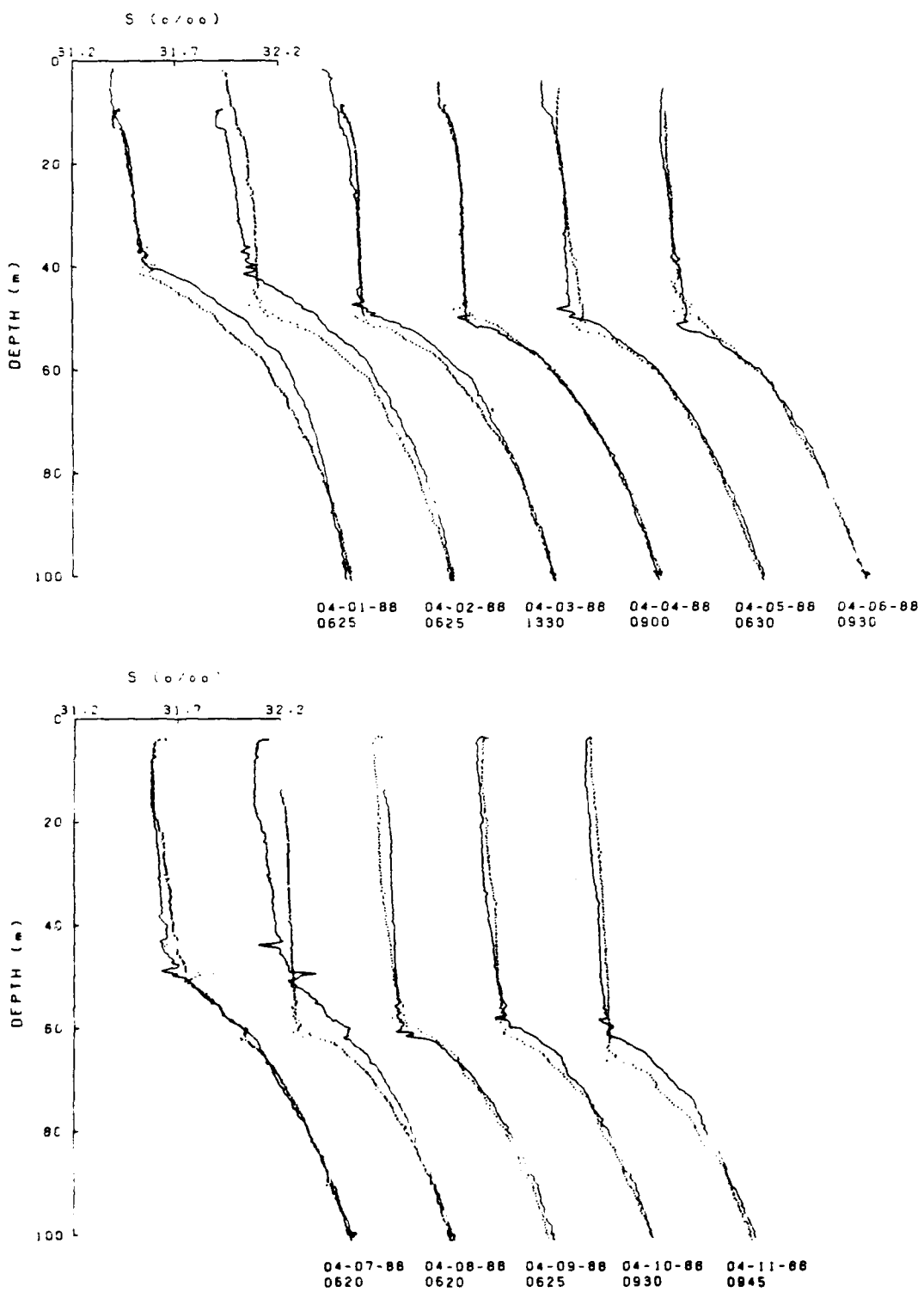


Figure 13. Comparison of successive pairs of salinity profiles showing mixing. Dates and times refer to the solid line in each of the pairs. The dotted line in each pair is a profile for the day after the solid line profile. To facilitate comparison of successive daily profiles, the dotted profile in each pair is the same as the solid line profile in the next pair.

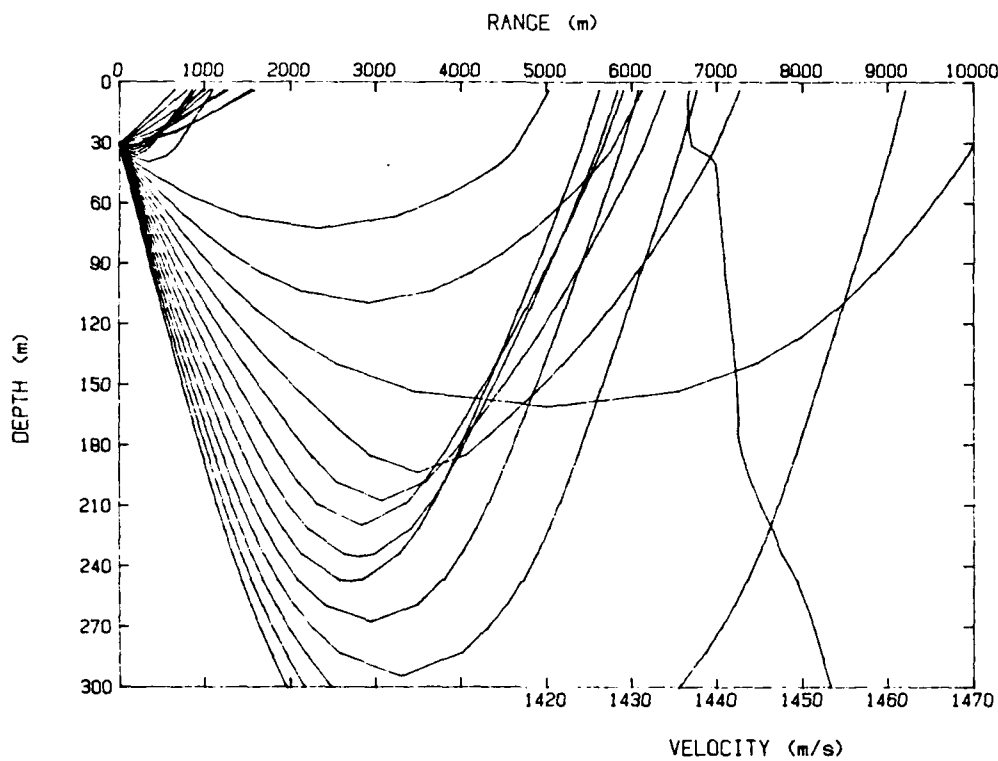


Figure 14. Ray trace with source depth near a thermocline (CTD cast No. 6). Ray angles from $+2^\circ$ to -10° at 0.5° decrements.

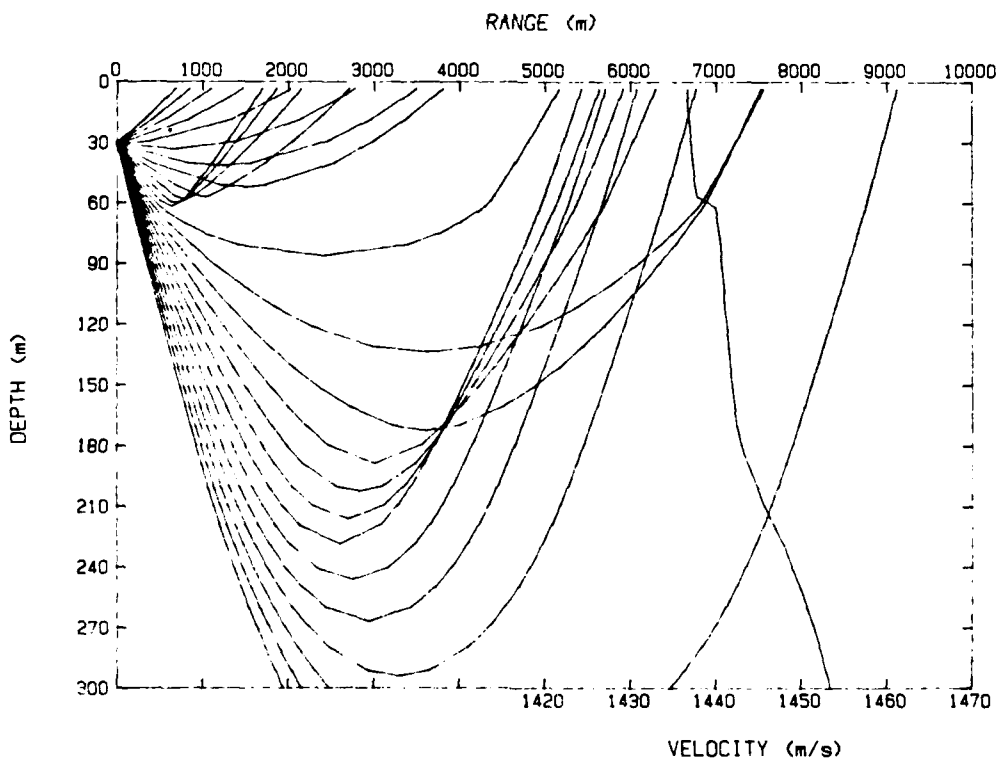


Figure 15. Ray trace with source away from a thermocline (CTD cast No. 32). Ray angles from $+2^\circ$ to -10° at 0.5° decrements.

VII. WATER SAMPLES

Water samples were needed for checking the calibration of the conductivity cells and for pH information useful in studying acoustic absorption. Samples were collected at eight depths using a Niskin bottle attached to the CTD cable 10 m above the sensor package. The sampling depth was determined from the depth sensor and corrected for the 10 m offset. Three 200 cc samples were taken from each cast, two for salinity analysis and one for pH analysis. Salinity analysis was done at the chemistry laboratory of the School of Oceanography, University of Washington, and pH analysis was done in the field using a VWR model 87 pH meter. The measured pH values were temperature-corrected to yield in-situ values. Table 2 shows the results of the water sample analyses. Salinity readings from two CTD casts bracketing the sampling time are also shown for comparison.

Table 2. Comparison of water sample analysis results and CTD readings.

Depth(m)	Water Samples 2 April 1700-1755		CTD Casts		Difference in Salinity Averages: Sample – Casts
	Salinity	pH	2 April 0630 Salinity	3 April 1330 Salinity	
15.8	31.509	8.23	31.453	31.543	+0.009
	31.506				
32.3	31.581	8.23	31.520	31.592	+0.024
	31.580				
64.4	32.213	8.09	32.224	32.171	+0.015
	32.211				
93.4	32.515	8.03	32.515	32.496	+0.009
	32.513				
153	32.924	7.97	32.904	32.934	+0.005
	32.924				
195	33.512	7.97	33.433	33.420	+0.088
	33.517				
288	34.613	8.11	33.572	34.560	+0.046
	34.611				
	4 April 0930		4 April 0900	4 April 1020	
243	34.254		34.212	34.224	+0.047
	34.268				

As shown in the right-hand column of the table, the analyzed salinity of the samples and the computed salinity from the casts differ somewhat. Samples taken at 153 m and shallower fall between the two CTD cast readings, indicating that the discrepancy was probably caused by mismatched sample and cast times. Below 195 m, however, the CTD readings were consistently lower than the sample by up to 0.09‰. This trend was also observed in 1986.¹

The conductivity cells were calibrated at the Northwest Regional Calibration Center (NRCC) prior to the ICEX 1-88 field trip to within 0.002‰ accuracy. The normal procedure for double checking the calibration called for consecutive casts with two different cells and temperature sensors. If the salinity and the temperature readings obtained from both casts agreed, all four sensors were assumed to still be in calibration. Two such casts (#24 and 25) showed good agreement in temperature readings to 0.003°C and salinity to 0.01‰ in the upper mixed layer. The discrepancy between CTD readings and sample analyses shown in Table 2 is therefore somewhat disturbing.

The pH readings, corrected for water temperature difference at sampling and analysis times, averaged 8.09 in-situ, exactly the same as that obtained in 1986.¹ The significance of the pH is that it is a measure of the dissociation of the ions of the boric acid, which influences low frequency sound absorption in the seawater. For example, a hypothetical change of pH from 8 to 9 for water at -1° C and 34‰ would increase absorption of 5 kHz sound from 0.39 to 0.77 dB/km, as given by Francois and Garrison's absorption equation.⁶

VIII. CURRENTS

Currents were usually estimated simply from the angle of the CTD cable, which was usually nearly vertical, implying a very low current. This method was adopted because no real interest in quantitative information had been expressed by the investigators at the ice camp. Other more pressing tasks also made this a low-priority measurement.

On 13 April, during a period of high winds, a large cable angle was noted on a CTD cast. The safety of an upcoming diving operation was in question, so a cast with a current meter (InterOcean S4) was made to assess the speed and direction of the current relative to the floe. The meter was attached to the end of the CTD cable and, to obtain stable current readings, was alternately lowered and stopped at depth intervals of about 5 m. Fifteen of the data points at each depth were used to obtain an average and a standard deviation. The results are shown in Figure 16.

04/13/88 0940 L

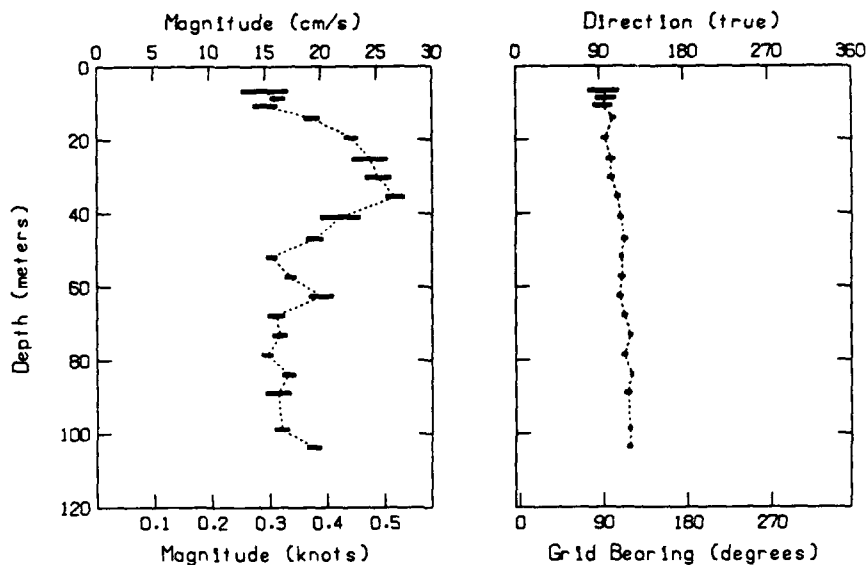


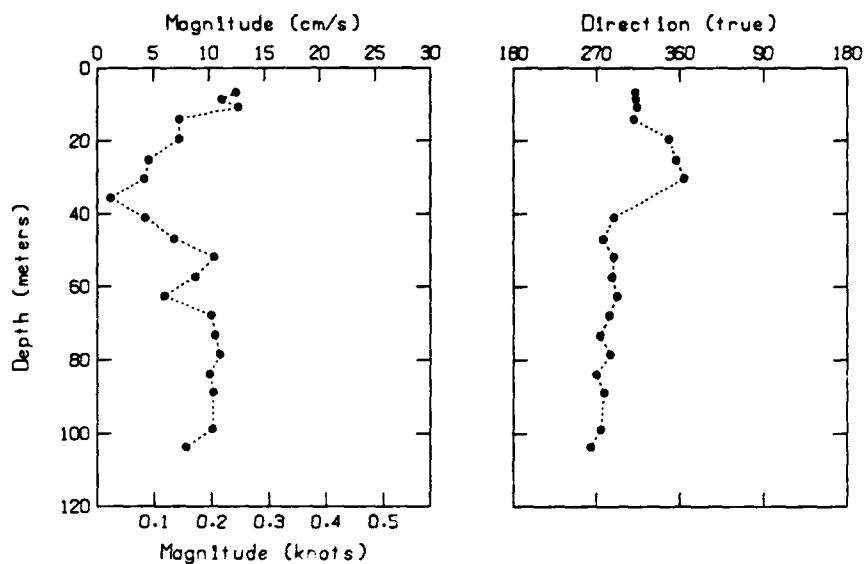
Figure 16. Vertical current profile relative to the floe during high wind. Horizontal bars indicate the standard deviation.

The absolute current (relative to the Earth) can be obtained by vector summing the relative current and the floe motion. Figure 17 shows the estimated absolute current computed with a floe drift speed of 26.1 cm/s and direction of 292°, as obtained by interpolation of NAVSAT data. It appears that the current at the shallow depths was induced by the ice pack, which was in turn driven by the wind. Below 40 m, there was a current layer flowing in the general direction of 270°.

IX. PROPERTIES OF ICE

Ice cores were taken with a 7.6-cm-diameter Sipre corer from the ~1.5 m thick refrozen lead to study the physical properties of the ice column in connection with acoustic experiments performed at the lead. Soon after the core was removed, temperature was measured at intervals along the core with a digital thermometer inserted into small drilled holes; the measurements are shown in Table 3. Cores #1 and #2 were taken from ice 135.5 cm and 141.1 cm thick, respectively; cores #3 and #4 did not reach the bottom of the ice. On cores #1 and #2, horizontal sections were removed and weighed. The

04/13/88 0940L

*Figure 17. Absolute current relative to Earth.*

approximate density was computed using the length, diameter, and weight of each section. Each core section was then melted in a covered glass jar and the salinity of the liquid determined with a salinometer. Because some brine was lost from the cores when they were pulled out of the surrounding ice, the density and the salinity readings for the bottom sections of the cores are considered low.

The sound speed within the ice can be estimated, based on elasticity theory, using Young's modulus of elasticity E , density ρ , and Poisson's ratio μ as follows:

$$c = \sqrt{[(E/\rho)(1-\mu)] / [(1+\mu)(1-2\mu)]} \quad (\text{m/s}) .$$

The modulus of elasticity can in turn be obtained from an empirical model based on the model of brine volume by Langleben and Pounder:⁷

$$E = (10.0 - 0.0351 V_b) 10^{10} \quad (\text{dynes/cm}^2) .$$

A model for Poisson's ratio is given by Weeks and Assur⁸:

$$\mu = 0.333 + 0.06105 \exp(T/5.48) \quad (T \text{ in } ^\circ\text{C}) .$$

Table 3. Measured ice core temperatures.

Core #1: 25 March, 1630 hours		Core #2: 3 April, 0900 hours	
Depth (cm)	Temperature (°C)	Depth (cm)	Temperature (°C)
7.0	-17.6	5.0	-21.1
16.0	-17.6	15.0	-18.3
23.0	-16.1	30.0	-16.4
35.0	-14.8	45.0	-14.2
45.0	-13.9	60.0	-12.4
60.0	-12.4	70.0	-10.7
70.0	-12.2	80.0	-9.2
80.0	-8.0	95.0	-7.5
95.0	-6.4	105.0	-5.9
108.0	-4.9	120.5	-4.0
118.5	-2.3	128.0	-2.4
125.5	-2.1	136.0	-1.8
131.5	-1.6		
134.0	-1.9		

Core #3: 8 April, 0930 hours		Core #4: 8 April, 1010 hours	
Depth (cm)	Temperature (°C)	Depth (cm)	Temperature (°C)
5.0	-24.2	5.0	-14.2
17.0	-22.3	12.0	-13.3
25.0	-20.7	24.0	-12.2
32.0	-19.5	38.0	-10.9
42.0	-18.1	50.0	-10.0
52.0	-16.6	66.0	-9.2
63.0	-14.4	76.0	-7.4
77.0	-13.2	89.0	-6.4
90.0	-11.1	96.0	-5.3
99.0	-10.2		

Finally, the brine volume is computed using the empirical relationships obtained by Frankenstein and Garner⁹ based on the measured temperature (°C) and salinity (‰):

$$V_b = S (-52.56/T - 2.28) \quad \text{for } -0.5 > T > -2.06$$

$$V_b = S (-45.917/T + 0.93) \quad -2.06 > T > -8.2$$

$$V_b = S (-43.795/T + 1.189) \quad -8.2 > T > -22.9 .$$

From the relationships above, it is clear that the sound speed in the ice depends on the fundamental properties: temperature, salinity, and density.

The measured and computed properties of cores #1 and #2 are given in Table 4 and plotted in Figure 18, along with the temperature profiles of cores #3 and #4. A linear trend is generally observed in the temperature profile of the cores. In fact, the major deviations from linearity were caused by the warming and cooling of the cores during the delay, sometimes lengthy, between the temperature measurements, which were done both indoors and outdoors.

Table 4. Measured and computed ice core properties.

Core #1: 25 March 1630 hours

Depth (cm)	Temperature (°C)	Salinity (‰)	Density (g/cc)	Brine Volume (‰)	Sound Speed (m/s)
6.0	-17.6	8.7	0.932	32.0	3795.1
30.0	-15.3	6.6	0.917	26.7	3875.1
49.0	-13.5	4.6	0.911	20.4	3946.5
81.0	-7.9	4.3	0.910	29.0	3958.2
103.0	-5.5	3.8	0.925	35.3	3946.7
116.0	-2.9	3.7	0.959	62.0	3787.9
121.0	-2.2	3.9	0.955	85.0	3643.0
126.8	-2.0	4.2	0.977	100.7	3472.7
132.5	-1.8	6.9	0.860	185.5	2731.0

Core #2: 3 April 0900 hours

Depth (cm)	Temperature (°C)	Salinity (‰)	Density (g/cc)	Brine Volume (‰)	Sound Speed (m/s)
3.6	-21.1	8.3	0.922	27.1	3843.9
22.8	-17.3	6.7	0.928	24.9	3857.0
29.6	-16.4	5.9	0.927	22.8	3878.5
45.6	-14.3	5.5	0.935	23.4	3868.1
61.1	-12.2	4.0	0.916	19.1	3956.0
73.8	-10.1	3.8	0.911	21.0	3977.4
90.7	-8.0	3.9	0.930	26.0	3935.9
106.8	-5.7	4.3	0.918	38.6	3927.5
122.9	-3.5	4.2	0.897	59.0	3904.9
129.5	-2.3	3.9	0.919	81.5	3738.7
136.0	-1.8	6.6	0.749	177.5	3042.8

Core #3 (Figure 18c) was obtained from an area where the surface snow had been removed about 18 days earlier and shows a surface temperature near that of the air, which averaged about -25°C. The core's temperature gradient was nearly constant, meaning a quasi-equilibrium between the air and water temperatures had been established since the removal of the surface snow layer.

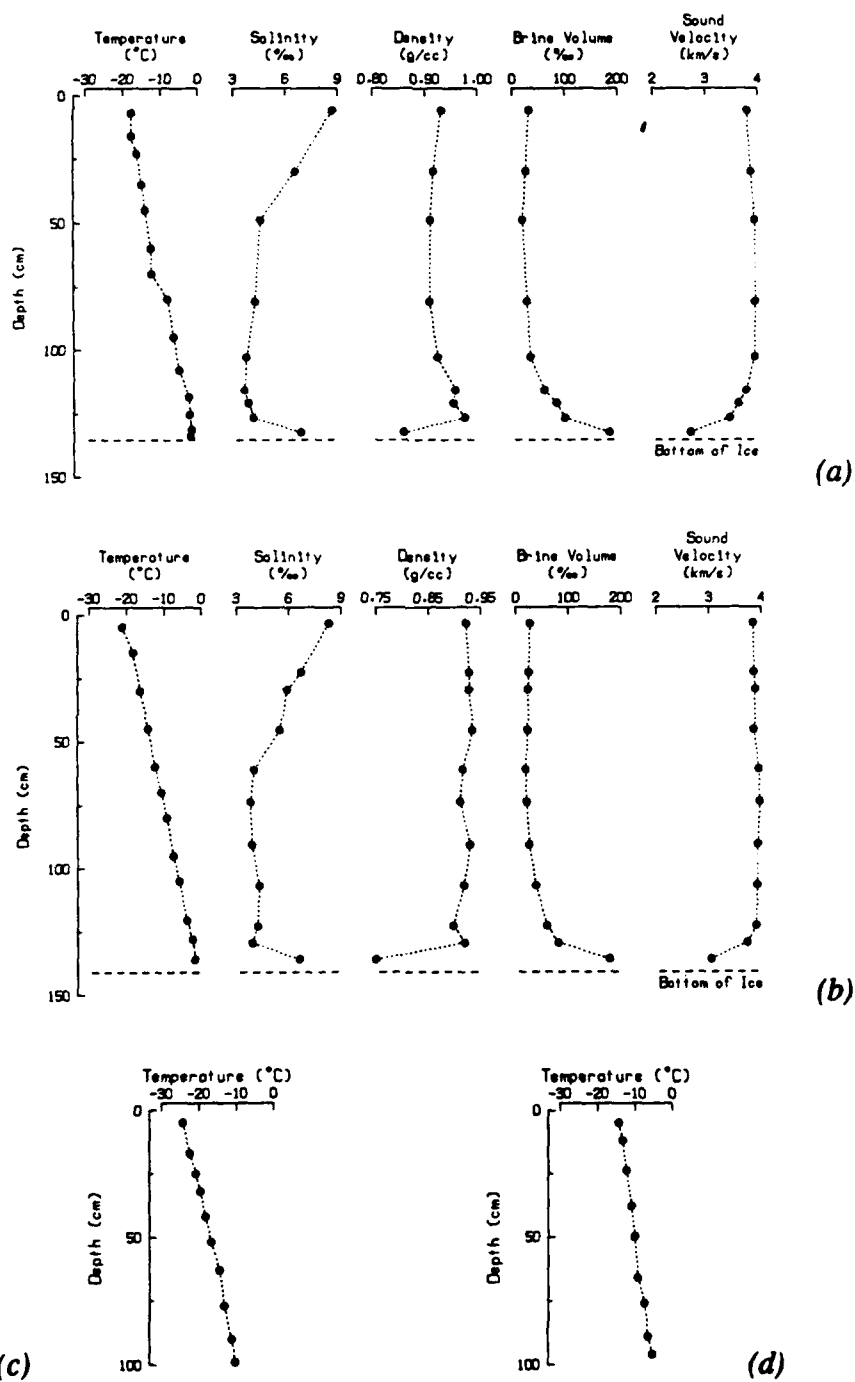


Figure 18. Measured and computed properties of ice cores: (a) 25 March, 1630; (b) 3 April, 0900; (c) 8 April, 0930; (d) 8 April, 1010.

The salinity profiles of Figures 18a and b show higher values at the top of the ice than at the bottom. This is consistent with the freezing process within the so-called skeletal layer near the bottom of the sea ice. As freezing takes place, brine is separated from the ice crystals and expelled. When the freezing is fast, as for thin ice, some of the brine does not have time to drain and gets trapped between the ice crystals, causing higher salinity in the ice that is to become the upper portion of the ice column. As the ice grows thicker, the freezing rate slows down and the brine has more time to drain, resulting in a lower salinity in what is to be the middle portion of the ice column. As mentioned before, brine drainage at the time of core removal was observed. The salinity measured in the skeletal layer at the bottom of the ice is therefore probably lower than the actual. However, the measured values of 6.6‰ and 6.9‰ agree with the value of 6.6‰ obtained from the sea ice salinity model of Cox and Weeks¹⁰:

$$S_i = K_{\text{eff}} S_w ,$$

where S_i is the salinity in ice, K_{eff} is the effective distribution coefficient, and S_w is the salinity of seawater;

$$K_{\text{eff}} = 0.26/[0.26 + 0.74 \exp(-7243V)]$$

for growth velocity $V > 3.6 \times 10^{-5}$ cm/s,

$$K_{\text{eff}} = 0.8925 + 0.0568 \ln(V)$$

for $2.0 \times 10^{-6} < V < 3.6 \times 10^{-5}$, and

$$K_{\text{eff}} = 0.12$$

for $V < 2 \times 10^{-6}$. The agreement is based on S_w of 32‰ and estimated growth rate of 5.8×10^{-6} cm/s (0.5 cm/day).

Although measured crudely, the density of the ice above the skeletal layer agrees well with that measured in 1986 during ICEX 1-86¹ (0.91–0.92 g/cc), when a more accurate immersion method was used.

The computed sound speed is noteworthy because it is nearly constant (3800–4000 m/s) for the upper portion (< 1 m) of the ice. These values agree well with the average of 3840 m/s obtained by Bunney¹¹ using direct speed measurements on samples cored from 1.5 m thick annual ice. A sharp drop-off in the sound speed is observed near the bottom. Unfortunately Bunney's measurements stopped at 10 cm from the bottom of the ice, so the low velocity in the skeletal layer cannot be confirmed. However, the lower part of Bunney's velocity profile does indicate a small decreasing trend.

X. UNDER-ICE AMBIENT NOISE

A comprehensive noise measurement program was carried out to study the temporal characteristics and the spatial correlation of under-ice noise. This section, however, presents only the daily measured background noise levels for a synoptic view. Detailed analysis of the data will be presented in a follow-up report.

A block diagram of the experimental setup is shown in Figure 19. Four omnidirectional hydrophones (ITC 6050C) with very low self-noise levels of -17 dBs were placed at 700 m from the camp to minimize interference from noise generated by activities at the camp. The hydrophones were deployed in the configuration of an orthogonal axis system with one as the origin (15.2 m deep) and the other three along X, Y, Z axes, each 15.2 m from the origin. With this layout, a noise burst received at the spatially separated hydrophones can be cross correlated to estimate the direction and range of the source.

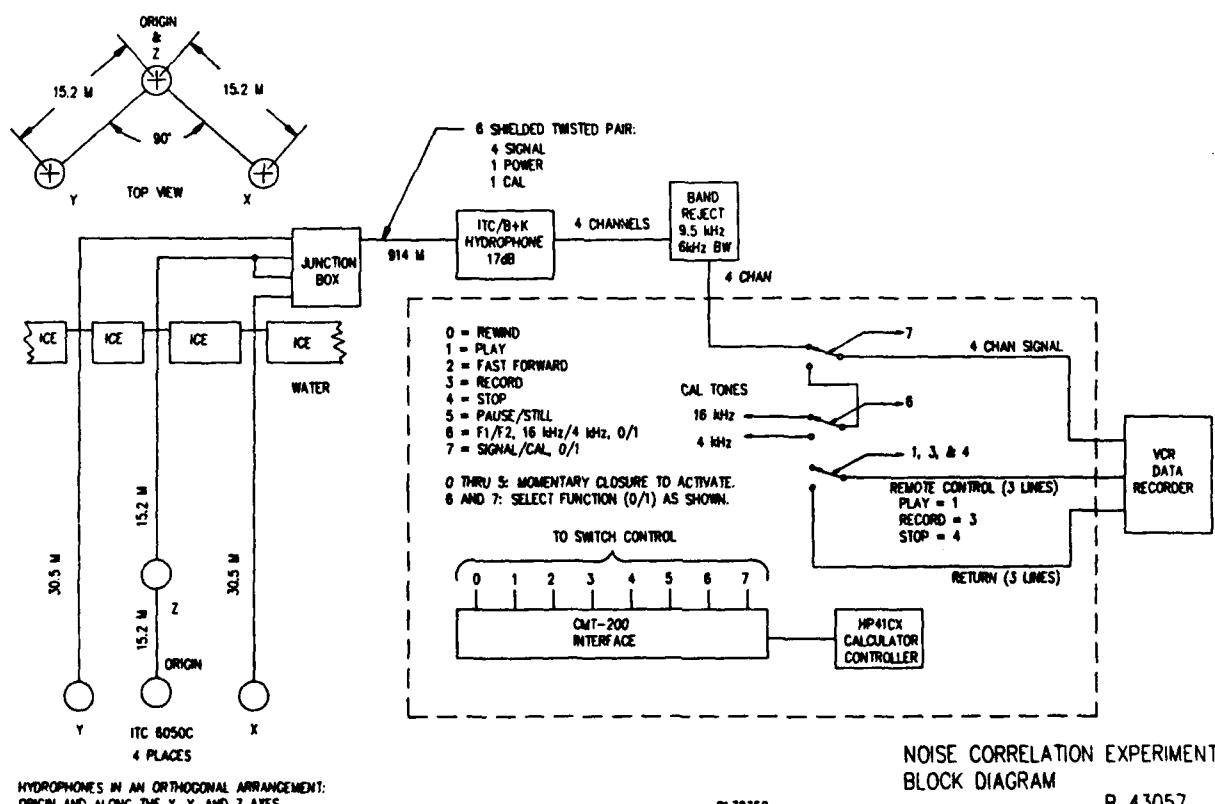


Figure 19. Block diagram of ambient noise measurement setup.

A 60 dB rejection notch filter centered at 9.5 kHz was sometimes used to reduce the interference from the signals generated by tracking and underwater communication. The ambient noise signals were then recorded on a 20 kHz-bandwidth VCR data recorder with two digital channels of 88 dB dynamic range and two HF channels of 75 dB dynamic range. An HP41 CX was used to control the recorder, turning it on at hourly intervals and shutting it off after a programmed recording period, typically 10 minutes.

In the Laboratory the data tapes were run through a spectrum analyzer using a Hanning window, and 64 consecutive spectra were ensemble-averaged to obtain a smoothed spectrum. The recording taken nearest 0000 hours of each day was used as a representative spectrum. Some additional noise spectra during the high wind period on 13 April are also given. Plots of the spectra are given in Appendix F. The sound level is given in spectral units, i.e., $\text{re } 1 \mu \text{Pa} // 1 \text{ Hz}$. Note that these spectra were obtained from the so-called 'steady-state' intervals during which there were no irregular noise bursts generated by ice cracking or ridging. Spectra with a dip centered at 9.5 kHz are those recorded with the notch filter enabled. Sometimes low level ambient noise at high frequency was masked by the self-noise limit of the hydrophones. The spectral lines at higher frequencies were caused by interfering electronic equipment. To minimize these spurious spectral lines we tried different ways of grounding and isolating equipment. The relatively low level of the lines and the ability to record low noise levels indicated reasonable success.

To illustrate the effect of wind speed on the under-ice ambient noise, noise level at arbitrarily selected frequencies of 1, 5, and 20 kHz (from the spectra in Appendix F) were plotted along with wind speed against day of month in Figure 20. Wherever a spurious peak was encountered, the local noise floor level near the selected frequencies was used. For example, the peak level of 61.2 dBs at 20 kHz on 7 April was replaced by an estimated floor level of 18 dBs. The figure shows that, with the exception of the data before 30 March, there is good correlation between the ambient noise and the wind speed. A probable mechanism to explain this apparent high degree of correlation is wind-blown snow impacting the surface. Although other wind-induced mechanisms may apply as well, such as drift¹² and ridging.¹³ If this is the case, then there is probably a critical wind speed below which there is no blowing snow and therefore no correlation between the noise and the wind. Figures 21–23 show the same ambient noise data shown in Figure 20 plotted against the wind speed. It is seen that the noise level was indeed nearly constant for wind speed less than ~3 m/s. If there is any correlation below this speed, it is negligible. Unfortunately there were no visual observations to verify this speed as the threshold for blowing snow conditions. Least squares fits for data with wind speeds above 3 m/s yield slopes of 1.3, 2.8, and 2.2 dBs/m/s, for 1, 5, and 20 kHz, respectively, as shown in Figures 21–23.

It should be mentioned that there are other causes of ambient noise such as wave action in an open lead, changing air temperature,¹⁴ radiant heat flux,¹⁵ and floe cracking/ridging (as happened on 13 April). Some of those factors may have accounted

for the low correlation between the wind speed and the noise levels of the data prior to 30 March. For the data after 30 March, the dominant factor appears to be the wind action on the surface of the ice, as discussed previously.

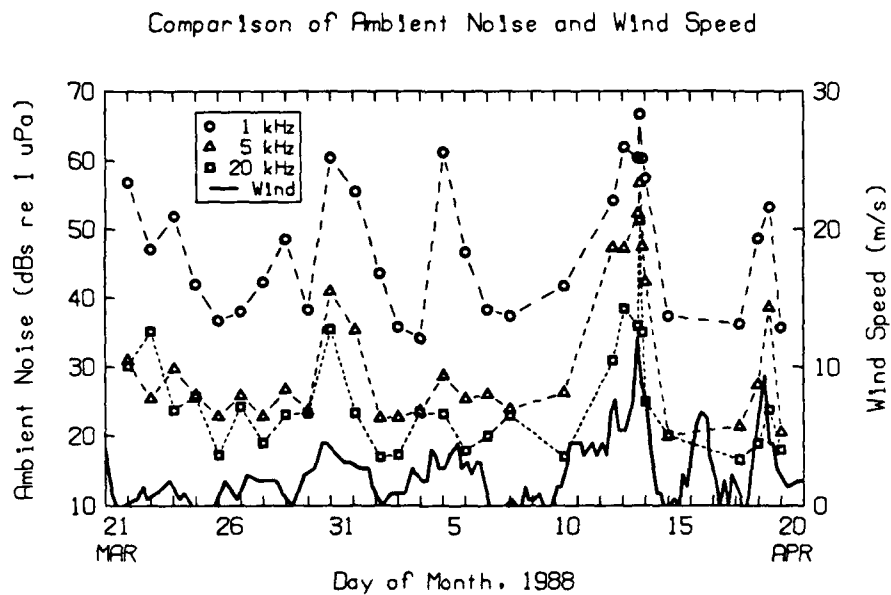


Figure 20. Daily ambient noise at 1, 5, and 20 kHz vs wind speed.

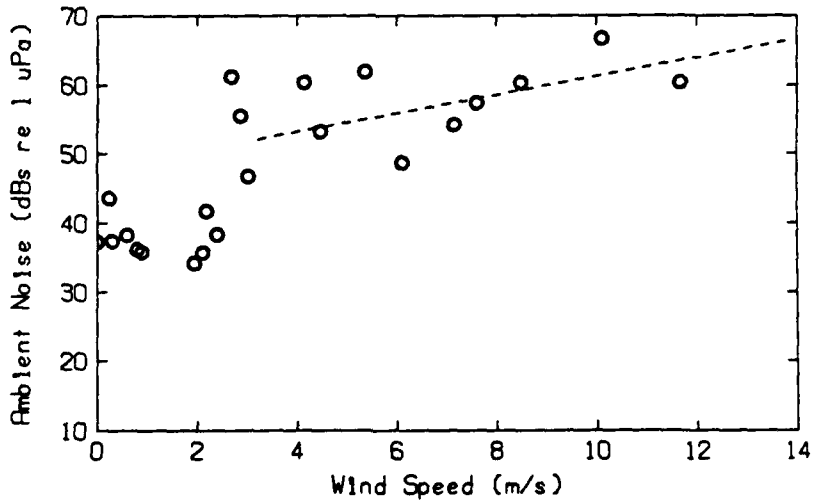


Figure 21. Ambient noise at 1 kHz vs wind speed. Slope of dashed line = 1.3 dBs/m/s.

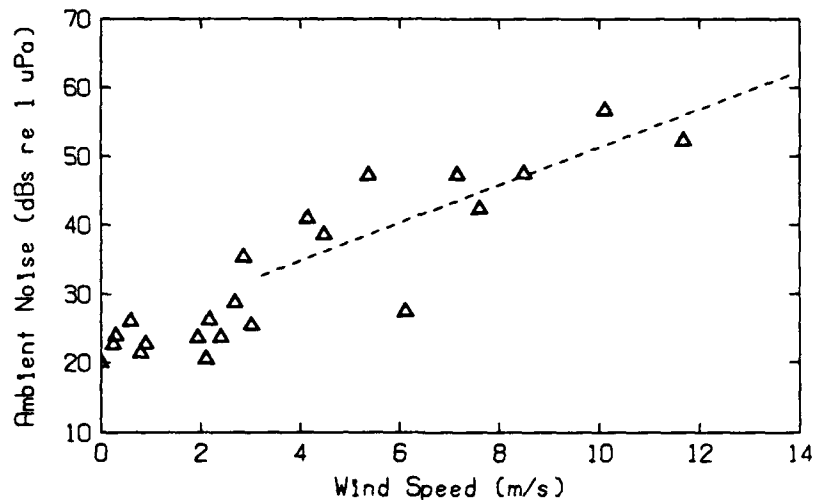


Figure 22. Ambient noise at 5 kHz vs wind speed. Slope of dashed line = 2.8 dBs/m/s.

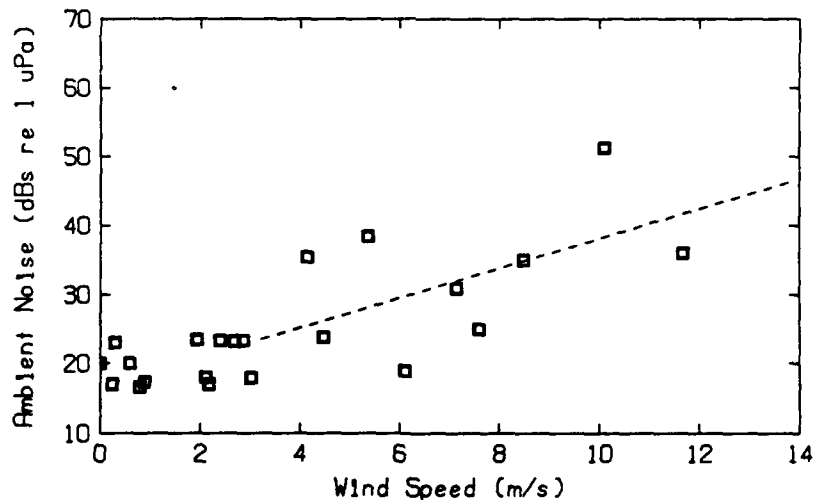


Figure 23. Ambient noise at 20 kHz vs wind speed. Slope of dashed line = 2.2 dBs/m/s.

Figure 24 shows a noise spectrum taken on 13 April at 1830 when the wind was blowing at 12.5 m/s, the maximum wind speed encountered at APLIS 88. Another spectrum shows the lowest level measured on 18 April when the wind was negligible. These two spectra, 30 dBs apart, are considered the maximum and the minimum noise levels measured during the camp period. The minimum level spectrum, about 10 dBs below

that of sea state 0 for open ocean, is also the lowest encountered at recent (since 1984) APL ice camps, where levels near sea state 0 were generally the lowest observed.^{1,2,16}

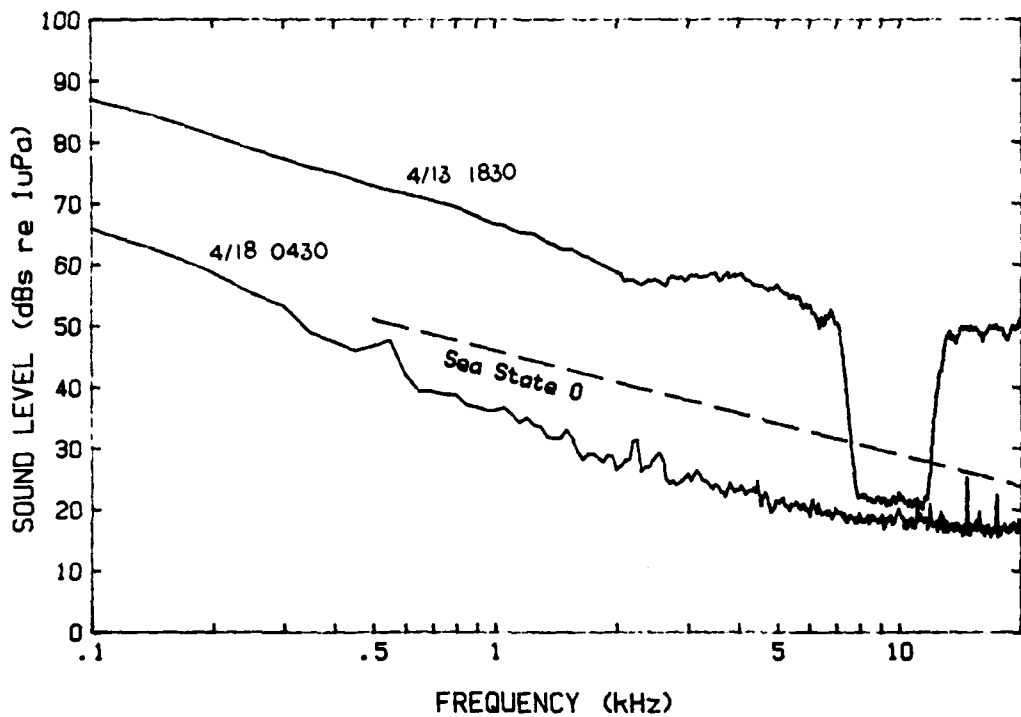


Figure 24. Maximum and minimum noise spectra at APLIS 88. The dip around 9.5 kHz in the maximum spectrum is caused by the notch filter.

It should be noted that the placement of hydrophones 700 m from camp was more than adequate to avoid contamination by noise generated at the camp. Measurements to verify this are given in Appendix G.

XI. REFERENCES

1. G. R. Garrison, T. Wen, R. E. Francois, W. J. Felton, and M. L. Welch, "Environmental Measurements in the Beaufort Sea, Spring 1986," APL-UW 4-86, Applied Physics Laboratory, University of Washington, Seattle, WA, January 1987.
2. T. Wen, R. P. Stein, F. W. Karig, R. T. Miyamoto, and W. J. Felton, "Environmental Measurements in the Beaufort Sea, Spring 1987," APL-UW 1-87, Applied Physics Laboratory, University of Washington, Seattle, WA, February 1988.
3. J. L. Hoerber, "Introduction to Satellite Navigation Systems," Tracor, Inc., Austin, TX, 1980.
4. S. D. Thompson, "An Introduction to the Global Positioning System," ARINC Research Corporation, Annapolis, MD, August 1985.
5. Data provided by Arctic Submarine Laboratory, Naval Ocean Systems Center; analysis by John L. Newton, Polar Research Laboratory, Carpenteria, CA.
6. R. E. Francois and G. R. Garrison, "Sound absorption based on ocean measurements: part II: Boric acid contribution and equation for total absorption," *J. Acoust. Soc. Am.*, **72**, 1879–1890, 1982.
7. M. P. Langenberg and E. R. Pounder, "Elastic parameters of sea ice," in *Ice and Snow: Process, Properties, and Applications*, Cambridge: MIT Press, 1963, 67–78.
8. W. F. Weeks and A. Assur, "The mechanical properties of sea ice," in *Cold Regions Science and Engineering Monograph II-C3*, Cold Regions Research and Engineering Laboratory, Hanover, NH, 1967.
9. F. Frankenstein and R. Garner, "Equations for determining the brine volume of sea ice from -0.5 to -22.9° C," *J. Glaciology*, **6**(48), 943–944, 1967.
10. G. F. N. Cox and W. F. Weeks, "On the profile properties of undeformed first-year sea ice," CRREL special report, Cold Regions Research and Engineering Laboratory, Hanover, NH. Presented at 2nd Ice Penetration Technology Workshop, 16–19 June 1986, Monterey, CA.
11. R. Bunney, "Feasibility of Acoustically Determining the Thickness of Sea Ice," APL-UW 7317, Applied Physics Laboratory, University of Washington, Seattle, WA, April 1974.

12. N. C. Makris and I. Dyer, "Environmental correlates of pack ice noise," *J. Acoust. Soc. Am.*, **79**, 1434–1440, 1986.
13. R. S. Pritchard, "Arctic ocean background noise caused by ridging of sea ice," *J. Acoust. Soc. Am.*, **75**, 419–427, 1984.
14. A. R. Milne and J. H. Ganton, "Ambient noise under arctic sea ice," *J. Acoust. Soc. Am.*, **36**, 885, 1964.
15. J. K. Lewis and W. W. Denner, "Higher frequency ambient noise in the Arctic Ocean," *J. Acoust. Soc. Am.*, **84**, 1444–1455, 1988.
16. G. R. Garrison, T. Wen, and M. L. Welch, "Environmental Measurements in the Beaufort Sea, Autumn 1984," APL-UW 3-85, Applied Physics Laboratory, University of Washington, Seattle, WA, March 1985.

APPENDIX A

Listing of ice camp positions obtained from NAVSAT system.

Data points have been smoothed with a 6-point running average filter. Times are given in UTC. To obtain local time, subtract 9 hours for days up to and including 2 April, and 8 hours afterward.

Coordinated

	Universal Time	North	West	Drift	Drift
Date	Time	Latitude	Longitude	Speed	Dir
mmdd	hhmm	dd mm.mm	ddd mm.mm	km/hr	true
0301	----	72 30.70	141 44.00	----	---
0303	1530	72 23.00	142 0.00	----	---
0304	0935	72 21.70	141 57.20	----	---
0305	----	72 22.20	142 34.70	----	---
0306	0930	72 26.80	142 53.30	----	---
0308	0125	72 32.67	143 9.68	----	---
0308	0333	72 32.84	143 10.90	0.35	294
0308	0444	72 32.92	143 11.57	0.34	293
0308	0545	72 32.97	143 12.22	0.35	288
0308	0657	72 33.12	143 13.30	0.47	291
0308	0800	72 33.17	143 13.82	0.43	292
0308	0904	72 33.22	143 14.35	0.29	287
0308	0955	72 33.25	143 14.78	0.29	284
0308	1039	72 33.27	143 15.12	0.28	283
0308	1210	72 33.31	143 15.61	0.21	284
0308	1340	72 33.33	143 15.98	0.16	281
0308	1520	72 33.35	143 16.37	0.14	278
0308	1706	72 33.36	143 16.77	0.12	276
0310	0417	72 32.44	143 16.79	----	---
0310	0721	72 32.66	143 18.91	0.60	282
0310	0802	72 32.74	143 19.60	0.59	289
0310	0848	72 32.85	143 20.60	0.79	291
0310	0942	72 33.02	143 21.70	0.76	297
0310	1042	72 33.14	143 22.51	0.49	295
0310	1141	72 33.36	143 23.51	0.70	306
0310	1242	72 33.57	143 24.40	0.63	308
0310	1337	72 33.73	143 25.25	0.60	302
0310	1431	72 33.92	143 25.99	0.59	309
0310	1512	72 34.10	143 26.48	0.63	320
0310	1552	72 34.27	143 27.15	0.74	310
0310	1632	72 34.41	143 27.68	0.58	310
0310	1736	72 34.58	143 28.69	0.60	299
0310	1832	72 34.76	143 29.79	0.75	299
0310	1935	72 34.94	143 30.75	0.59	301
0310	2038	72 35.10	143 31.80	0.63	296
0310	2145	72 35.25	143 32.82	0.57	296
0310	2251	72 35.45	143 33.91	0.65	301
0310	2331	72 35.61	143 34.46	0.63	314
0311	0012	72 35.76	143 34.94	0.55	314
0311	0047	72 35.89	143 35.53	0.71	307
0311	0121	72 36.10	143 36.51	1.17	305
0311	0157	72 36.30	143 37.11	0.85	318
0311	0248	72 36.57	143 37.98	0.80	315
0311	0410	72 37.05	143 39.30	0.85	321
0311	0532	72 37.49	143 40.50	0.76	320

Coordinated

Universal Time Date mmdd	Time hhmm	North dd	Latitude mm.mm	West ddd	Longitude mm.mm	Drift Speed km/hr	Drift Dir true
0311	0651	72	37.95	143	41.62	0.81	324
0311	0816	72	38.33	143	42.32	0.57	331
0311	0929	72	38.76	143	43.22	0.77	327
0311	1028	72	39.08	143	43.82	0.68	330
0311	1140	72	39.32	143	43.85	0.38	357
0311	1224	72	39.49	143	43.77	0.42	007
0311	1303	72	39.62	143	43.56	0.43	025
0311	1345	72	39.75	143	43.42	0.34	017
0311	1506	72	39.89	143	43.21	0.21	024
0311	1550	72	39.98	143	42.99	0.28	036
0311	1735	72	40.00	143	42.57	0.13	081
0311	1912	72	40.09	143	42.18	0.17	051
0311	2203	72	40.17	143	41.86	0.08	049
0312	0035	72	40.17	143	42.23	0.08	271
0312	0203	72	40.07	143	42.37	0.14	202
0312	0317	72	39.96	143	42.44	0.17	190
0312	0820	72	39.91	143	42.88	0.05	250
0312	1111	72	39.94	143	43.25	0.07	283
0312	1506	72	39.98	143	42.90	0.05	068
0312	1659	72	39.89	143	42.58	0.13	134
0312	1856	72	39.76	143	42.29	0.14	144
0312	2142	72	39.66	143	42.62	0.10	221
0312	2352	72	39.67	143	43.10	0.12	275
0313	0114	72	39.63	143	43.51	0.17	252
0313	0156	72	39.56	143	43.90	0.36	239
0313	0241	72	39.52	143	44.31	0.32	250
0313	0408	72	39.56	143	45.41	0.43	277
0313	0531	72	39.61	143	46.56	0.46	277
0313	0654	72	39.69	143	47.98	0.58	281
0313	0801	72	39.75	143	49.34	0.68	277
0313	0909	72	39.90	143	50.38	0.56	295
0313	1013	72	40.03	143	51.49	0.62	292
0313	1034	72	40.10	143	51.88	0.72	299
0313	1052	72	40.18	143	52.19	0.75	312
0313	1132	72	40.35	143	52.55	0.58	328
0313	1155	72	40.47	143	52.84	0.69	322
0313	1222	72	40.57	143	53.28	0.68	308
0313	1251	72	40.70	143	53.55	0.58	328
0313	1322	72	40.84	143	53.91	0.65	323
0313	1355	72	41.01	143	54.37	0.73	320
0313	1427	72	41.18	143	54.62	0.63	336
0313	1458	72	41.32	143	54.84	0.55	334
0313	1525	72	41.42	143	54.95	0.46	343
0313	1552	72	41.57	143	55.04	0.60	349
0313	1619	72	41.75	143	55.17	0.78	348
0313	1645	72	41.91	143	54.94	0.73	024
0313	1712	72	42.02	143	54.89	0.49	006
0313	1740	72	42.19	143	54.86	0.68	003
0313	1806	72	42.37	143	54.78	0.77	007
0313	1836	72	42.54	143	54.60	0.63	018
0313	1937	72	42.76	143	54.26	0.44	024
0313	2008	72	42.90	143	54.11	0.54	018

Coordinated

	Universal Time	North	West	Drift	Drift
Date	Time	Latitude	Longitude	Speed	Dir
mmdd	hhmm	dd mm.mm	ddd mm.mm	km/hr	true
0313	2058	72 43.04	143 53.65	0.43	043
0313	2148	72 43.20	143 53.07	0.52	048
0313	2233	72 43.33	143 52.66	0.45	042
0313	2318	72 43.45	143 52.11	0.50	054
0314	0003	72 43.52	143 51.56	0.44	065
0314	0052	72 43.62	143 50.71	0.61	068
0314	0119	72 43.60	143 50.17	0.67	097
0314	0150	72 43.60	143 49.62	0.58	089
0314	0219	72 43.55	143 49.07	0.66	108
0314	0249	72 43.52	143 48.58	0.55	100
0314	0315	72 43.51	143 48.13	0.58	093
0314	0417	72 43.33	143 47.51	0.46	134
0314	0520	72 43.21	143 46.89	0.39	123
0314	0620	72 43.04	143 46.27	0.47	132
0314	0720	72 42.90	143 45.71	0.40	130
0314	0821	72 42.75	143 45.07	0.45	128
0314	0924	72 42.57	143 44.54	0.42	138
0314	1023	72 42.45	143 44.10	0.34	133
0314	1137	72 42.28	143 43.68	0.31	143
0314	1258	72 42.08	143 43.26	0.32	147
0314	1333	72 41.97	143 43.00	0.42	144
0314	1436	72 41.84	143 42.68	0.29	144
0314	1507	72 41.74	143 42.52	0.39	153
0314	1620	72 41.54	143 42.20	0.33	154
0314	1703	72 41.44	143 42.07	0.29	159
0314	1744	72 41.30	143 41.94	0.39	163
0314	1824	72 41.18	143 41.83	0.35	165
0314	1904	72 41.08	143 41.66	0.31	152
0314	1949	72 40.93	143 41.56	0.38	168
0314	2100	72 40.74	143 41.38	0.30	163
0314	2210	72 40.56	143 41.40	0.30	181
0314	2250	72 40.45	143 41.48	0.31	192
0315	0010	72 40.21	143 41.36	0.34	171
0315	0056	72 40.09	143 41.34	0.29	176
0315	0147	72 39.94	143 41.33	0.32	179
0315	0258	72 39.71	143 41.47	0.36	190
0315	0407	72 39.50	143 41.48	0.35	180
0315	0516	72 39.29	143 41.57	0.34	187
0315	0626	72 39.12	143 41.68	0.27	190
0315	0737	72 38.92	143 41.95	0.33	201
0315	0841	72 38.75	143 42.13	0.31	197
0315	0935	72 38.63	143 42.18	0.27	186
0315	1020	72 38.53	143 42.36	0.27	210
0315	1111	72 38.40	143 42.58	0.33	206
0315	1153	72 38.29	143 42.77	0.32	206
0315	1317	72 38.07	143 42.85	0.29	185
0315	1428	72 37.88	143 42.91	0.30	185
0315	1527	72 37.72	143 42.93	0.29	182
0315	1627	72 37.56	143 42.92	0.30	178

Coordinated Universal Time		North		West		Drift	Drift
Date mmdd	Time hhmm	Latitude dd mm.mm	Longitude ddd mm.mm			Speed km/hr	Dir true
0315	1657	72 37.45	143 43.00			0.44	192
0315	1736	72 37.30	143 42.98			0.43	177
0315	1819	72 37.14	143 42.95			0.41	177
0315	1859	72 37.00	143 43.09			0.41	196
0315	1940	72 36.84	143 43.25			0.45	196
0315	2025	72 36.69	143 43.37			0.40	192
0315	2106	72 36.58	143 43.56			0.32	208
0315	2233	72 36.37	143 44.06			0.34	214
0315	2326	72 36.21	143 44.20			0.33	195
0316	0018	72 36.08	143 44.30			0.30	192
0316	0343	72 35.80	143 44.38			0.15	184
0316	0705	72 35.54	143 44.40			0.14	181
0316	1032	72 35.27	143 44.43			0.15	182
0316	1335	72 35.06	143 44.24			0.13	164
0316	1641	72 34.87	143 44.21			0.11	176
0316	1944	72 34.71	143 44.14			0.10	172
0316	2113	72 34.64	143 43.77			0.17	123
0316	2237	72 34.63	143 43.32			0.18	096
0317	0042	72 34.52	143 43.09			0.11	146
0317	0238	72 34.41	143 43.14			0.11	187
0317	0701	72 34.27	143 42.94			0.06	156
0317	1310	72 34.15	143 42.92			0.04	177
0317	1843	72 34.06	143 42.59			0.04	130
0317	2304	72 34.07	143 42.08			0.07	086
0318	0259	72 34.09	143 41.56			0.07	083
0318	0420	72 34.04	143 41.19			0.17	115
0318	1142	72 33.99	143 40.81			0.03	111
0318	1522	72 34.00	143 40.28			0.08	088
0318	1740	72 33.96	143 39.79			0.12	104
0319	0620	72 33.92	143 40.28			0.02	256
0319	1030	72 33.93	143 40.82			0.07	271
0319	2250	72 33.90	143 41.07			0.00	---
0320	0938	72 33.81	143 40.69			0.02	127
0320	1347	72 33.83	143 40.19			0.07	082
0320	1631	72 33.88	143 39.75			0.10	069
0320	1820	72 33.97	143 39.43			0.13	048
0320	1939	72 34.02	143 39.03			0.19	064
0320	2051	72 34.15	143 38.50			0.31	050
0320	2131	72 34.22	143 38.00			0.46	065
0320	2209	72 34.27	143 37.50			0.46	073
0320	2245	72 34.34	143 37.05			0.49	060
0320	2320	72 34.39	143 36.62			0.42	071
0320	2355	72 34.46	143 36.22			0.45	060
0321	0052	72 34.55	143 35.64			0.38	061
0321	0157	72 34.65	143 35.01			0.37	060
0321	0240	72 34.74	143 34.69			0.32	050
0321	0322	72 34.80	143 34.39			0.29	054
0321	0427	72 34.88	143 34.13			0.20	044
0321	0634	72 35.06	143 33.76			0.19	031
0321	0746	72 35.17	143 33.58			0.18	027
0321	1027	72 35.28	143 33.57			0.08	000
0321	1300	72 35.23	143 33.95			0.09	247

Coordinated

	Universal Time		North		West		Drift	Drift
	Date	Time	Latitude		Longitude		Speed	Dir
	mmdd	hhmm	dd mm.mm	ddd	mm.mm		km/hr	true
0321	1512	72	35.18	143	34.37	0.12	246	
0321	1722	72	35.07	143	34.78	0.14	227	
0321	1924	72	34.96	143	35.17	0.15	227	
0321	2050	72	34.83	143	35.37	0.18	205	
0321	2257	72	34.70	143	35.21	0.13	160	
0322	0035	72	34.56	143	35.10	0.16	166	
0322	0301	72	34.38	143	35.15	0.14	184	
0322	0440	72	34.29	143	35.33	0.12	209	
0322	0712	72	34.14	143	35.31	0.11	178	
0322	1055	72	34.00	143	35.14	0.07	158	
0322	1252	72	33.90	143	34.99	0.11	157	
0322	1512	72	33.87	143	34.56	0.10	101	
0322	1738	72	33.77	143	34.42	0.09	157	
0322	2011	72	33.66	143	34.46	0.08	186	
0323	0016	72	33.64	143	34.00	0.06	099	
0323	0246	72	33.60	143	33.62	0.09	106	
0323	1519	72	33.55	143	33.45	0.00	---	
0324	0034	72	33.54	143	32.98	0.03	091	
0324	1056	72	33.65	143	33.08	0.02	344	
0324	2312	72	33.63	143	33.16	0.00	---	
0325	0526	72	33.52	143	32.64	0.06	125	
0325	1004	72	33.60	143	32.97	0.05	308	
0325	2229	72	33.59	143	32.89	0.00	---	
0326	0353	72	33.51	143	32.61	0.04	130	
0326	0702	72	33.45	143	32.29	0.07	122	
0326	1340	72	33.53	143	32.58	0.03	310	
0326	2208	72	33.51	143	32.11	0.03	098	
0327	0106	72	33.62	143	31.79	0.09	039	
0327	0427	72	33.49	143	31.73	0.07	172	
0327	1633	72	33.57	143	31.70	0.00	---	
0327	2352	72	33.53	143	31.29	0.03	106	
0328	0310	72	33.45	143	30.86	0.09	121	
0328	0724	72	33.48	143	31.29	0.06	280	
0328	1016	72	33.44	143	31.71	0.09	252	
0328	1504	72	33.34	143	31.47	0.05	141	
0329	0341	72	33.42	143	31.65	0.00	---	
0329	1033	72	33.42	143	32.13	0.04	269	
0329	1956	72	33.41	143	32.59	0.03	265	
0329	2251	72	33.49	143	33.07	0.11	298	
0330	0157	72	33.46	143	33.45	0.07	254	
0330	0655	72	33.49	143	33.80	0.04	290	
0330	1826	72	33.47	143	34.30	0.02	260	
0330	1931	72	33.46	143	34.70	0.20	263	
0330	2040	72	33.45	143	35.11	0.20	266	
0330	2213	72	33.45	143	35.75	0.23	271	
0330	2316	72	33.46	143	36.34	0.31	273	
0331	0054	72	33.45	143	36.88	0.18	265	
0331	0228	72	33.47	143	37.24	0.13	280	
0331	1127	72	33.43	143	37.63	0.03	253	
0331	2055	72	33.32	143	37.73	0.02	194	
0401	0941	72	33.30	143	37.79	0.00	---	
0401	2226	72	33.26	143	37.78	0.00	---	

Coordinated							
Universal Time	North	West	Drift	Drift			
Date	Time	Latitude	Longitude	Speed	Dir		
mmdd	hhmm	dd mm.mm	ddd mm.mm	km/hr	true		
0402	1039	72 33.19	143 37.66	0.00	---		
0402	1537	72 33.33	143 37.62	0.05	005		
0402	2142	72 33.25	143 37.88	0.04	222		
0403	0945	72 33.27	143 37.85	0.00	---		
0403	2223	72 33.27	143 37.74	0.00	---		
0404	1124	72 33.19	143 37.72	0.00	---		
0404	2022	72 33.30	143 37.90	0.03	334		
0404	2250	72 33.34	143 38.48	0.13	282		
0405	0120	72 33.40	143 39.02	0.13	290		
0405	0333	72 33.46	143 39.47	0.12	291		
0405	0545	72 33.50	143 39.86	0.11	289		
0405	0811	72 33.55	143 40.28	0.10	290		
0405	1248	72 33.58	143 40.64	0.04	287		
0406	0106	72 33.52	143 40.50	0.00	---		
0406	0314	72 33.42	143 40.73	0.10	214		
0406	1531	72 33.42	143 40.54	0.00	---		
0407	0427	72 33.37	143 40.48	0.00	---		
0407	1656	72 33.31	143 40.49	0.00	---		
0408	0531	72 33.35	143 40.63	0.00	---		
0408	1738	72 33.35	143 40.41	0.00	---		
0408	2055	72 33.38	143 40.84	0.07	282		
0409	0922	72 33.41	143 40.56	0.00	---		
0409	2159	72 33.38	143 40.59	0.00	---		
0410	1050	72 33.31	143 40.66	0.00	---		
0410	1448	72 33.42	143 40.60	0.05	010		
0411	0253	72 33.32	143 40.70	0.02	196		
0411	1541	72 33.29	143 40.69	0.00	---		
0412	0358	72 33.27	143 40.60	0.00	---		
0412	1600	72 33.26	143 40.58	0.00	---		
0413	0436	72 33.36	143 40.87	0.02	318		
0413	0832	72 33.40	143 41.27	0.06	288		
0413	0918	72 33.44	143 41.61	0.27	292		
0413	1001	72 33.50	143 42.16	0.46	290		
0413	1047	72 33.61	143 43.05	0.70	291		
0413	1126	72 33.72	143 44.01	0.87	290		
0413	1209	72 33.86	143 44.98	0.84	296		
0413	1254	72 34.02	143 46.09	0.90	295		
0413	1339	72 34.19	143 47.22	0.93	296		
0413	1425	72 34.32	143 48.35	0.90	291		
0413	1510	72 34.45	143 49.46	0.87	291		
0413	1627	72 34.73	143 51.28	0.88	297		
0413	1757	72 35.07	143 53.71	0.99	295		
0413	1927	72 35.47	143 55.98	0.97	300		
0413	2058	72 35.86	143 58.34	1.00	299		
0413	2229	72 36.35	144 0.73	1.05	304		
0413	2359	72 36.82	144 2.95	1.00	304		
0414	0104	72 37.19	144 4.54	1.03	307		
0414	0217	72 37.61	144 6.02	0.94	313		
0414	0332	72 38.00	144 7.60	0.90	309		
0414	0445	72 38.38	144 8.89	0.82	314		
0414	0553	72 38.71	144 10.14	0.83	311		

Coordinated								
Universal Time		North		West	Drift	Drift		
Date	Time	Latitude		Longitude	Speed	Dir		
mmdd	hhmm	dd mm.mm	ddd	mm.mm	km/hr	true		
0414	0706	72 39.08	144	11.39	0.80	315		
0414	0827	72 39.47	144	12.71	0.75	314		
0414	0926	72 39.74	144	13.63	0.72	314		
0414	1019	72 39.94	144	14.35	0.63	314		
0414	1114	72 40.17	144	15.24	0.71	310		
0414	1214	72 40.37	144	16.10	0.60	307		
0414	1327	72 40.61	144	17.14	0.60	307		
0414	1426	72 40.78	144	17.87	0.52	307		
0414	1523	72 40.93	144	18.64	0.53	303		
0414	1627	72 41.14	144	19.44	0.55	311		
0414	1740	72 41.33	144	20.15	0.44	312		
0414	1847	72 41.53	144	20.74	0.44	318		
0414	1930	72 41.63	144	21.03	0.34	318		
0414	2020	72 41.78	144	21.46	0.44	320		
0414	2111	72 41.91	144	21.80	0.37	323		
0414	2222	72 42.08	144	22.20	0.32	323		
0414	2325	72 42.23	144	22.59	0.33	322		
0415	0042	72 42.37	144	22.97	0.27	321		
0415	0157	72 42.52	144	23.48	0.32	315		
0415	0309	72 42.66	144	23.82	0.27	324		
0415	0425	72 42.82	144	24.01	0.25	340		
0415	0520	72 42.91	144	24.21	0.22	325		
0415	0630	72 43.04	144	24.58	0.26	319		
0415	0754	72 43.14	144	24.77	0.16	330		
0415	0940	72 43.24	144	24.98	0.12	327		
0415	1149	72 43.32	144	25.28	0.10	312		
0415	1447	72 43.46	144	25.96	0.15	304		
0415	1740	72 43.60	144	26.61	0.15	305		
0415	2023	72 43.72	144	27.13	0.13	307		
0415	2239	72 43.84	144	27.67	0.17	306		
0416	0035	72 43.97	144	28.16	0.19	312		
0416	0215	72 44.12	144	28.84	0.28	307		
0416	0305	72 44.20	144	29.31	0.35	298		
0416	0431	72 44.34	144	29.91	0.29	308		
0416	0507	72 44.39	144	30.32	0.40	290		
0416	0546	72 44.42	144	30.78	0.40	284		
0416	0648	72 44.50	144	31.20	0.26	300		
0416	0716	72 44.53	144	31.55	0.43	290		
0416	0820	72 44.58	144	32.14	0.32	285		
0416	0859	72 44.67	144	32.66	0.50	299		
0416	0939	72 44.74	144	33.36	0.62	288		
0416	1018	72 44.82	144	34.07	0.63	290		
0416	1100	72 44.91	144	34.73	0.59	294		
0416	1142	72 45.01	144	35.64	0.77	291		
0416	1221	72 45.10	144	36.41	0.69	289		
0416	1250	72 45.18	144	36.98	0.72	295		
0416	1321	72 45.25	144	37.56	0.66	293		
0416	1354	72 45.27	144	38.26	0.71	275		
0416	1439	72 45.38	144	39.35	0.84	287		
0416	1532	72 45.50	144	40.40	0.70	291		
0416	1628	72 45.72	144	41.70	0.86	299		

Coordinated								
Universal Time	North	West	Drift	Drift				
Date	Time	Latitude	Longitude	Speed	Dir			
mmdd	hhmm	dd mm.mm	ddd mm.mm	km/hr	true			
0416	1732	72 45.94	144 43.06	0.81	298			
0416	1832	72 46.19	144 44.27	0.81	305			
0416	1929	72 46.51	144 45.48	0.92	311			
0416	2018	72 46.79	144 46.26	0.82	320			
0416	2102	72 47.08	144 46.98	0.93	324			
0416	2144	72 47.35	144 47.42	0.78	333			
0416	2225	72 47.61	144 47.70	0.73	342			
0416	2308	72 47.90	144 47.97	0.77	344			
0416	2354	72 48.16	144 48.15	0.67	348			
0417	0036	72 48.42	144 48.41	0.70	343			
0417	0121	72 48.67	144 48.41	0.62	359			
0417	0205	72 48.88	144 48.45	0.53	357			
0417	0243	72 49.06	144 48.44	0.51	000			
0417	0320	72 49.17	144 48.52	0.36	349			
0417	0357	72 49.28	144 48.60	0.33	347			
0417	0442	72 49.39	144 48.60	0.27	000			
0417	0633	72 49.54	144 49.15	0.22	313			
0417	0744	72 49.65	144 49.51	0.24	316			
0417	0856	72 49.76	144 49.75	0.20	327			
0417	1005	72 49.88	144 49.99	0.22	328			
0417	1108	72 49.96	144 50.36	0.24	306			
0417	1251	72 50.13	144 50.63	0.20	334			
0417	1459	72 50.23	144 51.02	0.13	310			
0417	1630	72 50.19	144 51.54	0.19	256			
0417	1810	72 50.13	144 52.09	0.19	249			
0417	1851	72 50.10	144 52.58	0.40	257			
0417	1927	72 50.08	144 53.00	0.40	260			
0417	2032	72 50.11	144 53.36	0.19	288			
0417	2104	72 50.13	144 53.74	0.40	279			
0417	2213	72 50.17	144 54.34	0.29	282			
0417	2326	72 50.27	144 55.01	0.34	296			
0418	0010	72 50.34	144 55.43	0.36	298			
0418	0159	72 50.41	144 55.93	0.17	295			
0418	0353	72 50.39	144 56.39	0.13	264			
0418	0748	72 50.35	144 56.84	0.07	251			
0418	0924	72 50.35	144 57.46	0.21	271			
0418	1055	72 50.42	144 57.87	0.17	301			
0418	1142	72 50.52	144 58.08	0.27	327			
0418	1439	72 50.62	144 58.53	0.10	307			
0418	1717	72 50.63	144 59.03	0.11	273			
0418	1951	72 50.59	144 59.73	0.15	258			
0418	2127	72 50.58	145 0.33	0.20	267			
0418	2222	72 50.62	145 0.85	0.32	282			
0418	2330	72 50.68	145 1.55	0.35	286			
0419	0052	72 50.75	145 2.30	0.32	288			
0419	0245	72 50.82	145 3.76	0.43	279			
0419	0434	72 50.90	145 5.34	0.48	279			
0419	0622	72 50.99	145 6.93	0.49	280			
0419	0809	72 51.08	145 8.74	0.56	279			
0419	0948	72 51.11	145 10.63	0.63	273			
0419	1110	72 51.14	145 12.37	0.69	273			
0419	1204	72 51.19	145 13.53	0.71	277			

Coordinated

Universal Date mmdd	Time hhmm	North dd mm.mm	West ddd mm.mm	Drift Speed km/hr	Drift true
0419	1250	72 51.22	145 14.56	0.74	275
0419	1354	72 51.26	145 15.94	0.71	275
0419	1444	72 51.30	145 16.95	0.67	277
0419	1531	72 51.37	145 17.77	0.60	286
0419	1621	72 51.42	145 18.74	0.64	280
0419	1710	72 51.49	145 19.67	0.64	284
0419	1803	72 51.56	145 20.66	0.63	283
0419	1838	72 51.64	145 21.32	0.67	291
0419	1912	72 51.68	145 22.12	0.77	279
0419	1944	72 51.75	145 22.74	0.67	290
0419	2012	72 51.82	145 23.25	0.67	295
0419	2051	72 51.89	145 23.93	0.61	289
0419	2138	72 52.01	145 24.64	0.57	299
0419	2225	72 52.12	145 25.24	0.48	302
0419	2316	72 52.26	145 25.72	0.44	315
0420	0006	72 52.37	145 26.26	0.44	304
0420	0118	72 52.52	145 26.66	0.30	322
0420	0219	72 52.66	145 26.77	0.26	347
0420	0417	72 52.86	145 26.50	0.20	022
0420	0528	72 52.95	145 26.21	0.19	044
0420	0638	72 53.03	145 25.93	0.19	044
0420	0835	72 53.14	145 25.76	0.11	025
0420	1123	72 53.26	145 25.93	0.09	338
0420	1259	72 53.36	145 26.18	0.14	322
0420	1444	72 53.45	145 26.48	0.13	315
0420	1641	72 53.54	145 26.74	0.11	319
0420	1817	72 53.62	145 27.06	0.14	310
0420	2043	72 53.73	145 28.33	0.30	286
0420	2235	72 53.82	145 29.40	0.33	286
0421	0025	72 53.91	145 30.51	0.34	284
0421	0224	72 53.98	145 31.67	0.33	281
0421	0424	72 54.04	145 32.96	0.35	278
0421	0631	72 54.11	145 34.23	0.33	280
0421	0714	72 54.09	145 34.66	0.32	262
0421	0852	72 54.07	145 35.53	0.29	265
0421	1007	72 54.02	145 35.98	0.21	250
0421	1126	72 54.01	145 36.55	0.24	266
0421	1208	72 53.98	145 36.90	0.29	250
0421	1344	72 53.95	145 37.63	0.25	263
0421	1440	72 53.87	145 38.14	0.35	239
0421	1543	72 53.75	145 38.67	0.34	233
0421	1641	72 53.64	145 39.20	0.36	236
0421	1747	72 53.54	145 39.75	0.33	236
0421	1846	72 53.44	145 40.23	0.32	235
0421	1939	72 53.33	145 40.80	0.42	235
0421	2041	72 53.23	145 41.36	0.35	238
0421	2132	72 53.11	145 41.81	0.38	228
0421	2224	72 53.13	145 42.42	0.39	275
0421	2305	72 53.16	145 42.92	0.41	283
0421	2347	72 53.03	145 43.50	0.56	232
0422	0029	72 52.91	145 43.82	0.40	218

Coordinated							
Universal Time		North		West		Drift	Drift
Date	Time	Latitude		Longitude		Speed	Dir
mmdd	hhmm	dd mm.mm	ddd	mm.mm		km/hr	true
0422	0057	72 52.85	145	44.14	0.46	234	
0422	0150	72 52.63	145	44.55	0.53	208	
0422	0224	72 52.42	145	44.77	0.70	197	
0422	0301	72 52.34	145	45.11	0.38	231	
0422	0343	72 52.25	145	45.51	0.39	233	
0422	0422	72 52.15	145	45.84	0.41	223	
0422	0505	72 52.00	145	46.14	0.45	210	
0422	0548	72 51.86	145	46.46	0.44	214	
0422	0627	72 51.71	145	46.72	0.47	207	
0422	0707	72 51.60	145	46.95	0.37	210	
0422	0832	72 51.41	145	47.31	0.29	208	
0422	0918	72 51.29	145	47.63	0.37	218	
0422	1006	72 51.20	145	47.91	0.27	225	
0422	1058	72 51.10	145	48.13	0.26	213	
0422	1159	72 50.96	145	48.35	0.28	204	
0422	1252	72 50.82	145	48.56	0.32	203	
0422	1341	72 50.70	145	48.67	0.28	194	
0422	1511	72 50.53	145	48.79	0.21	192	
0422	1620	72 50.41	145	48.84	0.20	186	
0422	1732	72 50.26	145	48.96	0.23	193	
0422	1845	72 50.10	145	48.88	0.25	172	
0422	1944	72 49.95	145	49.09	0.31	202	
0422	2050	72 49.86	145	49.40	0.22	223	
0422	2153	72 49.73	145	49.65	0.25	210	
0422	2302	72 49.62	145	49.87	0.21	210	
0423	0020	72 49.52	145	50.27	0.23	228	
0423	0150	72 49.37	145	50.77	0.26	224	
0423	0304	72 49.28	145	51.04	0.17	223	
0423	0520	72 49.13	145	51.45	0.16	217	
0423	0720	72 48.98	145	51.86	0.17	219	
0423	0856	72 48.91	145	52.18	0.14	232	
0423	1707	72 48.81	145	51.89	0.03	136	
0423	2321	72 48.68	145	51.71	0.04	158	
0424	0726	72 48.63	145	51.37	0.03	119	
0424	1157	72 48.52	145	51.25	0.05	162	
0424	1529	72 48.46	145	51.93	0.11	254	
0424	1727	72 48.47	145	52.44	0.14	273	
0424	1915	72 48.44	145	53.03	0.19	257	
0424	2003	72 48.41	145	53.43	0.28	256	
0424	2143	72 48.42	145	54.08	0.22	275	
0424	2224	72 48.44	145	54.51	0.35	278	
0424	2310	72 48.51	145	54.99	0.38	294	
0424	2351	72 48.55	145	55.41	0.36	290	
0425	0028	72 48.59	145	55.95	0.48	281	
0425	0105	72 48.64	145	56.37	0.41	295	
0425	0146	72 48.69	145	56.87	0.42	288	
0425	0233	72 48.76	145	57.47	0.45	291	
0425	0318	72 48.80	145	58.05	0.44	282	
0425	0407	72 48.85	145	58.71	0.45	283	
0425	0457	72 48.94	145	59.19	0.38	302	

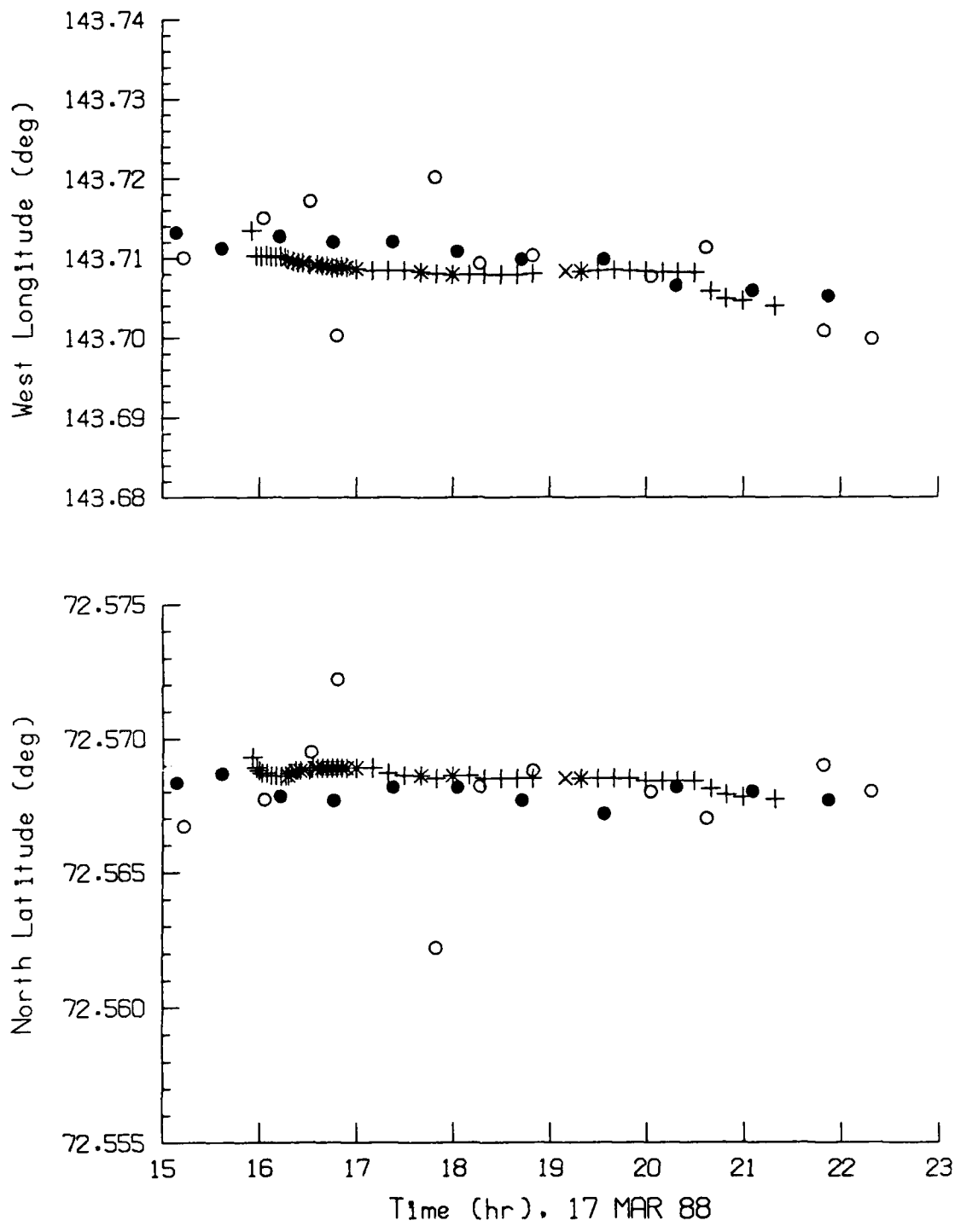
Coordinated

	Universal Time	North	West	Drift	Drift		
	Date	Time	Latitude	Longitude	Speed	Dir	
	mmdd	hhmm	dd mm.mm	ddd mm.mm	km/hr	true	
0425	0542	72	48.98	145	59.72	0.40	285
0425	0626	72	49.04	146	0.29	0.45	291
0425	0708	72	49.09	146	0.71	0.36	288
0425	0745	72	49.15	146	1.15	0.44	297
0425	0824	72	49.21	146	1.68	0.47	291
0425	0904	72	49.26	146	2.26	0.48	284
0425	0950	72	49.29	146	2.97	0.52	278
0425	1034	72	49.33	146	3.63	0.50	281
0425	1115	72	49.36	146	4.31	0.55	277
0425	1202	72	49.34	146	5.12	0.57	266
0425	1237	72	49.36	146	5.74	0.58	274
0425	1321	72	49.39	146	6.46	0.54	278
0425	1407	72	49.43	146	7.29	0.60	280
0425	1507	72	49.45	146	8.32	0.57	274
0425	1605	72	49.46	146	9.39	0.61	271
0425	1700	72	49.53	146	10.38	0.60	282
0425	1800	72	49.55	146	11.48	0.60	274
0425	1850	72	49.58	146	12.48	0.67	276
0425	1933	72	49.61	146	13.26	0.61	275
0425	2008	72	49.64	146	14.08	0.76	277
0425	2047	72	49.68	146	14.90	0.71	280
0425	2120	72	49.73	146	15.65	0.77	282
0425	2156	72	49.81	146	16.27	0.62	293

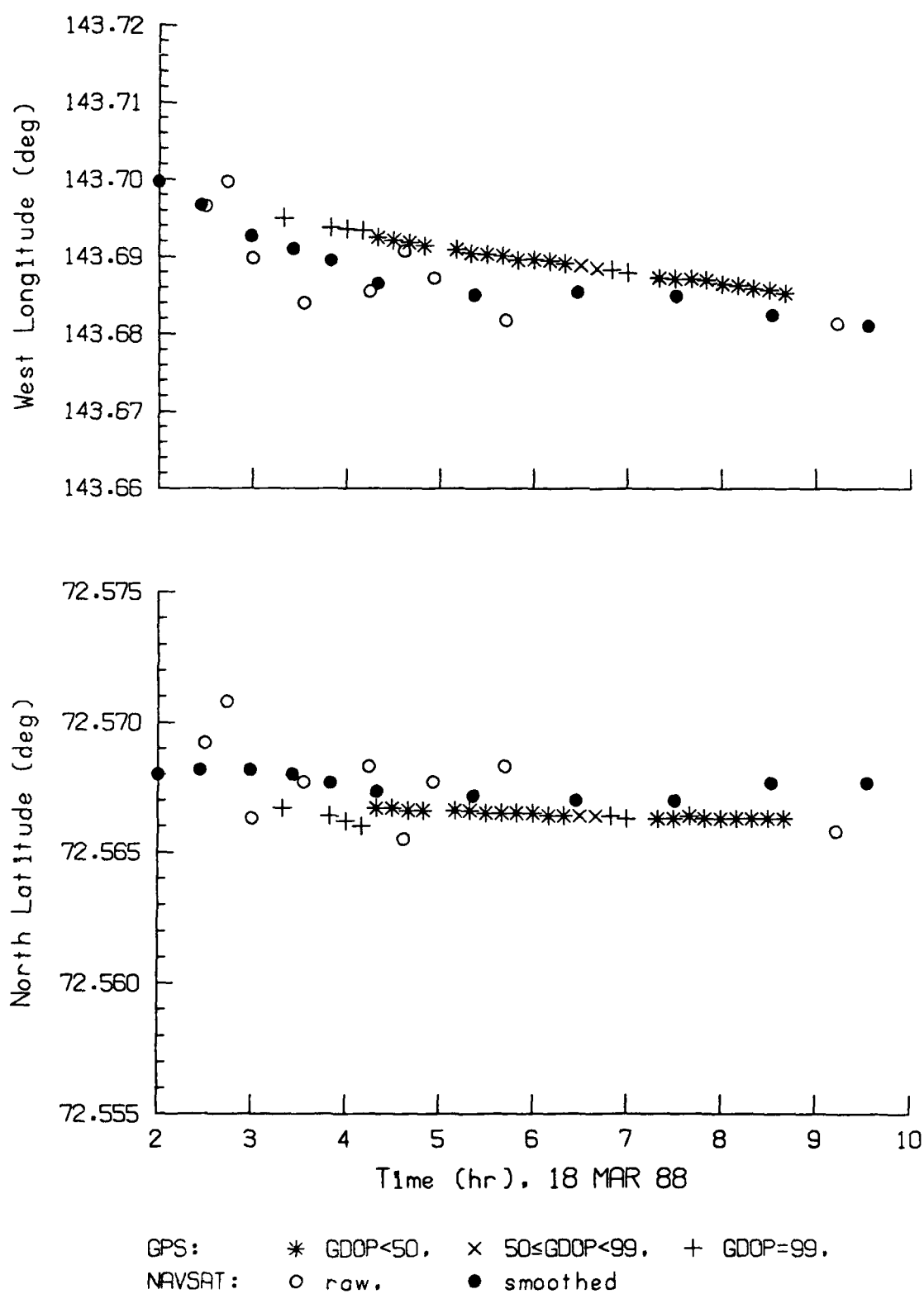
APPENDIX B

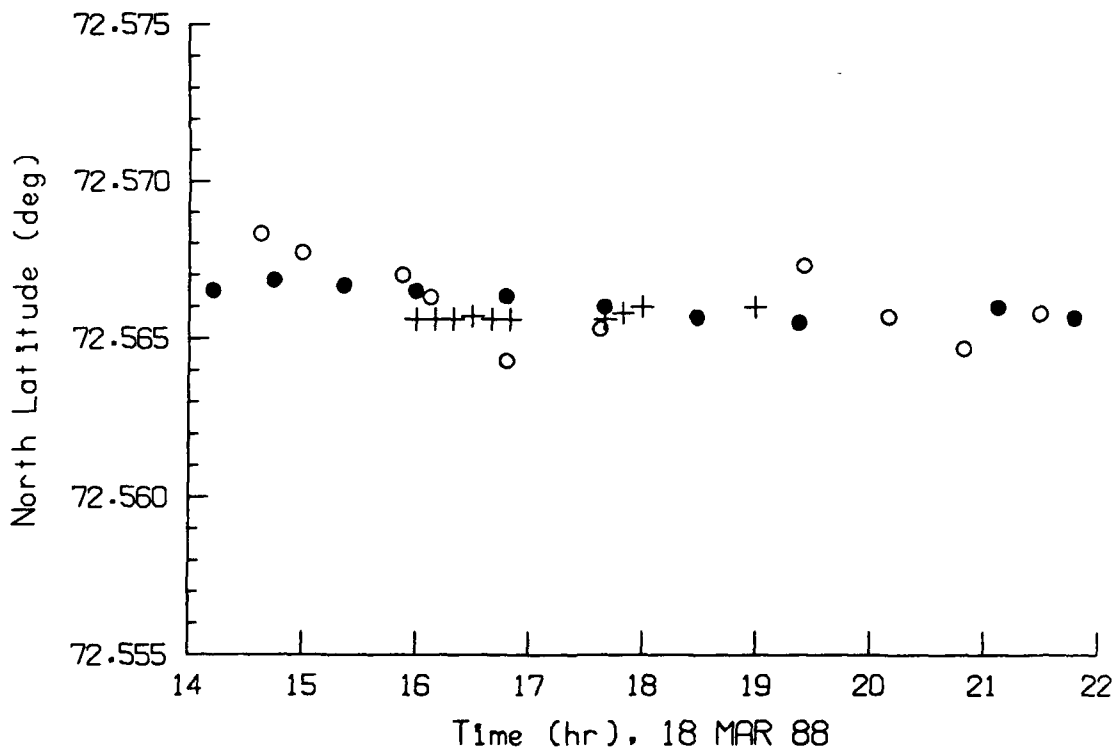
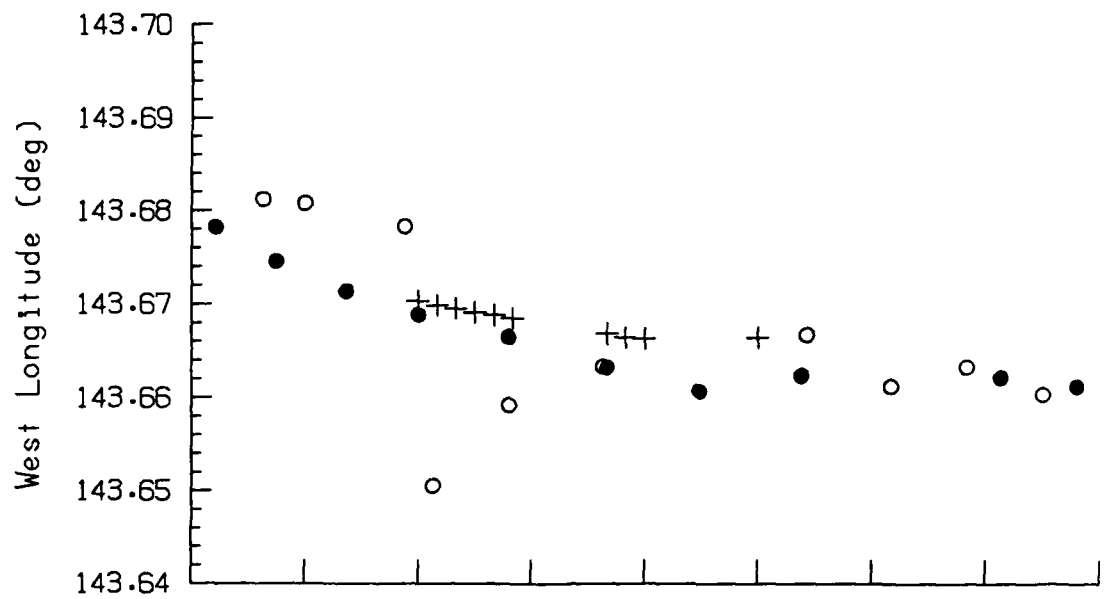
Comparison of NAVSAT and GPS Fixes at Various Time Periods

Times are given in UTC. To obtain local time, subtract 9 hours for days up to and including 2 April, and 8 hours afterward. For GPS, the geometrical dilution of precision (GDOP) is a measure of the accuracy.

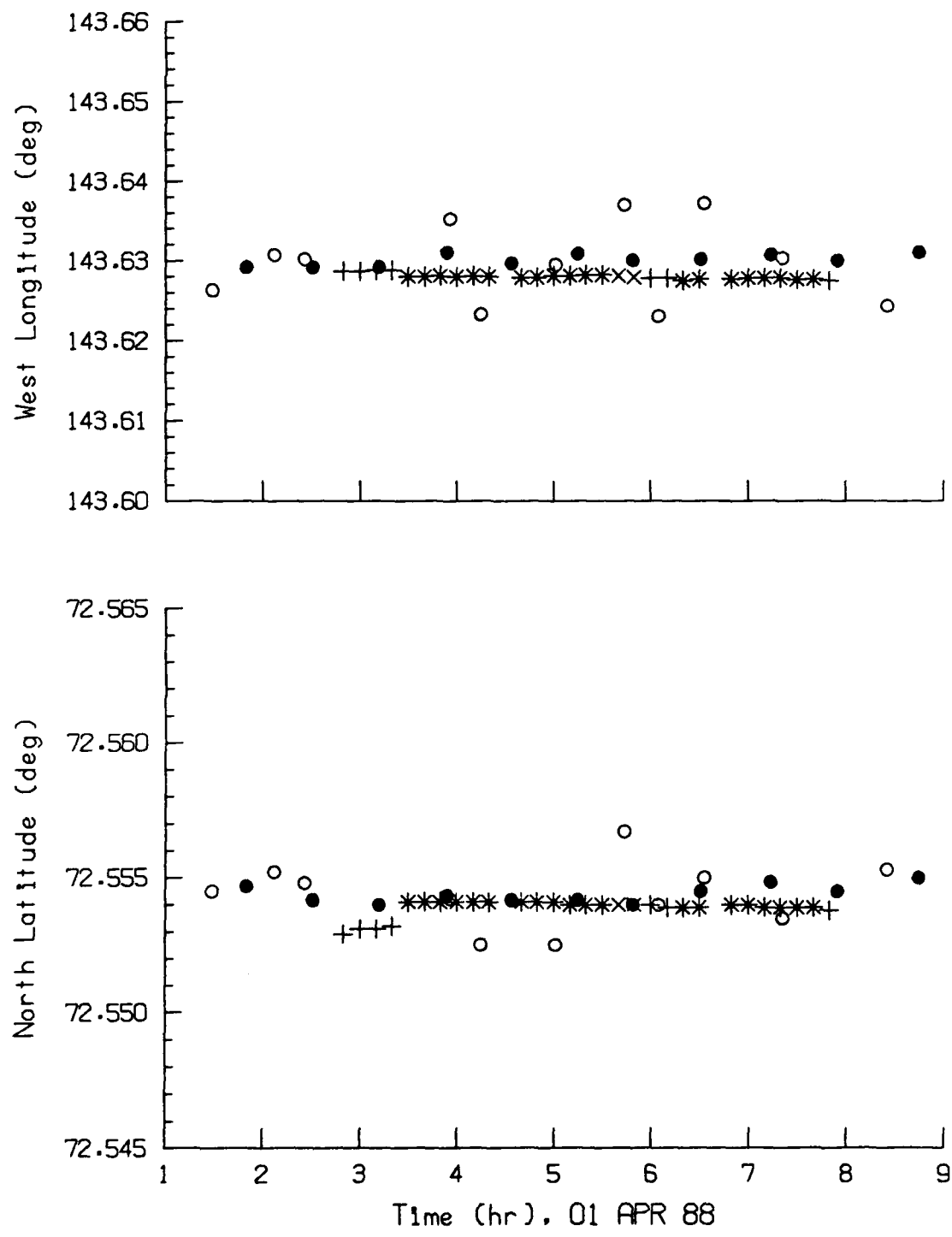


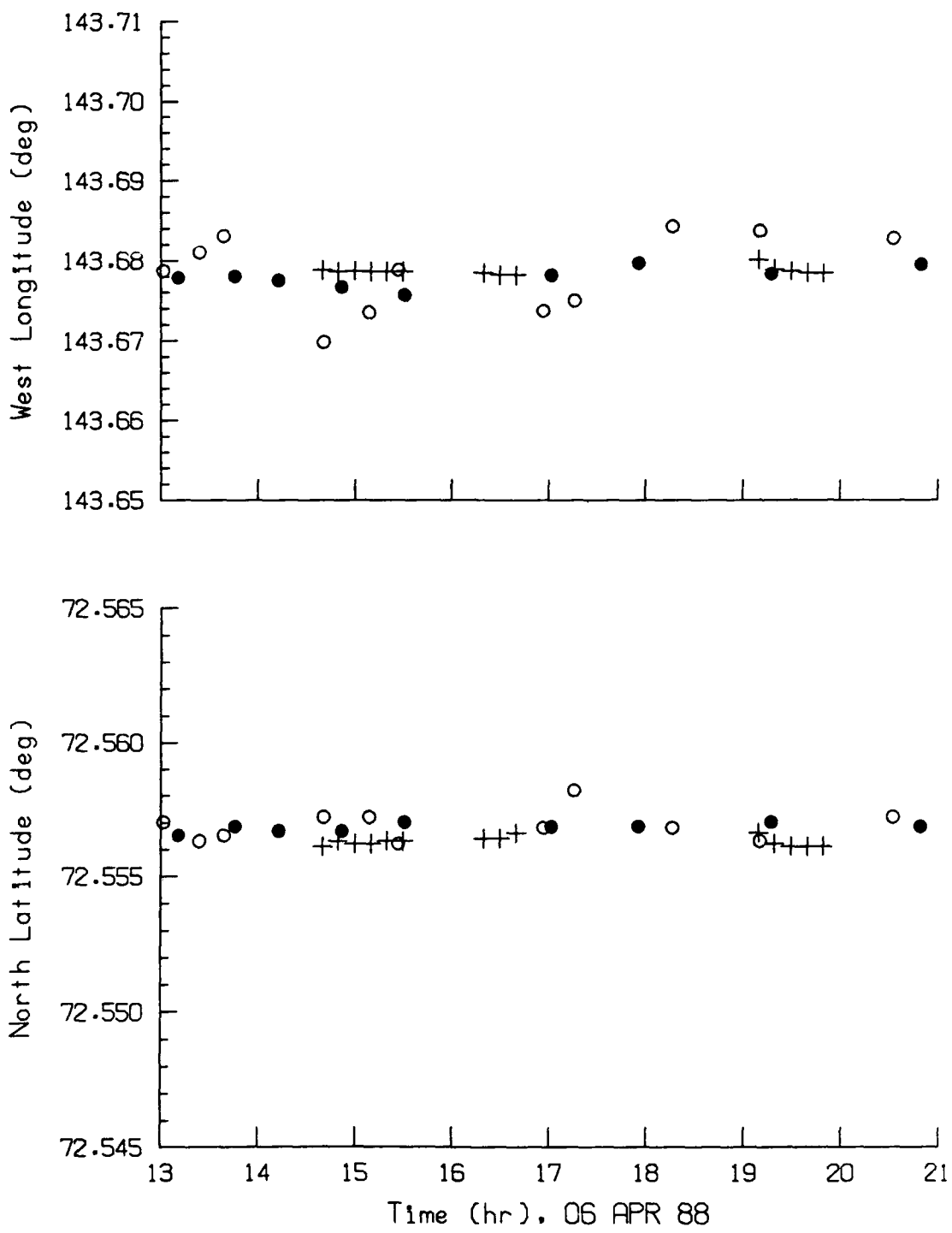
GPS: * $\text{GDOP} < 50$, $\times 50 \leq \text{GDOP} < 99$, + $\text{GDOP} \geq 99$.
 NAVSAT: ○ raw, ● smoothed



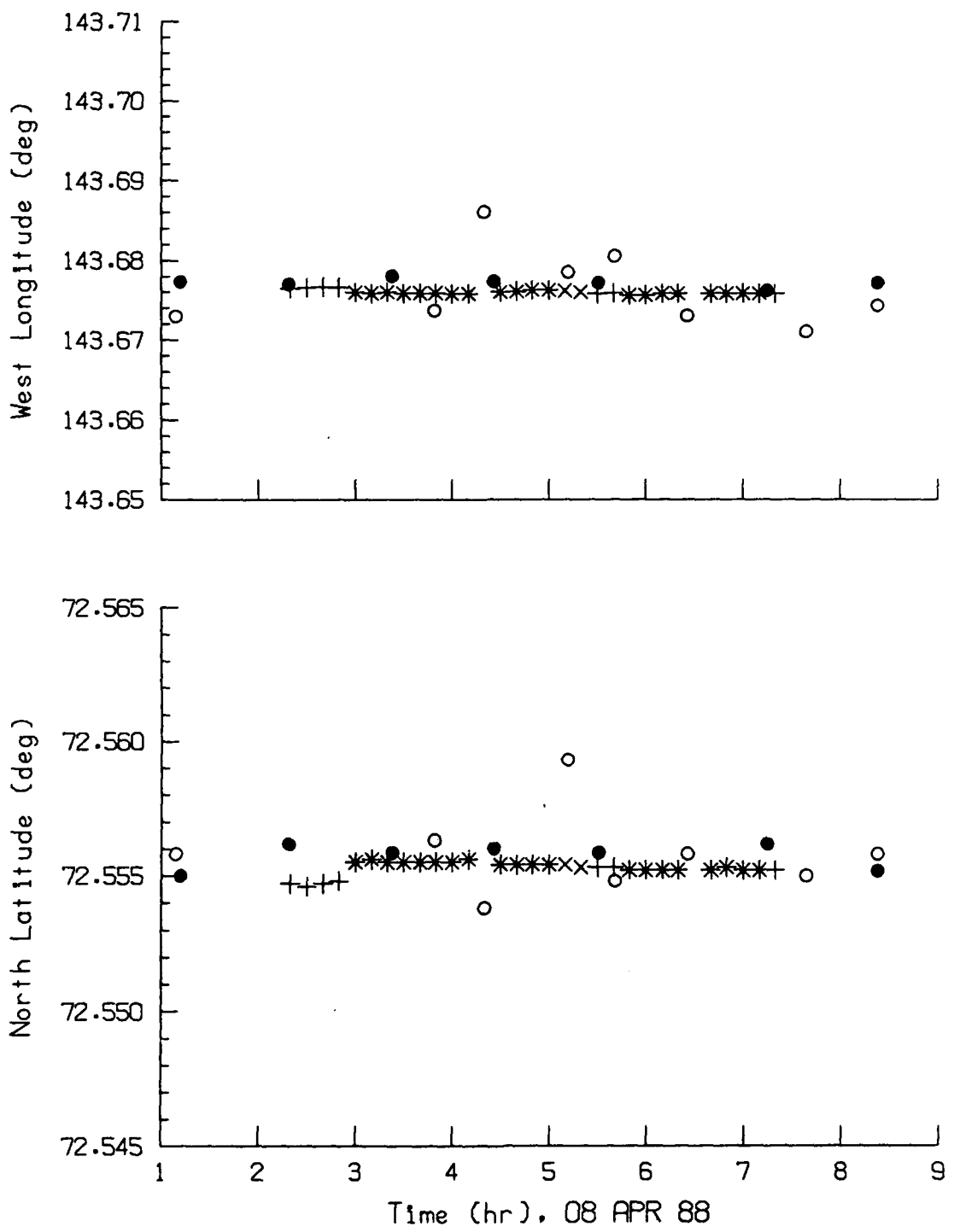


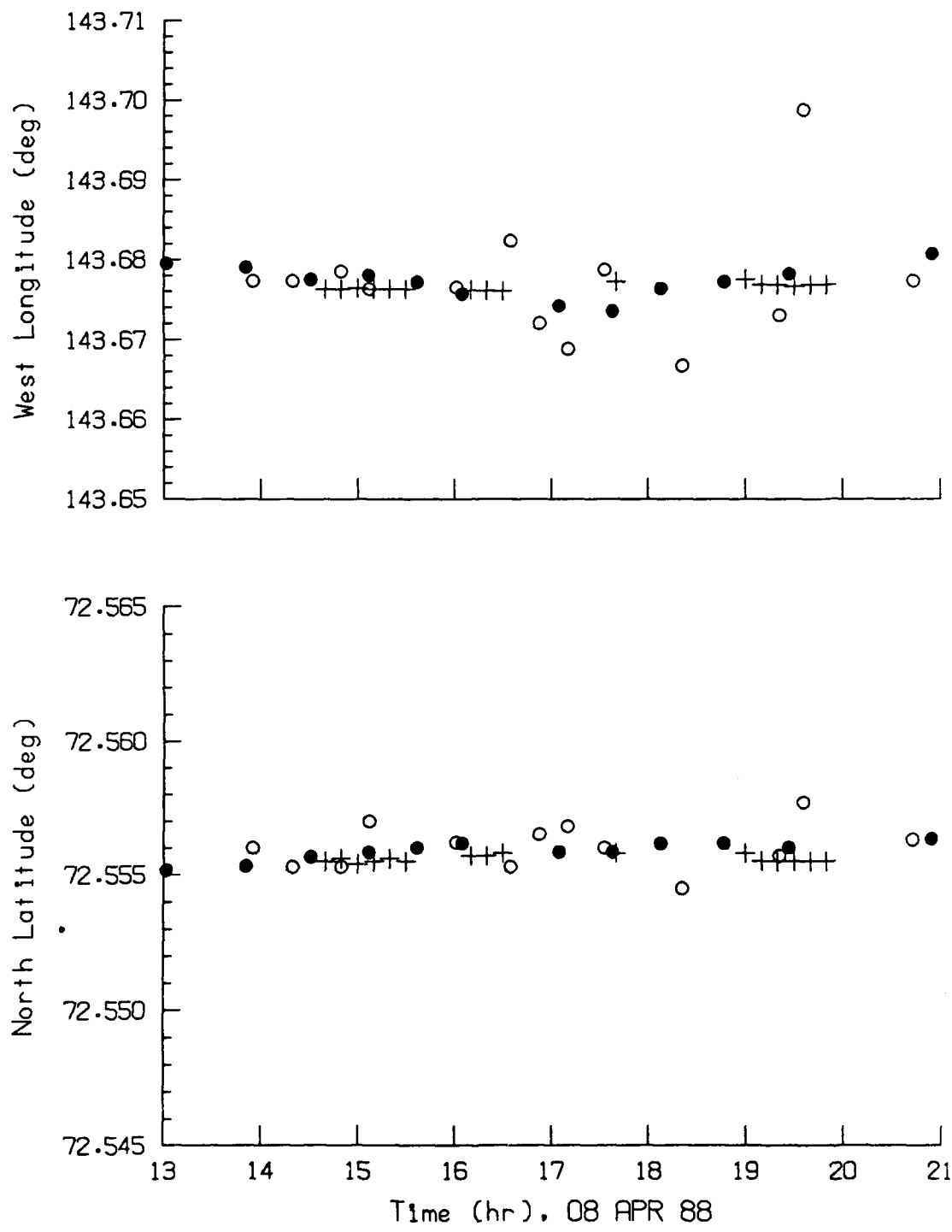
GPS: * GDOP<50, X 50≤GDOP<99, + GDOP=99,
 NAVSAT: ○ raw, ● smoothed



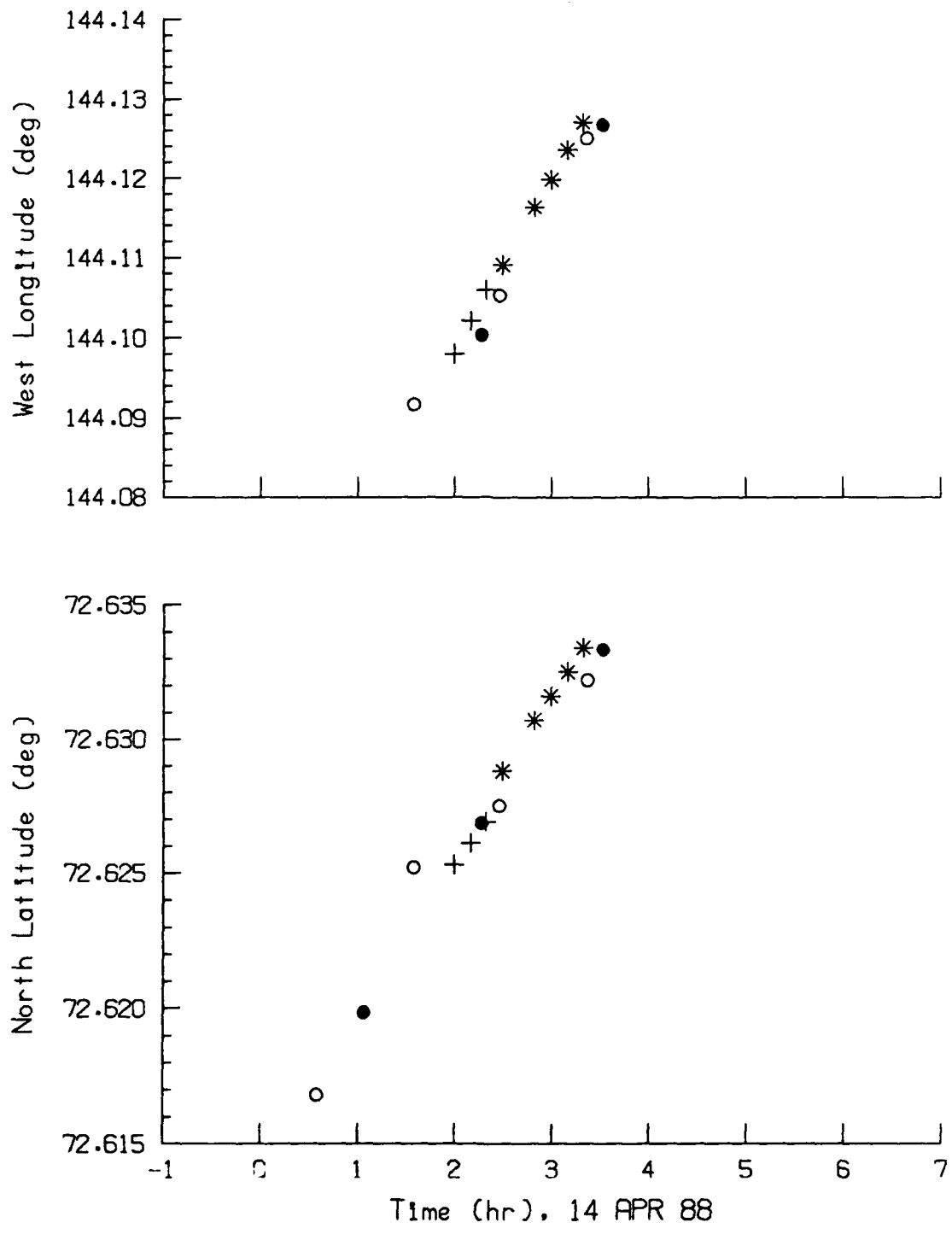


GPS: * GDOP<50, x 50≤GDOP<99, + GDOP=99.
 NAVSAT: o raw, ● smoothed

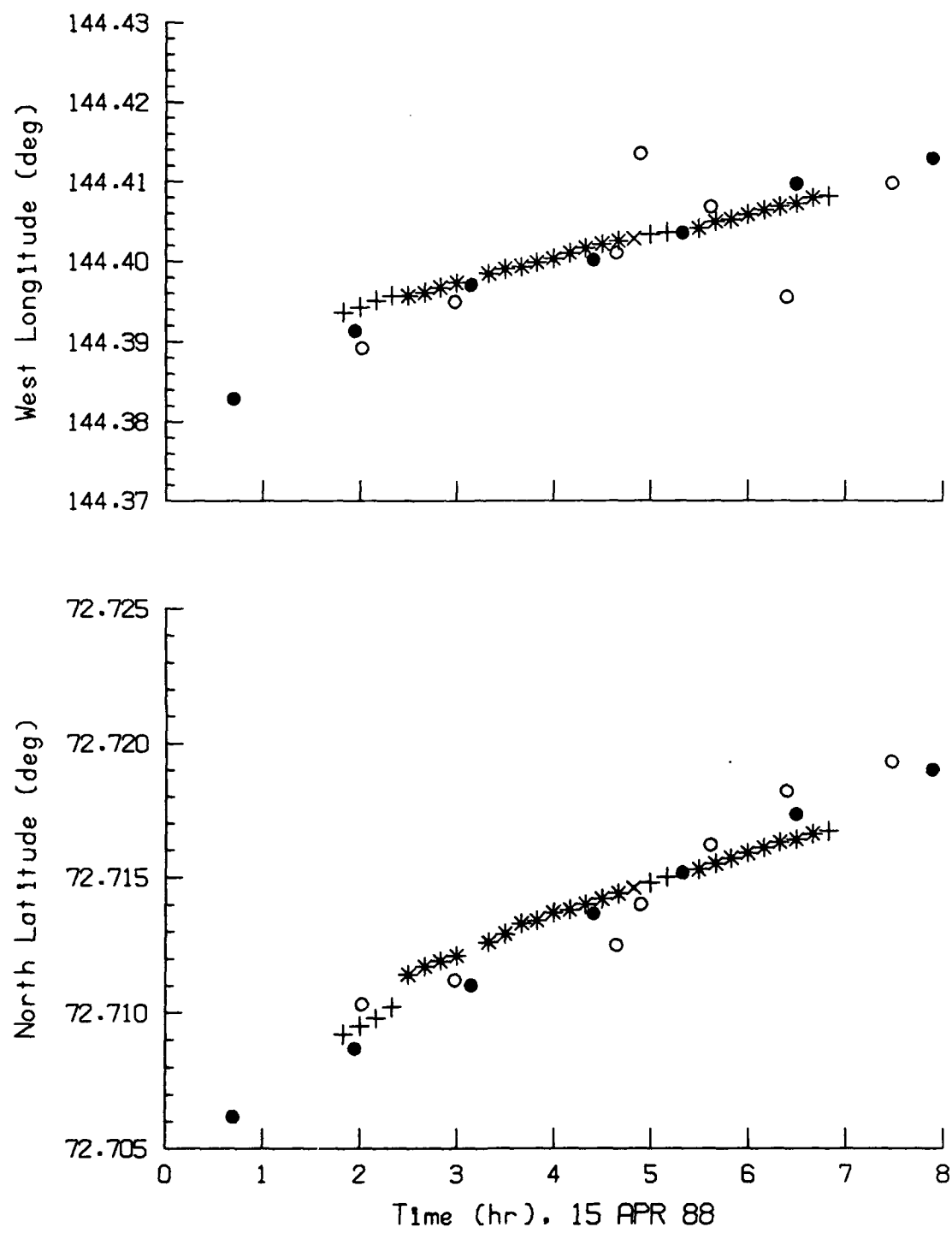




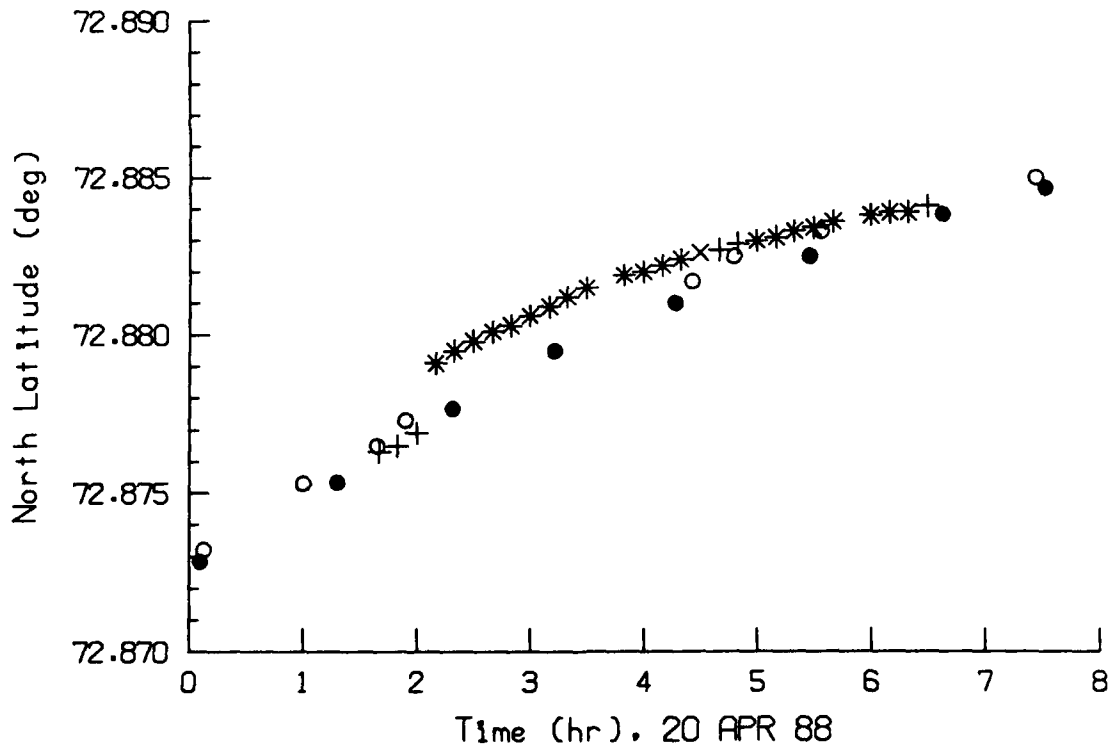
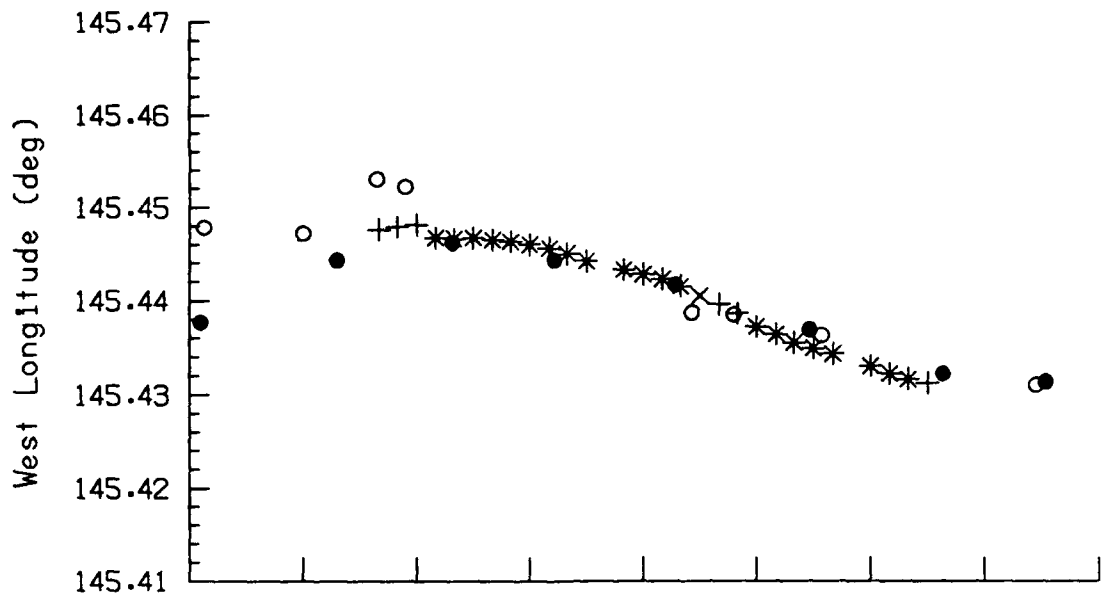
GPS: * GDOP<50. x 50≤GDOP<99. + GDOP=99.
 NAVSAT: ○ raw, ● smoothed



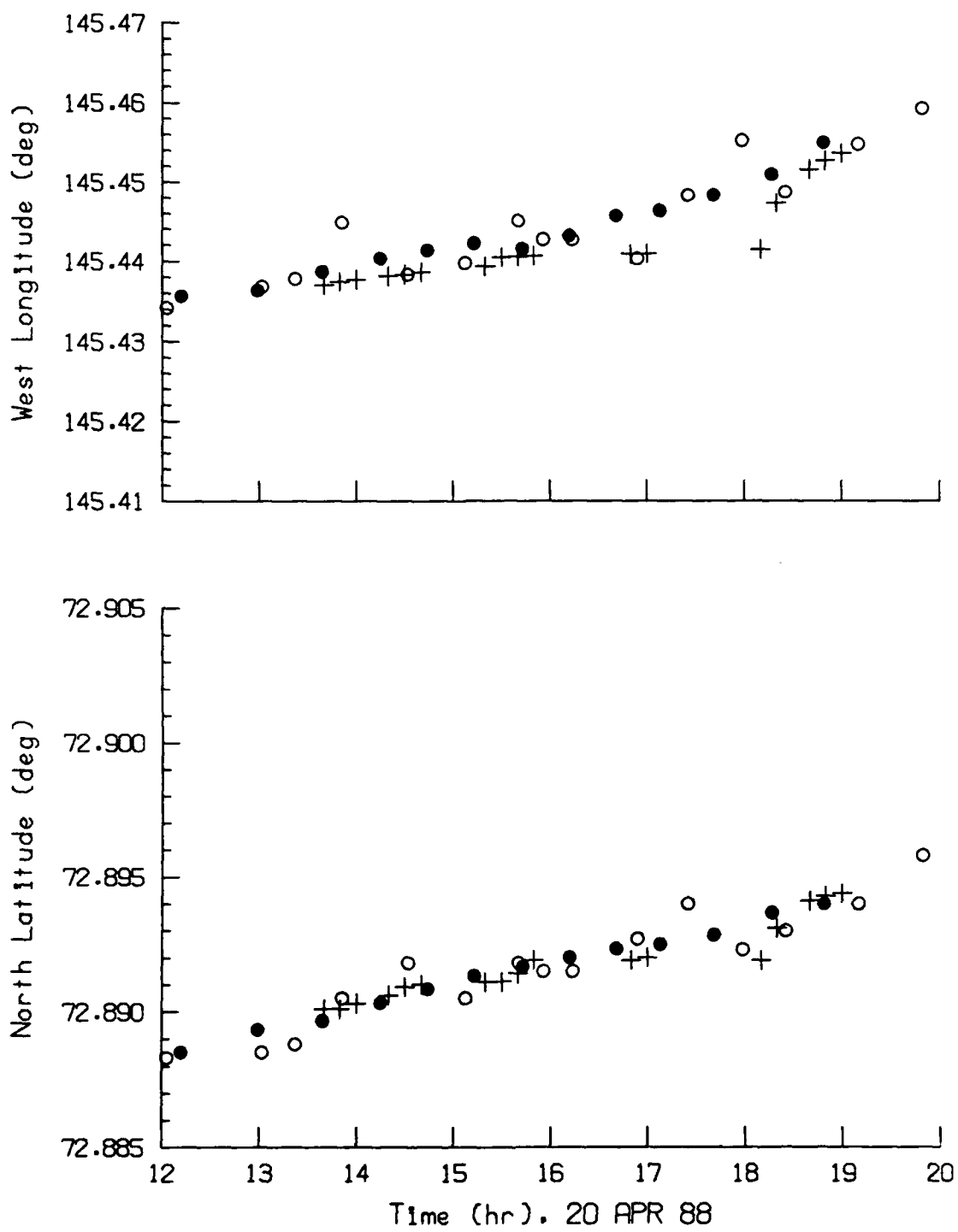
GPS: * GDOP<50. X 50≤GDOP<99. + GDOP=99.
 NAVSAT: ○ raw. ● smoothed



TR 8822 B-9



GPS: * GDOP<50, × 50≤GDOP<99, + GDOP=99.
NAVSAT: ○ raw, ● smoothed



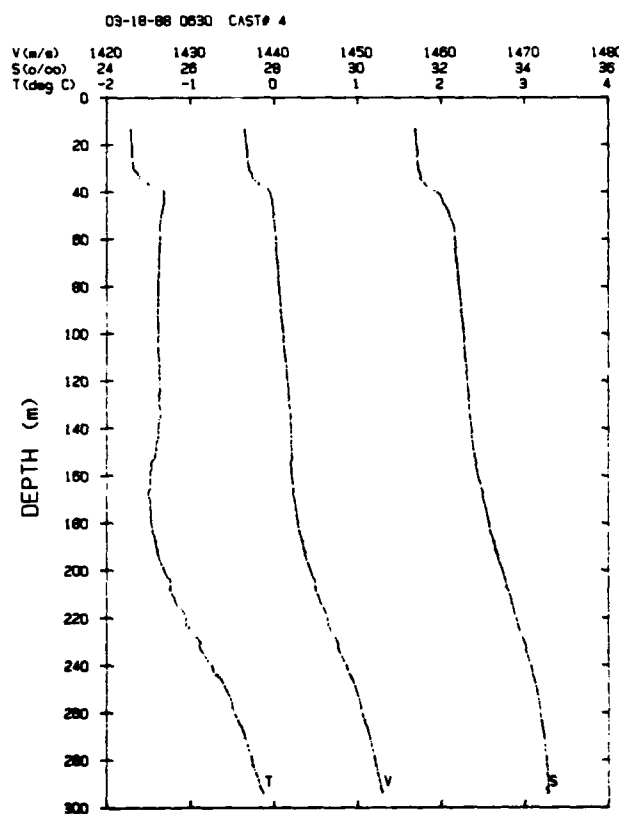
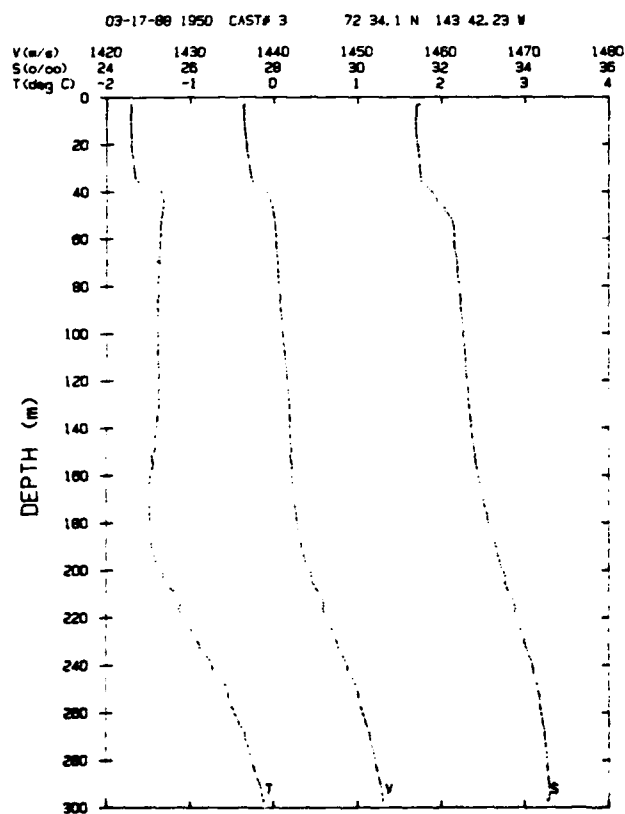
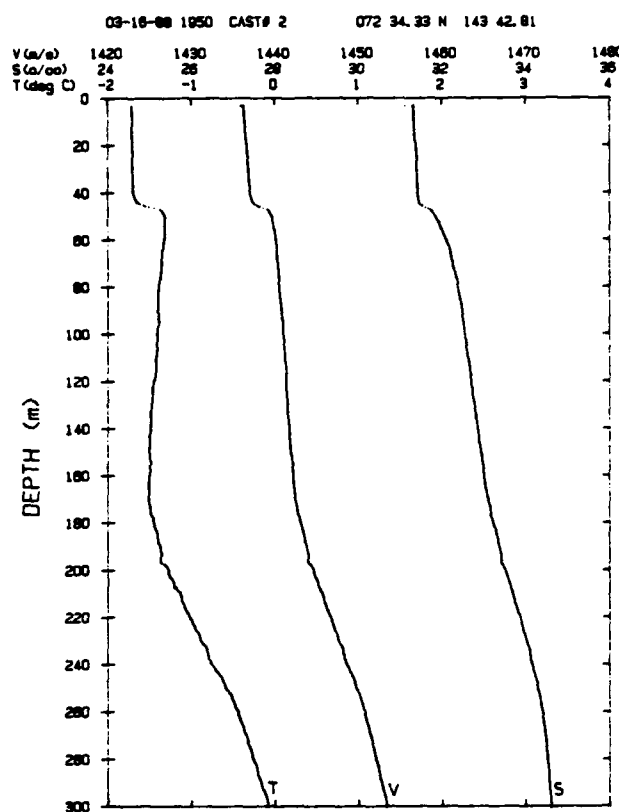
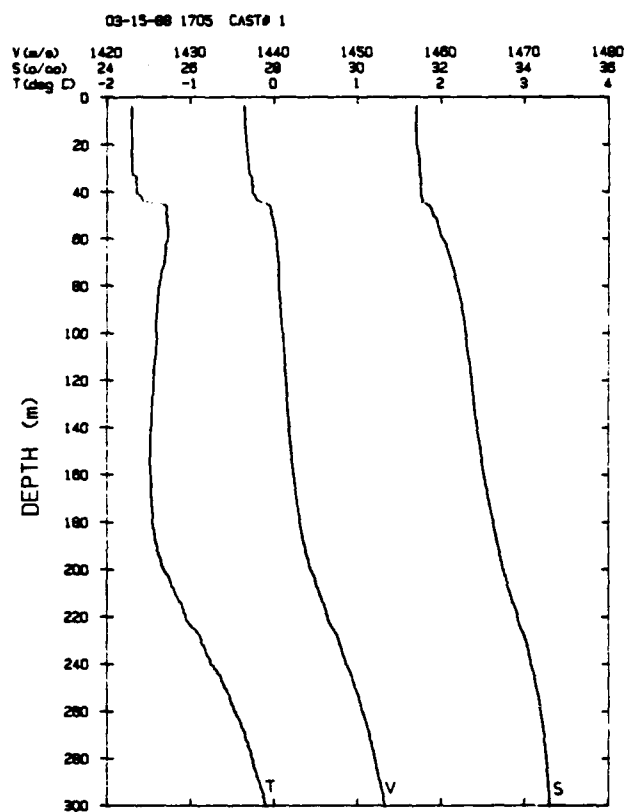
GPS: * $\text{GDOP} < 50$, $\times 50 \leq \text{GDOP} < 99$, + $\text{GDOP} = 99$.
 NAVSAT: ○ raw, ● smoothed

APPENDIX C

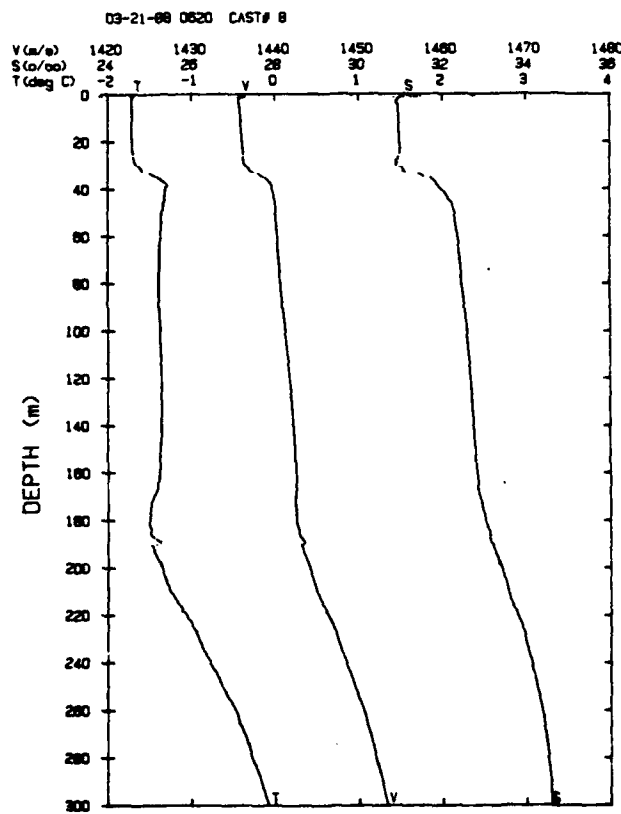
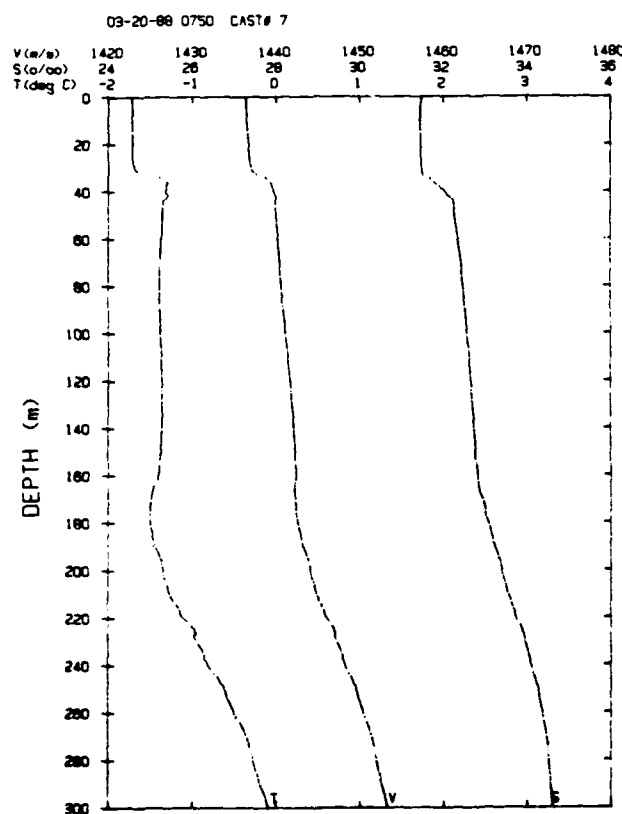
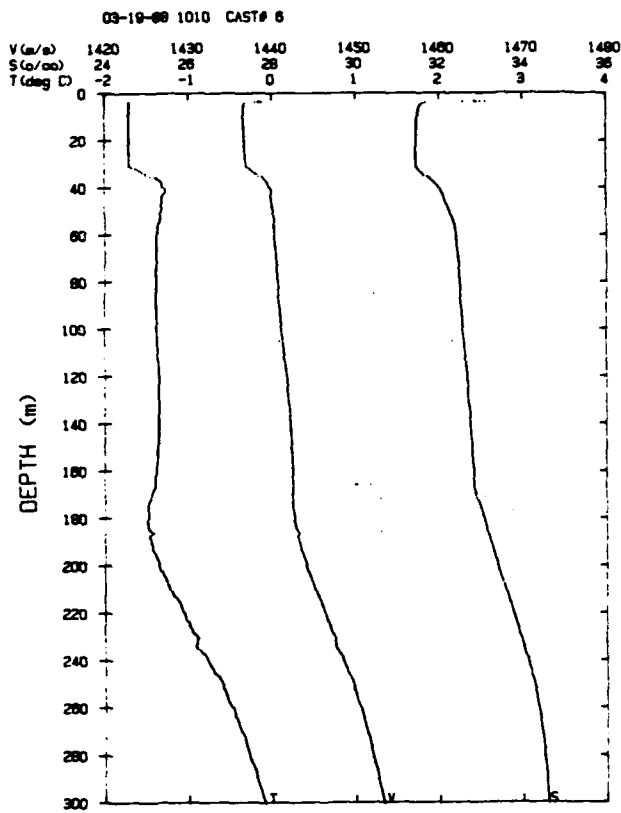
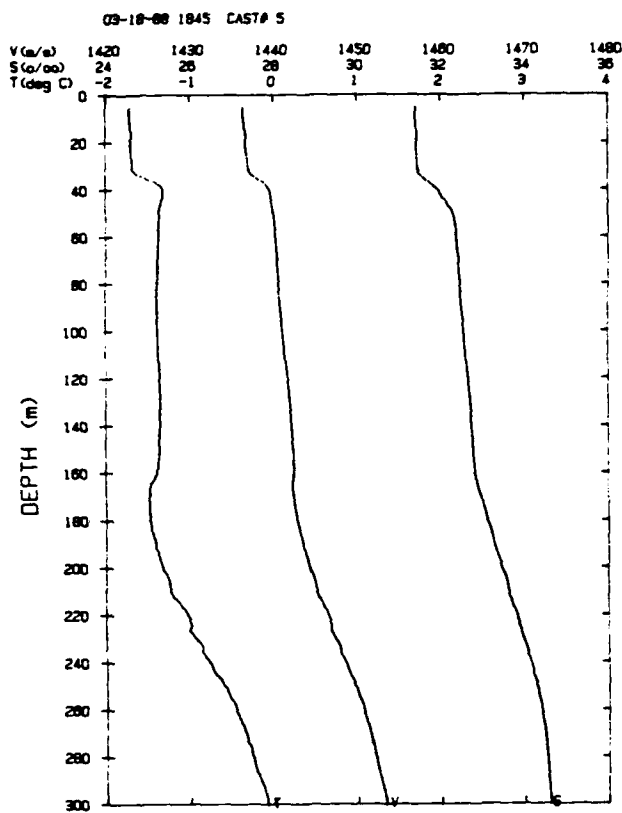
CTD Profiles at APLIS 88

All times are local.

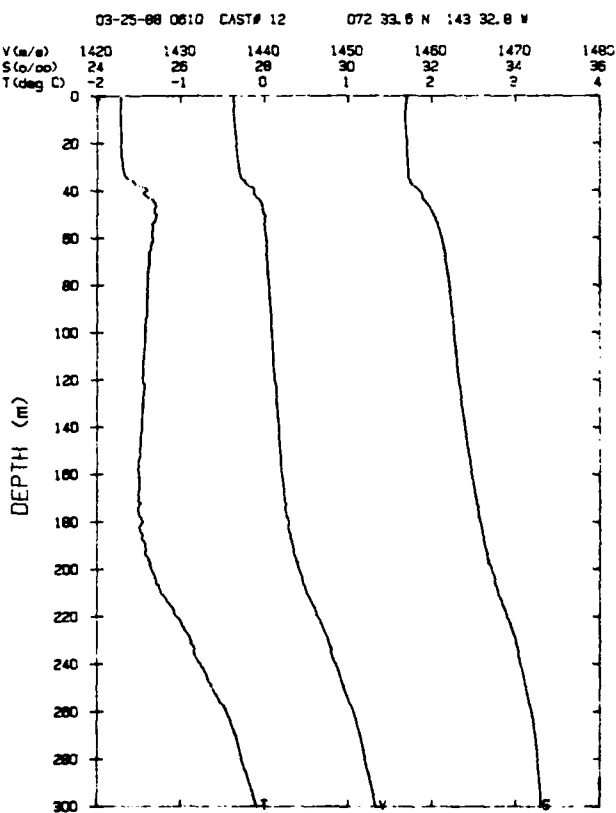
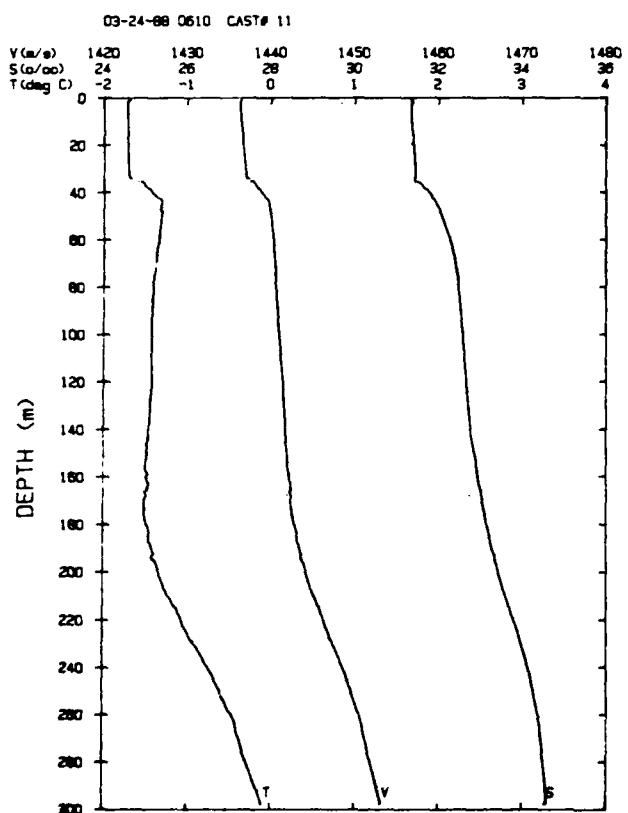
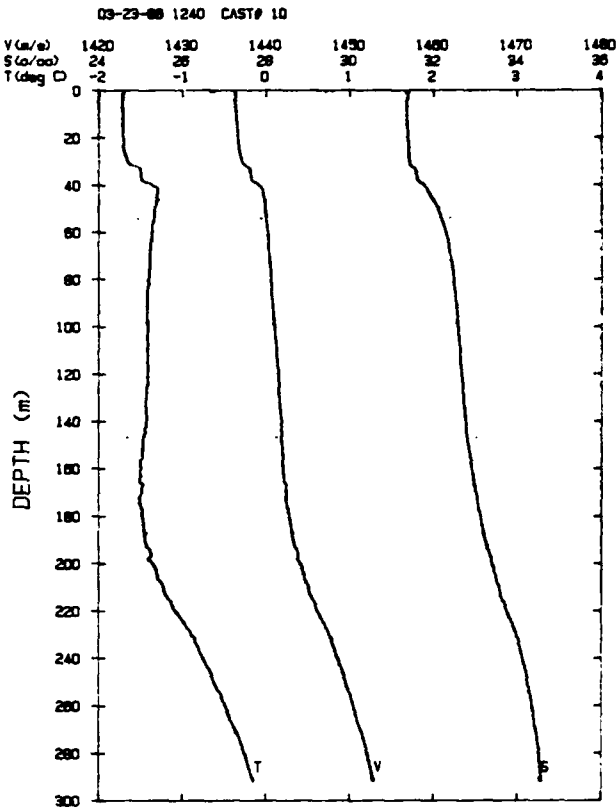
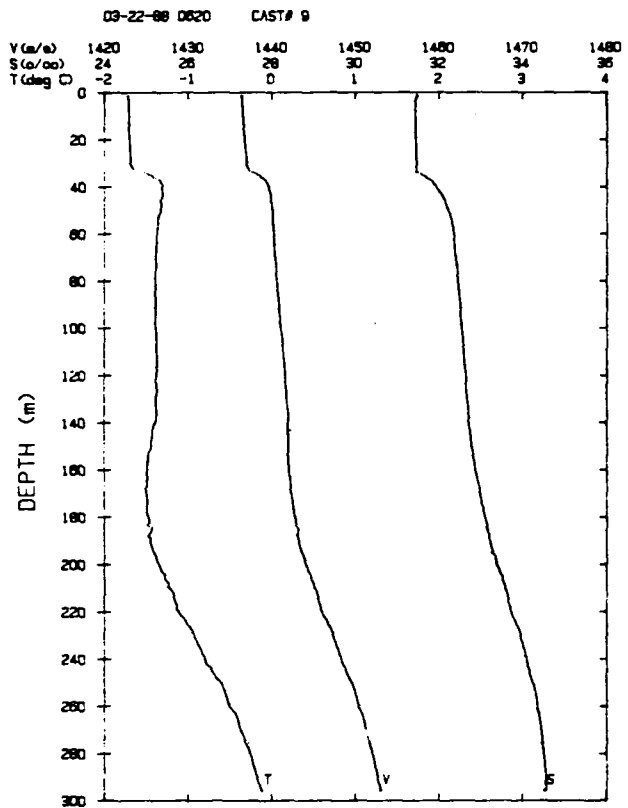
S = salinity
T = temperature
V = sound speed

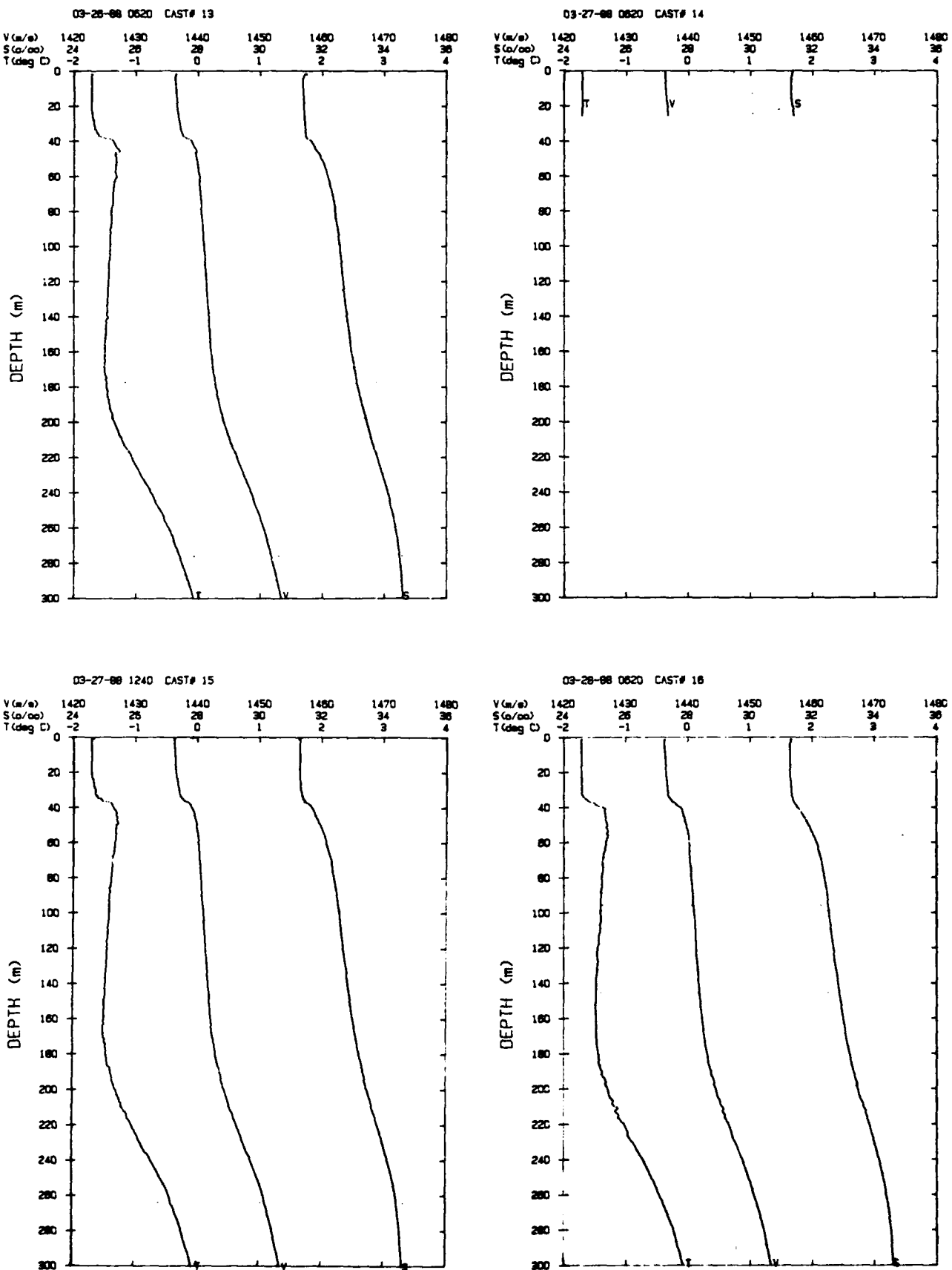


TR 8822 C-1

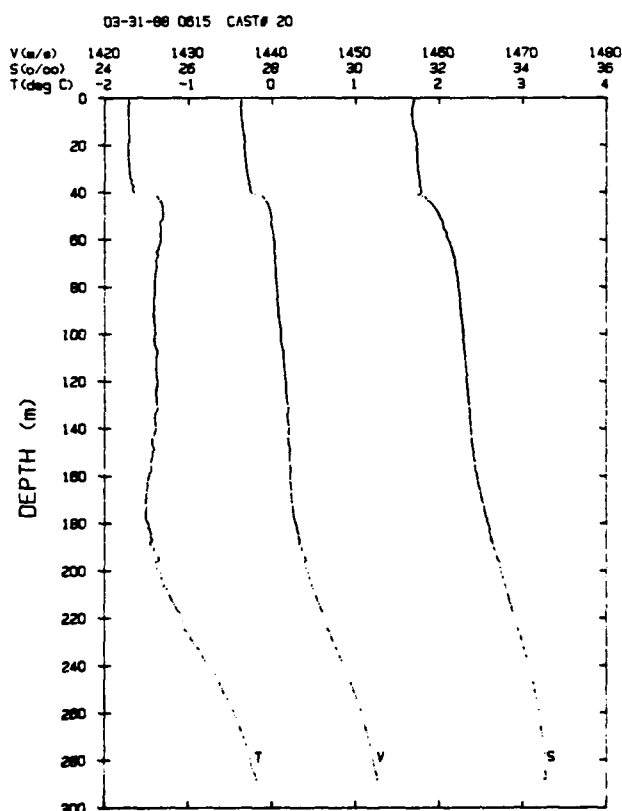
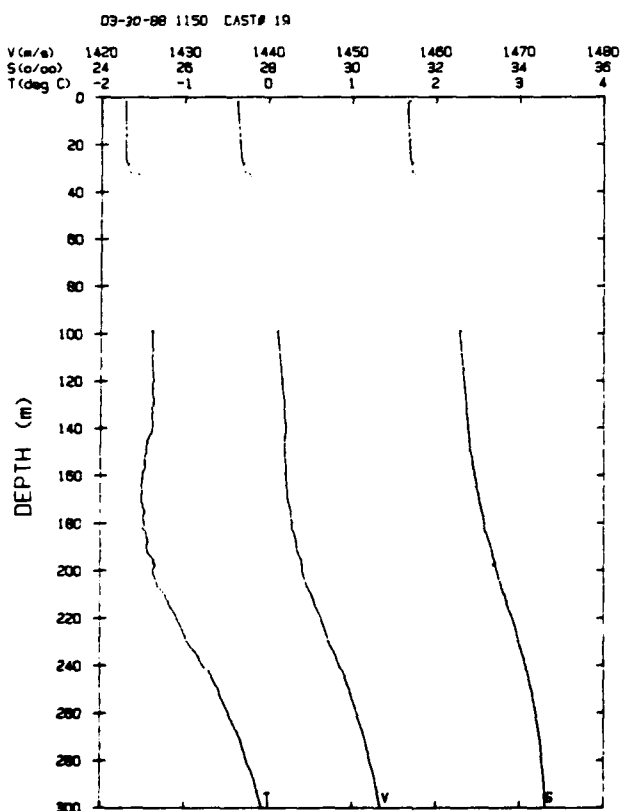
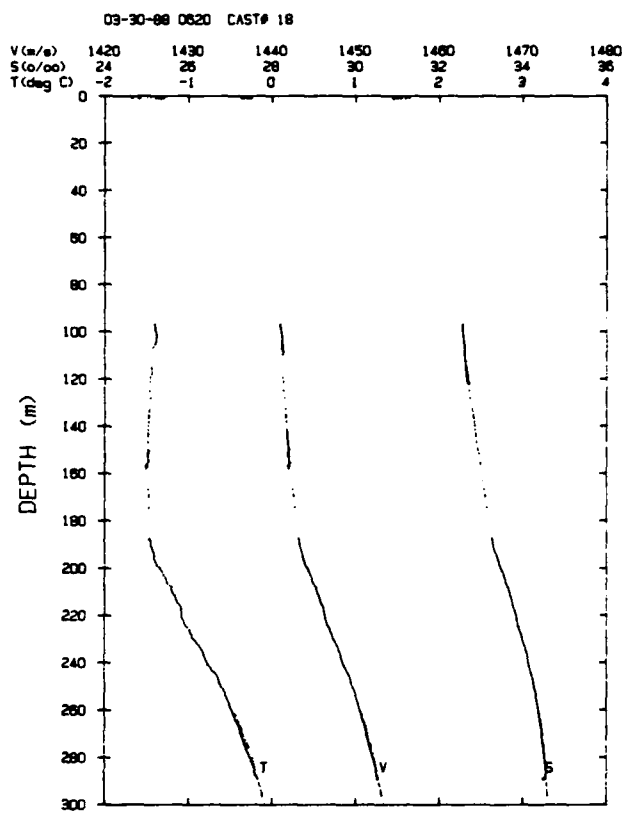
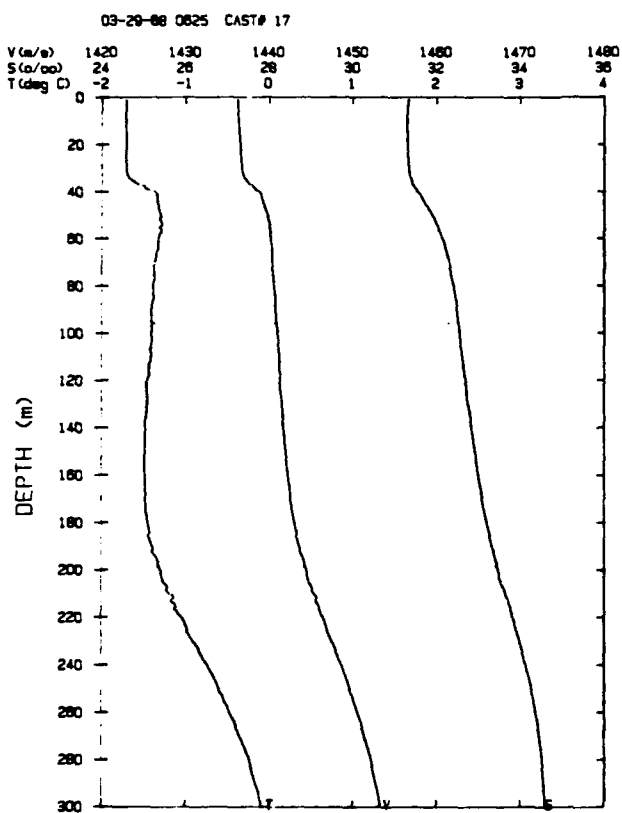


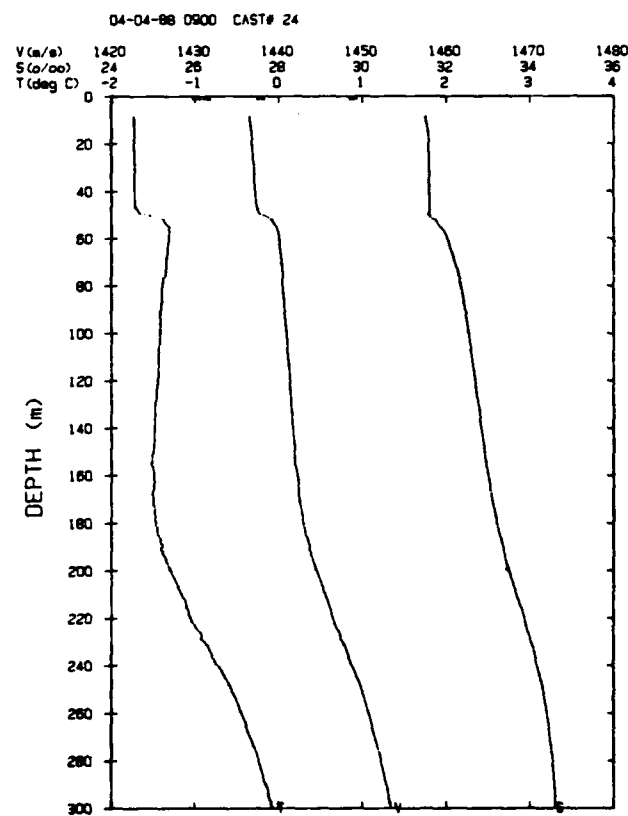
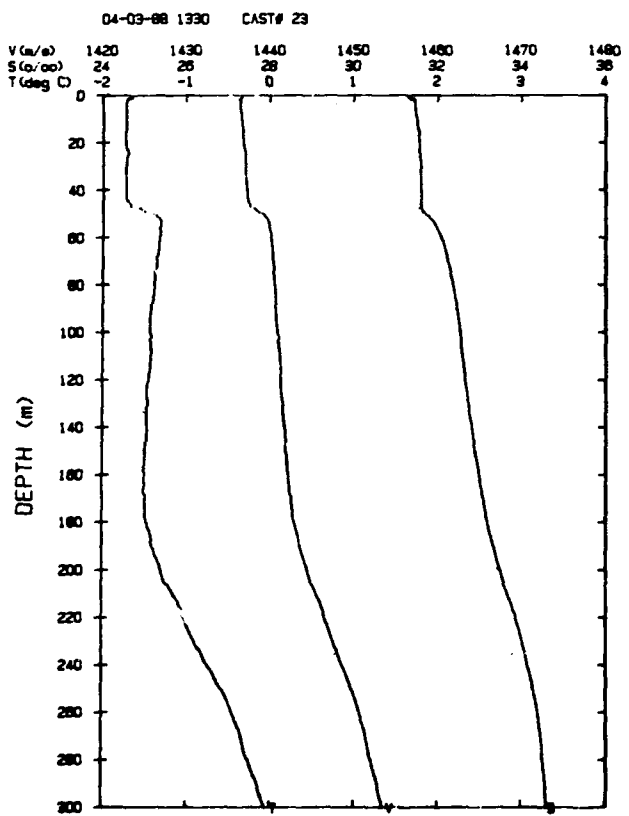
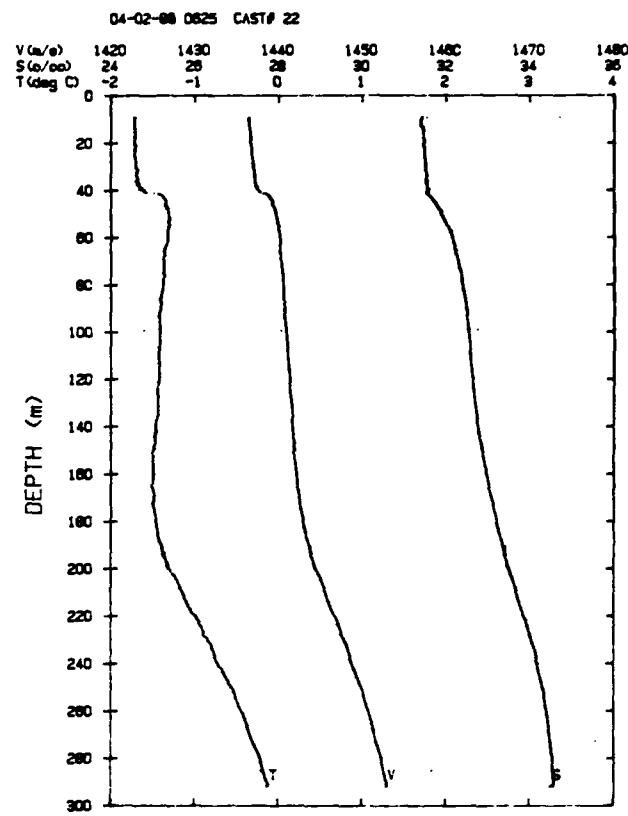
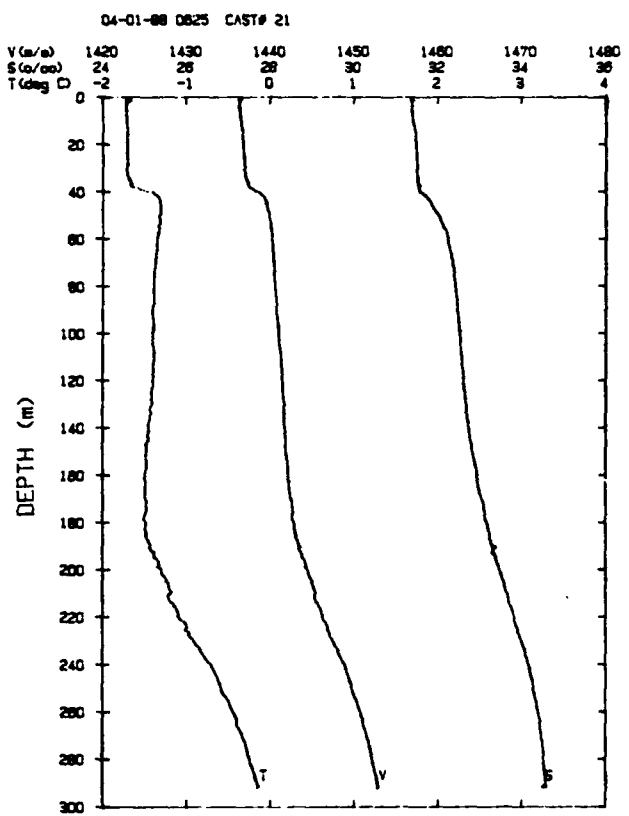
C-2 TR 8822

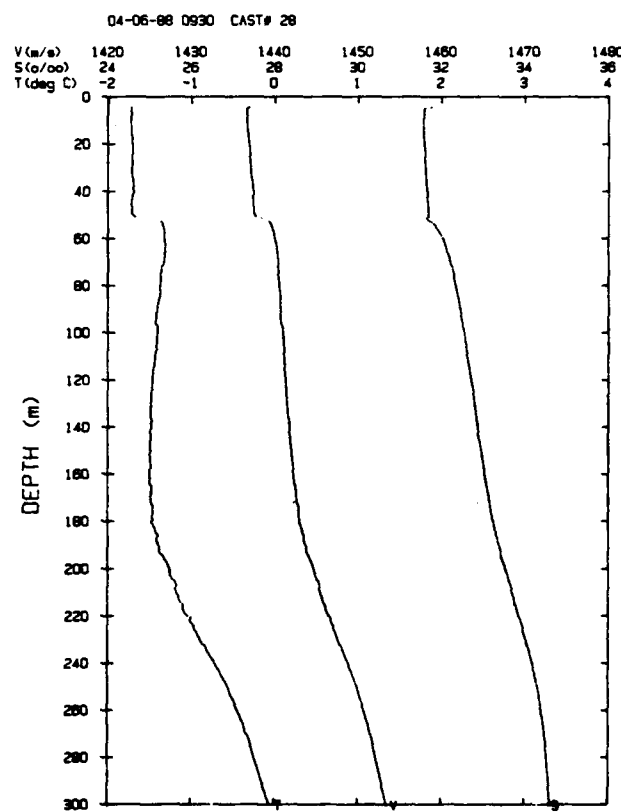
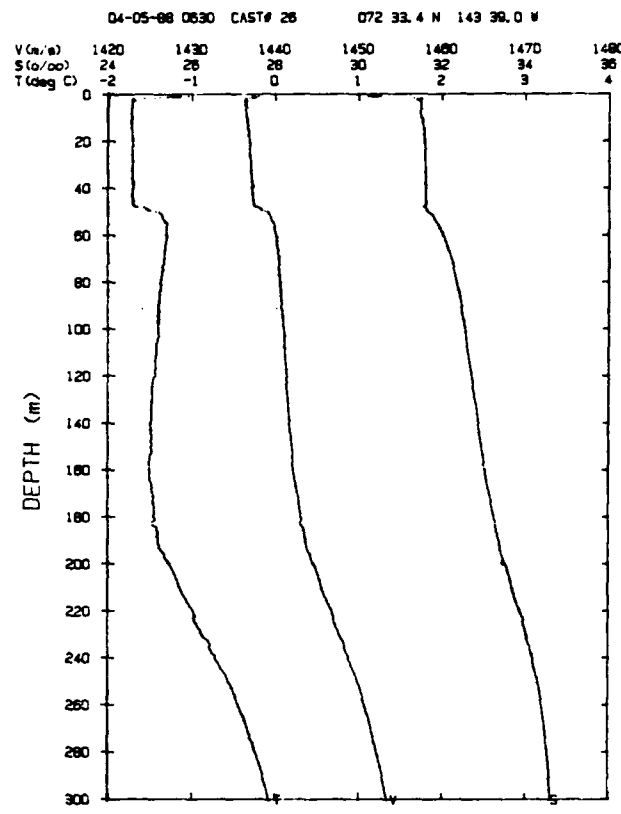
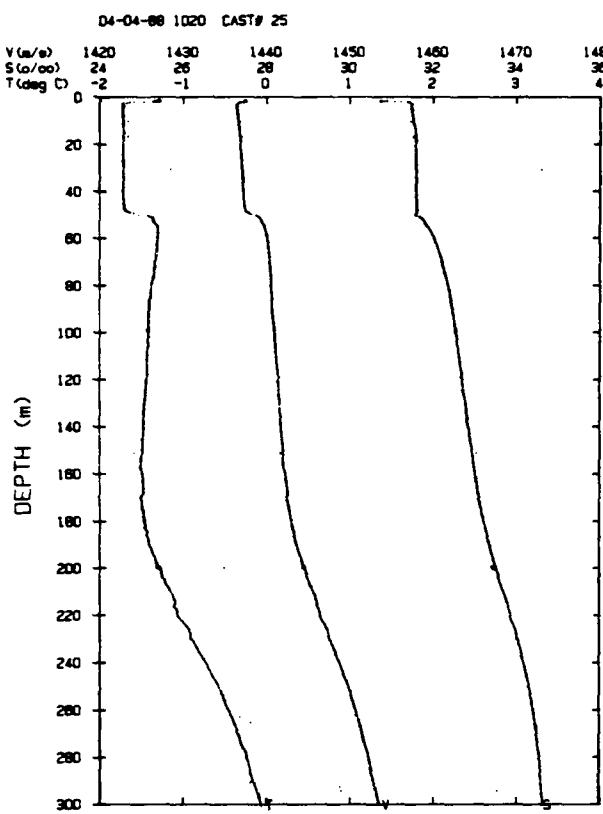




C-4 TR 8822



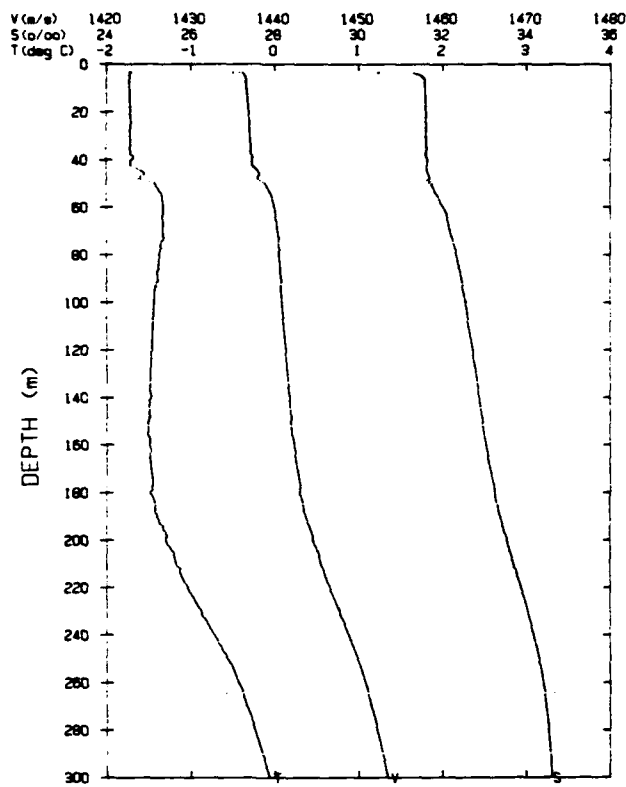




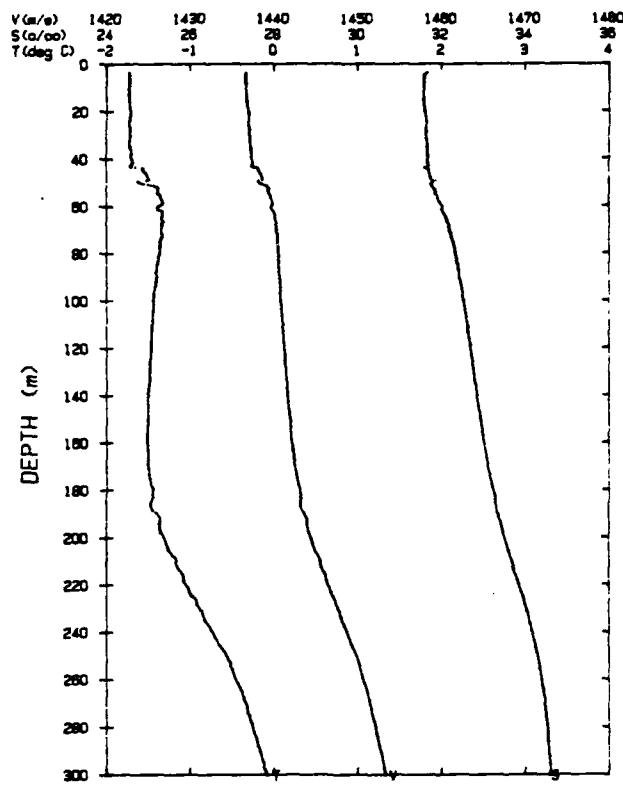
No Cast #27

TR 8822 C-7

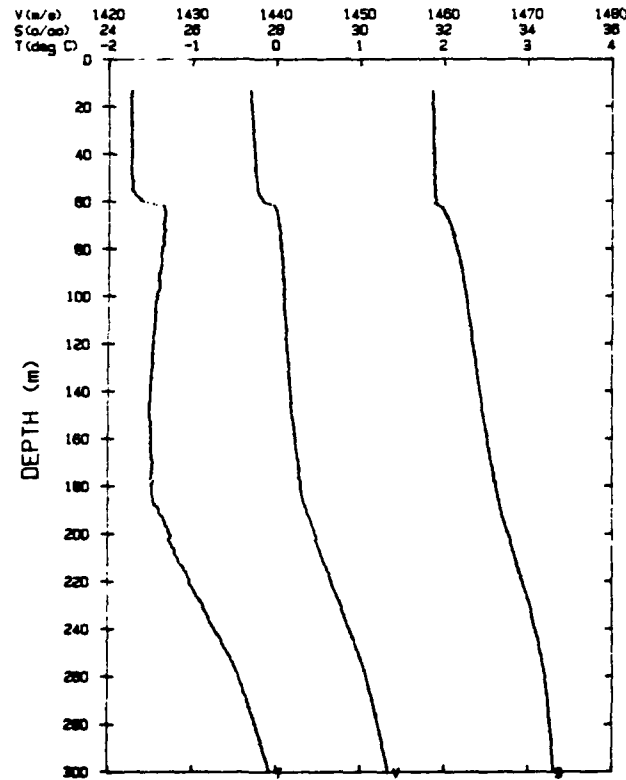
04-07-88 0620 CAST# 29



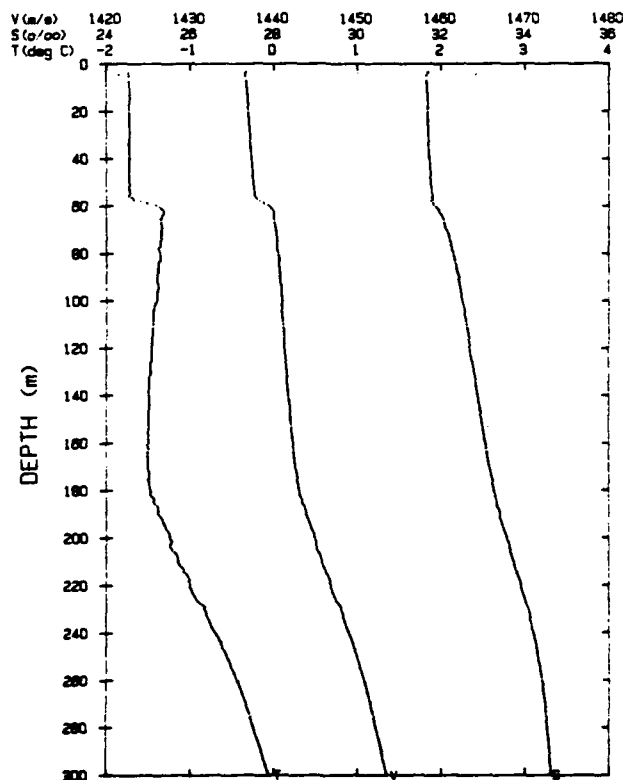
04-08-88 0620 CAST# 30



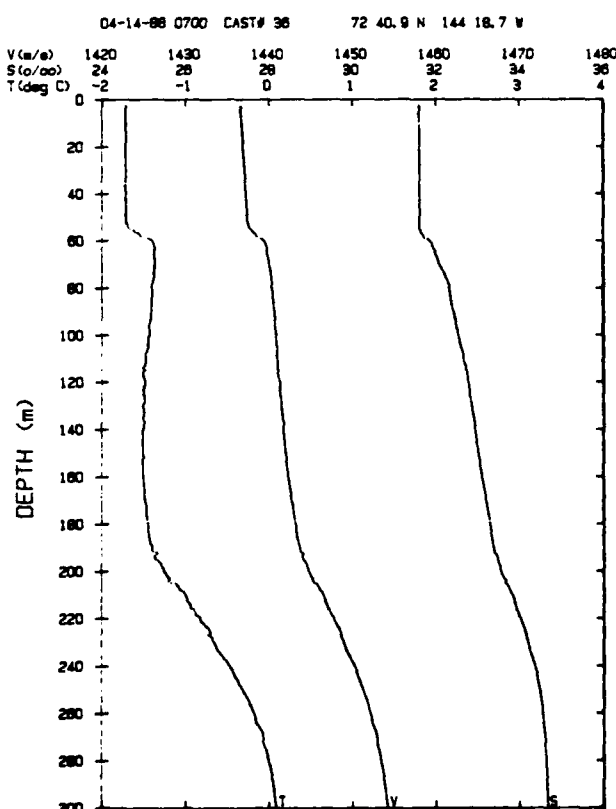
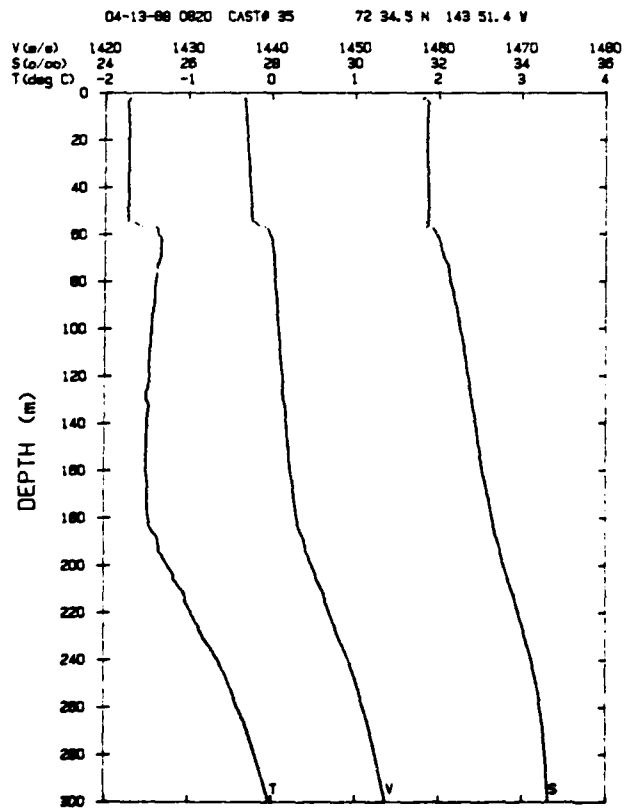
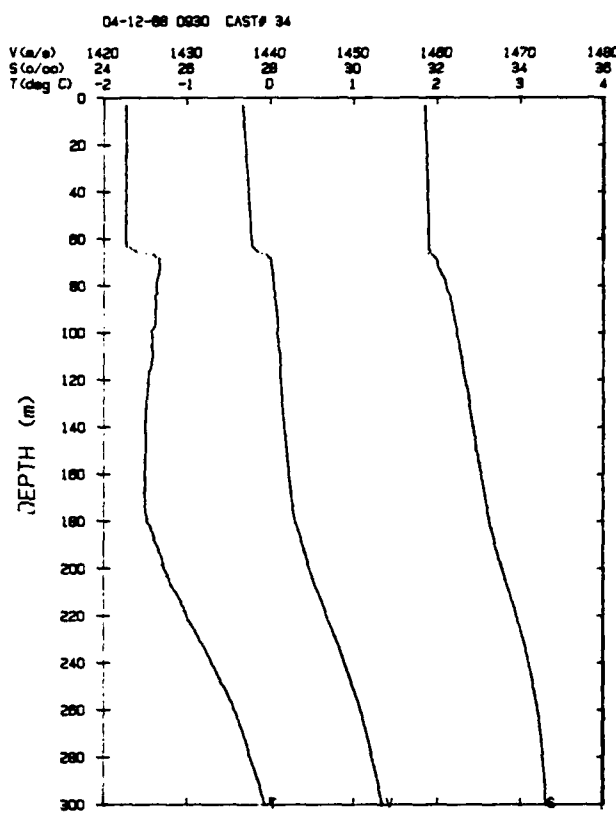
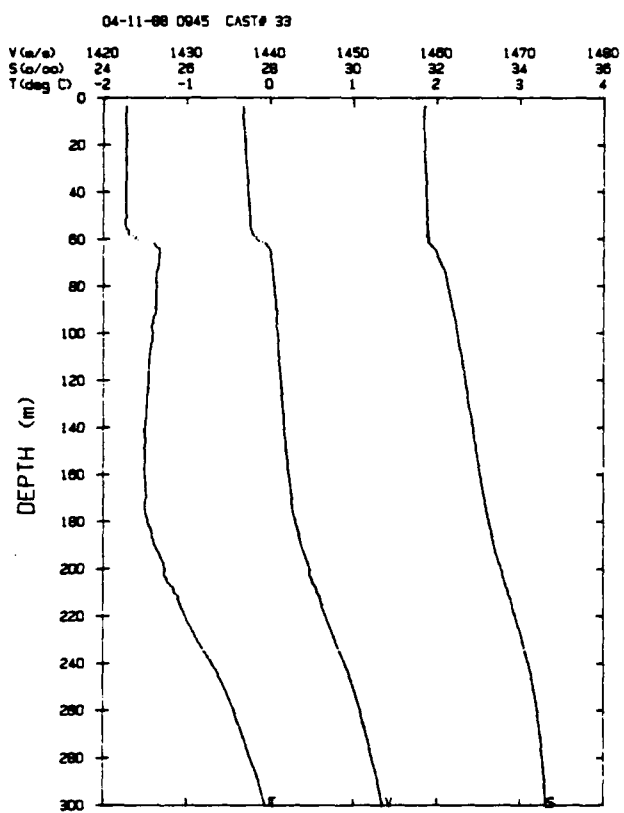
04-09-88 0625 CAST# 31



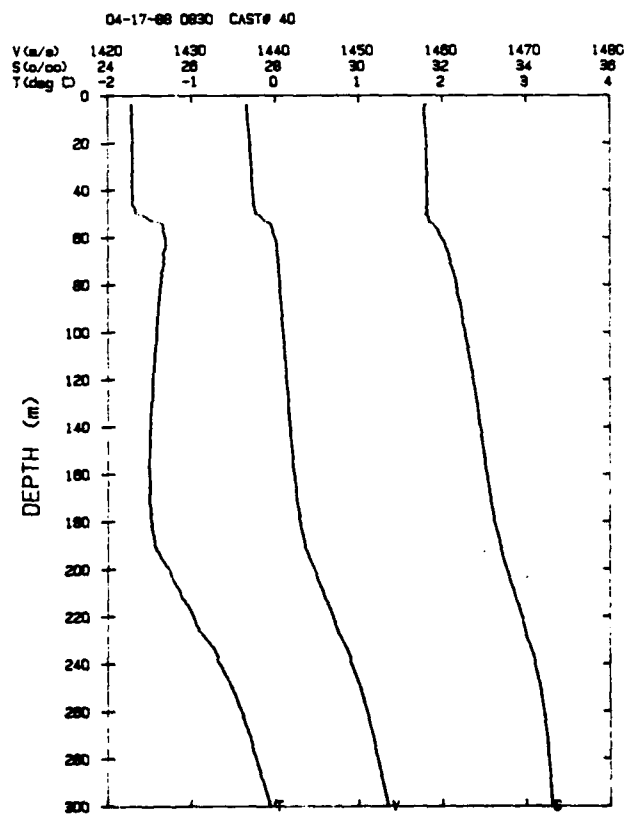
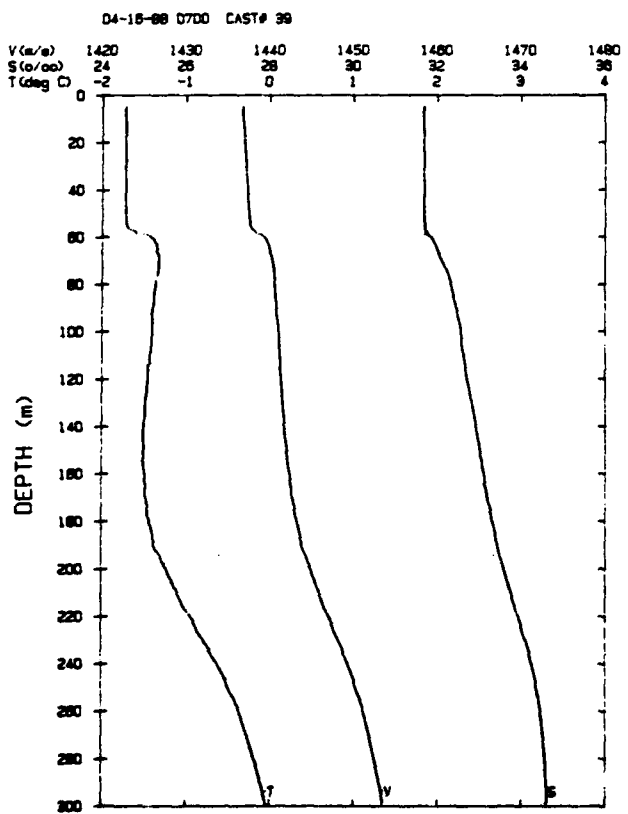
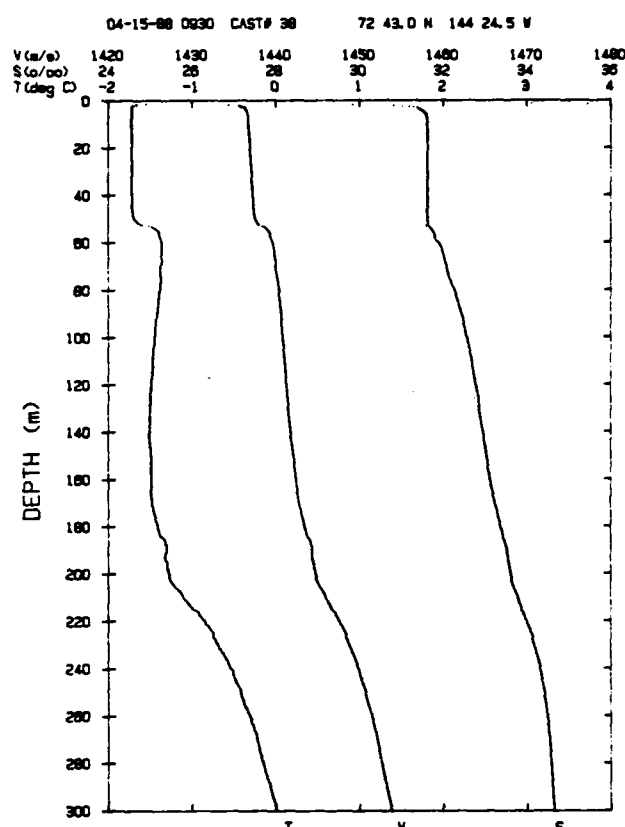
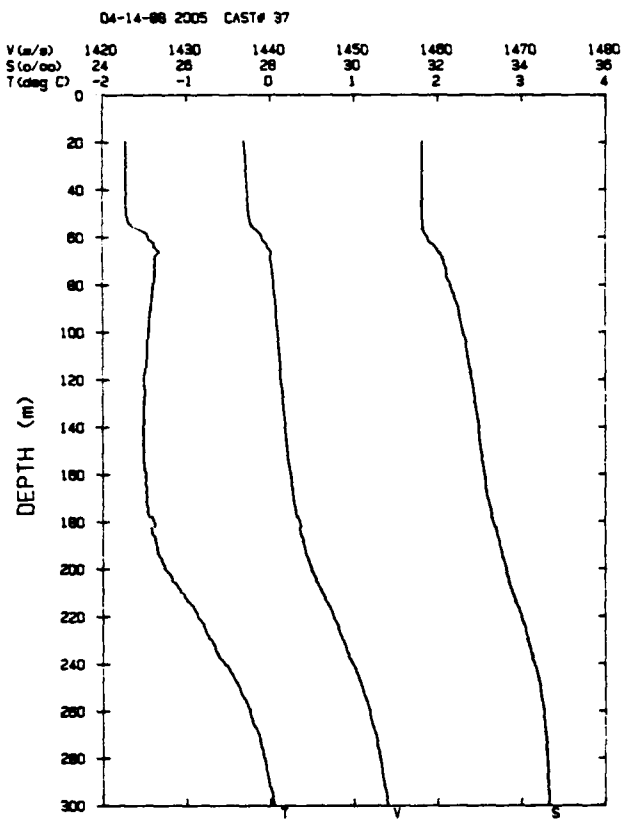
04-10-88 0930 CAST# 32

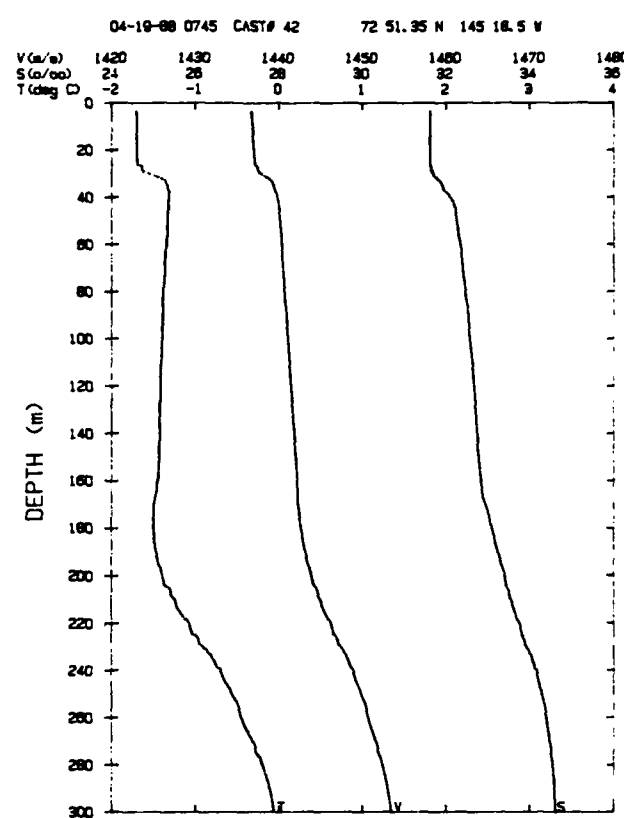
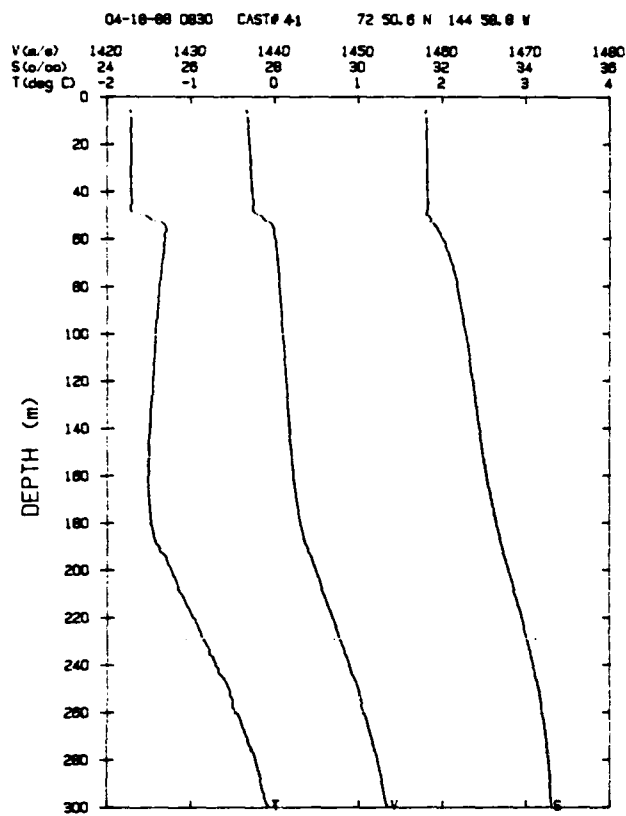


C-8 TR 8822



TR 8822 C-9





APPENDIX D

Sound Speed Profiles Computed from CTD Casts

03-15-88 1705 CAST #1		03-16-88 1950 CAST #2		03-17-88 1950 CAST #3		03-18-88 0630 CAST #4	
d(m)	sv(m/s)	d(m)	sv(m/s)	d(m)	sv(m/s)	d(m)	sv(m/s)
3.81	1436.41	4.07	1436.25	3.68	1436.36	13.31	1436.50
10.97	1436.50	12.66	1436.40	8.89	1436.43	18.37	1436.61
18.88	1436.64	21.73	1436.64	17.46	1436.61	23.80	1436.80
26.90	1436.88	31.03	1436.83	24.32	1436.86	29.61	1436.98
32.57	1437.03	40.41	1437.07	31.80	1437.13	31.54	1437.20
33.35	1437.21	42.72	1437.26	35.53	1437.44	32.32	1437.33
34.50	1437.28	44.13	1437.42	39.13	1438.92	34.12	1437.42
38.62	1437.40	45.54	1437.99	40.29	1439.24	36.05	1438.07
40.54	1437.43	46.44	1438.59	44.26	1439.54	37.46	1438.68
42.08	1437.71	47.46	1439.20	51.42	1440.04	39.39	1439.41
43.36	1437.86	48.35	1439.33	63.77	1440.28	40.54	1439.60
44.52	1438.39	49.63	1439.52	78.32	1440.53	46.18	1439.87
45.28	1439.20	51.80	1439.70	97.66	1440.98	51.93	1440.03
46.31	1439.50	57.54	1439.99	110.50	1441.26	56.78	1440.15
47.46	1439.57	66.56	1440.25	131.77	1441.80	65.29	1440.32
49.50	1439.66	75.55	1440.44	152.10	1441.94	71.63	1440.44
57.41	1440.12	84.37	1440.59	172.13	1442.41	76.05	1440.52
65.29	1440.39	93.03	1440.87	189.09	1443.22	81.35	1440.63
73.40	1440.48	102.03	1441.03	202.35	1444.43	88.26	1440.76
81.09	1440.56	111.12	1441.20	217.30	1445.96	96.16	1440.98
88.64	1440.76	119.92	1441.33	230.39	1447.53	102.78	1441.09
96.16	1440.89	128.57	1441.44	243.74	1449.03	109.75	1441.31
102.53	1441.13	137.30	1441.62	252.71	1450.02	116.21	1441.52
110.25	1441.23	145.88	1441.80	265.69	1451.08	122.64	1441.69
117.82	1441.36	154.66	1442.11	277.22	1451.89	131.52	1441.90
125.36	1441.48	162.93	1442.21	289.13	1452.66	137.92	1441.96
133.00	1441.61	171.40	1442.51	296.89	1453.04	147.59	1442.06
140.86	1441.78	179.72	1443.02			154.54	1442.00
148.44	1441.96	188.01	1443.59			160.86	1442.12
156.00	1442.16	196.03	1443.99			167.05	1442.27
163.53	1442.42	204.25	1445.05			173.46	1442.57
171.40	1442.71	212.80	1445.89			179.84	1442.85
179.24	1443.04	221.08	1446.82			185.97	1443.26
186.93	1443.39	229.56	1447.60			191.01	1443.58
194.36	1443.93	237.89	1448.43			195.43	1443.88
202.35	1444.68	246.07	1449.41			202.71	1444.62
210.08	1445.41	254.46	1450.24			209.96	1445.20
217.54	1446.21	262.46	1450.88			217.30	1446.08
225.09	1447.12	270.43	1451.49			224.50	1446.68
232.38	1447.96	278.48	1451.98			231.21	1447.61
239.88	1448.56	286.85	1452.54			238.25	1448.34
247.36	1449.47	295.18	1453.11			245.26	1449.25
254.69	1450.12					252.13	1449.95
262.22	1450.81					265.23	1451.01
269.50	1451.40					272.04	1451.58
277.22	1451.88					278.71	1451.97
284.90	1452.34					285.47	1452.39
291.99	1452.77					291.99	1452.74

03-18-88 1845		03-19-88 1010		03-20-88 0750		03-21-88 0620	
CAST #5		CAST #6		CAST #7		CAST #8	
d(m)	sv(m/s)	d(m)	sv(m/s)	d(m)	sv(m/s)	d(m)	sv(m/s)
5.37	1436.38	4.07	1436.74	.67	1436.39	1.85	1435.72
14.09	1436.56	8.76	1436.55	10.06	1436.49	7.59	1435.77
23.67	1436.79	17.85	1436.64	18.88	1436.67	14.48	1435.90
30.51	1437.00	25.35	1436.79	23.41	1436.76	21.21	1436.04
32.96	1437.29	31.29	1437.03	27.68	1436.88	28.71	1436.23
34.38	1437.76	34.38	1438.13	31.03	1437.07	30.38	1436.50
35.28	1438.16	36.82	1439.23	33.09	1437.62	32.19	1436.92
36.30	1438.62	40.16	1439.81	34.38	1438.84	33.99	1438.10
37.72	1439.08	42.72	1439.89	36.56	1439.44	35.53	1438.90
39.13	1439.38	47.59	1440.03	38.87	1439.63	37.33	1439.36
40.54	1439.60	57.03	1440.18	43.23	1439.98	39.26	1439.62
42.98	1439.72	66.56	1440.38	51.93	1440.06	41.06	1439.72
47.72	1439.95	76.18	1440.58	61.23	1440.26	42.85	1439.83
57.29	1440.19	85.50	1440.79	70.11	1440.44	46.31	1439.98
66.69	1440.35	94.78	1441.04	79.08	1440.61	53.33	1440.09
75.67	1440.54	103.78	1441.27	87.76	1440.80	60.34	1440.25
85.00	1440.73	112.73	1441.53	96.28	1441.01	67.58	1440.38
94.41	1440.97	126.47	1441.87	106.02	1441.32	74.79	1440.52
103.78	1441.20	140.00	1442.18	119.80	1441.68	81.85	1440.67
112.86	1441.46	153.57	1442.42	128.69	1441.86	88.89	1440.85
121.41	1441.70	166.93	1442.54	140.00	1442.14	95.91	1441.05
130.17	1441.92	175.87	1442.52	149.05	1442.30	104.15	1441.27
139.14	1442.14	185.13	1442.96	159.65	1442.34	112.73	1441.52
147.59	1442.26	198.54	1444.02	169.59	1442.27	121.16	1441.73
156.25	1442.38	209.25	1445.07	180.57	1442.63	129.43	1441.94
164.50	1442.22	221.67	1446.49	189.09	1443.18	137.67	1442.08
172.73	1442.46	234.14	1447.59	198.42	1444.05	146.12	1442.27
181.05	1442.82	247.01	1449.35	210.79	1444.98	154.66	1442.40
189.21	1443.42	259.33	1450.46	221.32	1446.33	162.93	1442.49
197.46	1444.08	271.23	1451.42	233.56	1447.70	171.52	1442.38
205.56	1444.86	283.07	1452.19	243.16	1448.59	180.20	1442.54
213.87	1445.67	298.71	1453.22	254.34	1449.90	186.57	1442.92
222.14	1446.70			266.50	1451.12	187.41	1443.03
230.39	1447.41			278.71	1451.96	188.25	1443.25
238.48	1448.32			287.30	1452.47	189.57	1443.50
246.54	1449.28			299.16	1453.24	190.41	1443.07
254.46	1450.12					192.68	1443.31
262.69	1450.88					196.75	1443.72
271.00	1451.49						
279.17	1452.03						
286.73	1452.51						
294.15	1453.04						

03-22-88 0620 CAST #9		03-23-88 1240 CAST #10		03-24-88 0610 CAST #11		03-25-88 0610 CAST #12	
d(m)	sv(m/s)	d(m)	sv(m/s)	d(m)	sv(m/s)	d(m)	sv(m/s)
1.46	1436.40	1.59	1436.27	1.98	1436.27	1.07	1436.31
8.76	1436.48	5.37	1436.32	6.02	1436.30	8.37	1436.38
16.81	1436.64	12.01	1436.43	12.66	1436.42	14.99	1436.52
25.22	1436.84	19.01	1436.59	18.88	1436.60	22.51	1436.69
29.35	1436.94	26.39	1436.84	25.22	1436.75	30.38	1436.96
33.09	1437.31	28.32	1436.98	31.93	1436.92	34.38	1437.20
33.86	1437.90	30.13	1437.11	33.86	1437.07	36.30	1437.73
34.76	1438.30	31.93	1437.64	35.53	1437.86	38.36	1438.44
35.53	1438.64	33.73	1438.10	38.75	1438.66	39.52	1438.82
36.43	1438.93	36.05	1438.21	42.85	1439.54	40.67	1438.78
37.33	1439.29	37.46	1438.31	46.44	1439.75	42.34	1438.98
38.62	1439.48	39.26	1438.96	52.95	1440.05	44.26	1439.49
39.77	1439.58	41.18	1439.52	59.19	1440.23	46.18	1439.74
41.95	1439.74	42.98	1439.65	68.97	1440.44	48.74	1439.83
46.18	1439.91	45.16	1439.73	78.83	1440.53	52.70	1440.12
50.40	1440.13	48.74	1439.88	89.89	1440.74	56.39	1440.13
58.69	1440.19	56.14	1440.09	99.03	1440.93	64.28	1440.28
66.94	1440.35	63.39	1440.27	109.38	1441.15	72.51	1440.42
75.42	1440.53	70.74	1440.42	119.55	1441.39	80.59	1440.56
83.74	1440.69	78.07	1440.57	129.55	1441.54	88.26	1440.73
91.65	1440.90	85.37	1440.66	139.76	1441.70	96.16	1440.85
98.53	1441.01	92.53	1440.80	149.79	1441.90	104.90	1441.02
106.52	1441.28	98.41	1440.98	159.53	1442.17	112.98	1441.12
113.97	1441.47	104.40	1441.09	170.19	1442.39	120.79	1441.28
121.41	1441.58	111.49	1441.29	179.84	1442.81	128.57	1441.52
128.57	1441.73	118.56	1441.44	189.45	1443.42	136.32	1441.66
136.20	1441.94	125.61	1441.56	199.73	1444.23	143.80	1441.81
143.80	1441.90	132.39	1441.65	209.36	1445.09	151.86	1441.97
151.37	1441.96	139.26	1441.84	218.84	1446.28	159.41	1442.13
159.04	1442.03	146.00	1441.91	228.27	1447.22	167.17	1442.34
166.68	1442.24	152.71	1441.97	239.65	1448.61	175.02	1442.57
174.42	1442.52	159.16	1442.08	250.97	1449.73	182.85	1442.89
182.13	1442.88	165.47	1442.21	258.40	1450.42	191.01	1443.51
189.69	1443.23	171.76	1442.43	269.62	1451.25	197.22	1443.96
194.72	1443.61	178.04	1442.74	280.77	1452.00	206.87	1444.84
201.87	1444.36	184.53	1443.01	291.41	1452.82	215.53	1445.91
210.55	1445.30	190.53	1443.34	296.66	1453.15	223.80	1446.94
218.84	1445.90	196.98	1443.89			231.68	1447.77
226.51	1447.01	204.02	1444.55			239.77	1448.53
234.14	1447.79	211.50	1445.19			248.06	1449.33
241.99	1448.49	218.37	1446.02			256.08	1450.18
250.04	1449.66	225.09	1447.00			263.84	1450.95
257.82	1450.22	231.80	1447.86			271.46	1451.54
265.58	1451.02	238.36	1448.42			279.28	1451.97
273.54	1451.59	244.91	1449.13			286.73	1452.47
281.58	1452.20	251.67	1449.71			294.27	1452.94
288.90	1452.62	258.17	1450.32				
295.18	1453.02	264.54	1450.84				
		271.00	1451.42				
		277.56	1451.94				
		284.10	1452.35				
		289.93	1452.72				

03-26-88 0620 CAST #13		03-27-88 1240 CAST #15		03-28-88 0620 CAST #16		03-29-88 0625 CAST #17	
d(m)	sv(m/s)	d(m)	sv(m/s)	d(m)	sv(m/s)	d(m)	sv(m/s)
1.85	1436.41	.81	1436.30	2.11	1436.21	1.33	1436.21
8.37	1436.40	6.28	1436.25	5.37	1436.23	8.50	1436.28
17.33	1436.57	10.58	1436.32	13.05	1436.36	15.77	1436.40
26.00	1436.80	16.94	1436.42	20.57	1436.49	23.54	1436.56
34.76	1437.34	21.60	1436.51	27.68	1436.65	32.06	1436.77
37.97	1437.98	25.87	1436.74	29.87	1436.71	34.12	1436.96
38.75	1438.50	30.51	1437.04	32.06	1436.77	36.05	1437.38
39.52	1438.86	33.09	1437.14	34.12	1436.96	38.36	1438.07
40.41	1439.01	34.12	1437.35	36.05	1437.38	40.29	1438.86
41.31	1439.12	35.53	1437.71	38.36	1438.07	42.47	1439.10
42.21	1439.22	36.69	1438.06	40.29	1438.86	44.39	1439.25
43.11	1439.33	37.85	1438.71	42.47	1439.10	48.23	1439.61
44.39	1439.58	39.77	1438.99	44.39	1439.25	53.21	1439.96
45.16	1439.70	41.95	1439.31	47.08	1439.48	61.23	1440.23
46.05	1439.77	43.11	1439.43	49.12	1439.68	69.48	1440.33
47.72	1439.63	45.67	1439.63	51.17	1439.81	77.69	1440.56
49.89	1439.80	50.91	1439.86	54.35	1440.06	85.62	1440.74
54.23	1439.99	56.01	1440.05	56.39	1440.16	93.40	1440.85
63.13	1440.23	60.97	1440.20	59.45	1440.16	99.16	1440.99
71.75	1440.42	66.31	1440.32	65.55	1440.29	106.39	1441.13
80.21	1440.56	71.50	1440.39	73.90	1440.46	114.72	1441.23
88.26	1440.74	77.06	1440.52	82.10	1440.65	121.90	1441.32
96.16	1440.90	82.23	1440.61	89.77	1440.76	129.31	1441.51
106.14	1441.11	87.51	1440.68	97.91	1440.96	137.18	1441.67
115.71	1441.27	92.78	1440.79	104.03	1441.09	144.90	1441.84
124.87	1441.41	97.91	1440.92	111.62	1441.26	153.08	1442.06
133.62	1441.56	103.28	1441.03	119.18	1441.28	161.11	1442.30
142.33	1441.74	108.76	1441.10	126.84	1441.47	168.98	1442.56
151.01	1441.91	114.97	1441.22	134.35	1441.63	177.07	1442.88
159.29	1442.09	121.28	1441.39	142.21	1441.79	184.77	1443.25
167.77	1442.30	127.09	1441.50	150.27	1441.99	192.68	1443.77
176.23	1442.69	133.00	1441.62	158.31	1442.22	198.06	1444.25
184.89	1443.07	138.90	1441.76	166.20	1442.46	204.97	1444.79
193.76	1443.67	144.78	1441.86	174.30	1442.75	213.28	1445.68
206.28	1444.79	150.76	1441.97	182.13	1443.15	221.55	1446.72
214.82	1445.73	156.85	1442.11	189.93	1443.67	229.68	1447.50
223.44	1446.66	163.05	1442.31	197.58	1444.23	237.89	1448.44
231.91	1447.65	169.59	1442.47	204.49	1444.78	246.19	1449.32
240.47	1448.62	176.47	1442.84	212.80	1445.61	254.34	1450.08
249.45	1449.55	183.09	1443.20	221.20	1446.68	262.46	1450.83
258.29	1450.38	189.09	1443.67	229.33	1447.44	270.66	1451.47
266.85	1451.12	193.88	1443.95	237.43	1448.36	278.94	1452.14
275.26	1451.76	200.56	1444.50	245.72	1449.28	287.07	1452.60
283.30	1452.30	206.99	1445.06	253.87	1450.05	295.52	1453.06
291.53	1452.86	213.40	1445.82	262.11	1450.79		
299.39	1453.31	219.55	1446.43	270.19	1451.45		
		225.80	1447.16	278.48	1452.10		
		231.80	1447.71	286.73	1452.58		
		237.89	1448.50	294.72	1453.04		
		244.09	1449.17				
		250.50	1449.84				
		256.78	1450.51				
		263.03	1450.91				
		269.62	1451.45				
		276.18	1451.94				
		282.49	1452.30				
		289.02	1452.71				
		294.72	1453.08				

03-30-88 1150		03-31-88 0615		04-01-88 0625		04-02-88 0625	
CAST #19		CAST #20		CAST #21		CAST #22	
d(m)	sv(m/s)	d(m)	sv(m/s)	d(m)	sv(m/s)	d(m)	sv(m/s)
1.98	1436.28	1.98	1436.27	1.33	1436.37	9.28	1436.49
8.24	1436.32	9.02	1436.36	6.93	1436.38	13.18	1436.53
13.83	1436.43	16.29	1436.63	15.25	1436.67	17.98	1436.67
20.31	1436.57	23.93	1436.77	24.06	1436.84	23.28	1436.79
25.35	1436.66	31.67	1436.99	28.32	1436.91	28.97	1436.93
31.41	1437.04	39.64	1437.45	33.09	1437.05	35.02	1437.19
32.83	1437.68	40.93	1437.99	34.63	1437.16	37.85	1437.28
35.28	1437.98	41.57	1438.85	35.53	1437.25	39.52	1437.54
39.13	1438.91	42.85	1439.12	38.10	1437.51	40.93	1437.86
40.54	1439.19	44.00	1439.36	39.39	1438.12	41.82	1438.66
41.95	1439.31	44.77	1439.47	40.16	1438.64	42.72	1438.90
42.98	1439.41	46.69	1439.68	41.06	1438.88	43.88	1439.08
45.67	1439.71	48.74	1439.81	42.59	1439.30	44.90	1439.24
48.35	1439.81	52.57	1439.90	44.77	1439.52	46.44	1439.24
52.82	1440.02	60.72	1440.26	47.08	1439.70	49.50	1439.69
58.05	1440.10	68.72	1440.35	51.80	1439.97	54.10	1439.95
70.36	1440.39	77.06	1440.50	56.52	1440.14	60.72	1440.18
71.63	1440.43	85.25	1440.67	66.05	1440.33	67.07	1440.27
76.68	1440.51	93.15	1440.86	76.05	1440.49	73.40	1440.44
80.21	1440.59	98.91	1441.04	85.50	1440.70	79.46	1440.61
81.60	1440.62	105.15	1441.22	93.03	1440.84	85.88	1440.64
99.03	1441.09	121.16	1441.71	98.91	1440.97	92.28	1440.77
107.64	1441.30	141.72	1442.03	108.26	1441.25	98.66	1440.93
117.45	1441.58	155.39	1442.16	116.21	1441.36	102.53	1441.00
126.97	1441.81	164.02	1442.20	124.00	1441.48	110.50	1441.15
136.56	1441.99	174.30	1442.50	132.14	1441.58	118.69	1441.32
145.76	1441.89	182.13	1443.00	140.37	1441.70	126.84	1441.49
155.15	1442.04	187.17	1443.26	148.57	1441.83	135.21	1441.69
164.02	1442.14	196.27	1443.85	156.73	1442.06	143.68	1441.77
172.97	1442.48	206.04	1444.71	165.11	1442.25	152.23	1441.97
182.01	1442.77	216.95	1446.03	173.58	1442.59	160.74	1442.19
190.89	1443.37	227.56	1447.06	182.25	1442.83	169.35	1442.55
197.46	1444.07	235.90	1448.07	190.05	1443.38	178.28	1442.93
206.51	1444.58	247.82	1449.49	197.58	1444.22	186.81	1443.38
215.53	1445.71	258.40	1450.50	206.63	1445.12	194.12	1443.93
224.86	1446.72	267.43	1451.28	215.05	1445.80	198.66	1444.31
234.14	1447.82	279.05	1452.05	224.15	1446.84	201.87	1444.74
243.39	1448.99	287.42	1452.56	233.32	1447.96	206.51	1445.28
252.36	1449.85			242.57	1449.09	215.76	1446.18
261.30	1450.64			251.78	1449.89	224.62	1447.34
269.85	1451.41			260.83	1450.77	233.67	1448.27
278.59	1452.01			269.50	1451.44	243.62	1449.19
287.07	1452.64			278.02	1452.01	252.48	1450.15
295.63	1453.12			286.04	1452.53	261.53	1450.88
				290.16	1452.76	270.54	1451.52
						279.51	1452.26
						288.33	1452.78

04-03-88 1330		04-04-88 0900		04-04-88 1020		04-05-88 0630	
CAST #23		CAST #24		CAST #25		CAST #26	
d(m)	sv(m/s)	d(m)	sv(m/s)	d(m)	sv(m/s)	d(m)	sv(m/s)
1.59	1436.33	8.76	1436.55	4.07	1436.43	2.76	1436.51
6.80	1436.46	14.86	1436.72	9.28	1436.57	7.06	1436.45
13.44	1436.62	19.66	1436.83	15.51	1436.77	12.53	1436.63
19.66	1436.78	24.84	1436.92	22.12	1436.88	18.24	1436.80
27.42	1436.97	30.51	1437.03	28.84	1436.99	24.58	1436.94
35.92	1437.13	36.18	1437.13	36.18	1437.14	30.64	1437.05
44.00	1437.26	42.34	1437.25	43.23	1437.27	37.08	1437.15
46.18	1437.58	47.84	1437.53	47.46	1437.38	42.85	1437.25
48.35	1438.30	49.76	1437.90	49.50	1437.93	47.46	1437.45
50.40	1439.22	50.65	1438.59	50.27	1438.75	48.74	1438.14
52.44	1439.69	51.80	1439.02	51.04	1439.10	49.50	1438.42
54.61	1439.87	52.70	1439.32	52.70	1439.41	50.53	1439.09
56.78	1439.93	54.35	1439.63	54.48	1439.73	51.80	1439.33
60.97	1440.17	55.88	1439.84	56.14	1439.87	52.70	1439.43
69.35	1440.30	57.54	1439.96	57.92	1439.99	54.10	1439.61
77.82	1440.51	59.07	1440.03	61.48	1440.12	55.25	1439.80
86.13	1440.66	62.37	1440.14	64.91	1440.25	56.65	1439.88
94.28	1440.73	68.72	1440.32	72.26	1440.45	57.79	1439.96
98.28	1440.81	75.04	1440.50	79.46	1440.52	59.45	1440.06
108.14	1441.13	81.60	1440.54	86.63	1440.65	62.63	1440.17
117.32	1441.26	87.89	1440.67	93.91	1440.78	65.55	1440.25
126.47	1441.38	94.78	1440.83	99.53	1440.92	69.48	1440.35
135.70	1441.62	99.28	1440.94	109.13	1441.15	75.80	1440.47
145.02	1441.87	109.01	1441.13	118.19	1441.37	82.23	1440.61
154.18	1442.03	117.69	1441.35	127.34	1441.53	88.39	1440.70
163.17	1442.28	126.47	1441.51	136.69	1441.71	94.78	1440.88
172.37	1442.58	135.58	1441.67	146.24	1441.90	99.41	1440.98
181.41	1443.03	144.41	1441.83	155.76	1442.06	112.11	1441.19
190.05	1443.60	152.84	1441.97	165.23	1442.45	121.41	1441.29
198.30	1444.36	161.23	1442.30	175.02	1442.75	130.66	1441.48
207.46	1445.29	169.47	1442.51	185.01	1443.31	140.12	1441.68
216.47	1446.35	177.92	1442.89	194.72	1444.10	149.66	1441.97
225.56	1447.17	186.69	1443.51	207.46	1445.34	159.29	1442.15
234.50	1448.15	195.19	1444.12	215.88	1446.05	168.86	1442.55
243.51	1449.10	208.18	1445.38	224.62	1447.16	178.40	1443.04
252.48	1450.07	217.66	1446.29	233.56	1448.04	188.01	1443.51
261.41	1450.81	227.21	1447.39	242.69	1449.07	197.22	1444.25
270.43	1451.47	236.72	1448.38	252.01	1450.05	210.08	1445.63
279.74	1452.07	246.31	1449.50	261.30	1450.78	220.85	1446.90
289.02	1452.75	255.97	1450.41	270.43	1451.52	231.68	1447.96
297.57	1453.29	265.46	1451.13	279.86	1452.20	242.57	1449.11
		275.15	1451.87	289.02	1452.76	253.29	1450.22
		284.79	1452.48	298.36	1453.38	264.19	1451.09
		294.15	1453.03			274.92	1451.85
						285.36	1452.55
						295.75	1453.16

04-06-88 0930		04-07-88 0620		04-08-88 0620		04-09-88 0625	
CAST #28		CAST #29		CAST #30		CAST #31	
d(m)	sv(m/s)	d(m)	sv(m/s)	d(m)	sv(m/s)	d(m)	sv(m/s)
5.24	1436.55	9.41	1436.63	3.94	1436.63	13.57	1436.84
9.41	1436.61	19.92	1436.85	8.63	1436.62	19.79	1436.98
18.24	1436.81	29.48	1437.05	13.05	1436.69	28.84	1437.14
27.68	1437.02	40.80	1437.31	19.79	1436.91	38.62	1437.34
37.08	1437.26	42.21	1437.32	31.03	1437.16	48.35	1437.49
46.05	1437.36	46.05	1438.16	38.49	1437.35	55.76	1437.73
48.35	1437.44	48.10	1437.91	45.80	1438.32	58.81	1438.19
50.53	1437.59	52.06	1439.24	48.35	1438.59	60.34	1438.62
52.82	1439.19	56.90	1439.72	49.63	1438.10	62.63	1439.83
54.86	1439.55	60.34	1439.98	52.57	1439.28	68.72	1440.17
57.16	1439.78	68.84	1440.32	57.29	1439.72	74.41	1440.42
61.36	1440.06	79.08	1440.53	64.79	1440.12	80.34	1440.55
65.93	1440.26	89.39	1440.73	69.98	1440.32	86.00	1440.70
70.49	1440.35	99.66	1440.83	77.69	1440.51	92.03	1440.76
79.46	1440.51	109.88	1441.05	85.75	1440.60	99.78	1440.87
88.26	1440.62	120.79	1441.29	93.40	1440.73	109.38	1441.03
99.41	1440.97	131.65	1441.51	99.78	1440.83	119.55	1441.25
110.37	1441.15	142.57	1441.78	110.12	1441.04	129.43	1441.46
119.68	1441.26	153.44	1442.00	119.68	1441.24	140.37	1441.65
128.44	1441.45	164.02	1442.41	129.68	1441.46	149.79	1441.87
139.51	1441.74	174.54	1442.86	139.76	1441.64	159.29	1442.24
148.44	1441.94	185.13	1443.39	150.03	1441.91	169.59	1442.63
159.29	1442.24	195.55	1444.25	160.01	1442.16	180.20	1442.93
170.07	1442.59	208.89	1445.41	169.71	1442.50	190.41	1443.70
181.05	1443.07	219.55	1446.49	180.08	1443.09	201.40	1444.76
189.81	1443.69	230.27	1447.71	190.65	1443.78	209.96	1445.52
200.44	1444.81	240.59	1448.85	201.28	1444.59	220.14	1446.60
209.25	1445.50	250.97	1449.97	211.14	1445.58	230.62	1447.80
218.13	1446.29	261.30	1450.88	220.61	1446.58	240.82	1448.85
228.74	1447.55	271.69	1451.65	229.80	1447.66	251.43	1449.98
239.42	1448.77	282.15	1452.34	241.17	1448.87	261.88	1450.87
250.04	1449.93	292.44	1452.99	250.50	1449.91	271.92	1451.60
261.07	1450.85	299.61	1453.39	260.26	1450.69	282.04	1452.30
271.69	1451.68			269.62	1451.49	291.99	1452.91
282.27	1452.32			279.51	1452.09	301.09	1453.48
292.21	1452.96			289.02	1452.67		
300.18	1453.46			300.41	1453.36		

04-10-88 0930		04-11-88 0945		04-12-88 0930		04-13-88 0820	
CAST #32		CAST #33		CAST #34		CAST #35	
d(m)	sv(m/s)	d(m)	sv(m/s)	d(m)	sv(m/s)	d(m)	sv(m/s)
3.55	1436.65	3.68	1436.70	3.42	1436.66	2.76	1436.61
8.24	1436.71	9.80	1436.77	10.32	1436.81	7.59	1436.83
18.75	1436.91	19.40	1436.96	20.18	1437.02	15.90	1436.97
29.48	1437.11	28.97	1437.14	30.00	1437.21	24.32	1437.11
40.41	1437.32	41.06	1437.36	40.03	1437.37	34.25	1437.29
51.29	1437.59	50.14	1437.55	49.63	1437.55	43.88	1437.45
56.52	1437.79	58.05	1437.88	59.45	1437.73	54.48	1437.62
59.07	1438.80	60.34	1438.44	63.39	1437.84	57.03	1439.14
61.74	1439.91	62.63	1439.57	66.31	1438.94	57.92	1439.53
64.40	1440.03	65.04	1439.99	67.19	1439.63	59.96	1439.68
69.73	1440.20	67.19	1440.09	68.72	1440.03	62.25	1439.97
75.04	1440.38	71.88	1440.27	71.12	1440.17	67.19	1440.17
80.72	1440.55	81.35	1440.51	80.84	1440.41	69.48	1440.24
90.65	1440.71	90.77	1440.81	90.40	1440.75	79.20	1440.38
100.53	1440.94	100.16	1440.93	99.91	1440.82	88.76	1440.59
111.37	1441.07	109.25	1441.01	109.38	1441.15	98.16	1440.76
121.04	1441.31	119.43	1441.26	118.81	1441.23	107.89	1440.96
131.03	1441.52	131.15	1441.50	128.20	1441.42	117.20	1441.16
141.10	1441.72	140.86	1441.68	139.76	1441.63	126.72	1441.30
151.01	1441.97	150.40	1441.91	151.13	1442.02	135.21	1441.64
160.50	1442.21	159.53	1442.20	160.14	1442.25	144.29	1441.83
169.95	1442.49	168.62	1442.54	168.86	1442.48	153.08	1442.06
179.48	1442.96	177.80	1442.86	179.96	1442.96	161.35	1442.30
188.85	1443.79	189.21	1443.69	188.85	1443.78	169.71	1442.66
200.32	1444.87	200.44	1444.78	199.49	1444.62	177.92	1442.94
209.48	1445.68	209.60	1445.61	210.43	1445.84	186.21	1443.54
219.07	1446.76	218.72	1446.57	218.96	1446.69	194.48	1444.18
228.62	1447.93	228.04	1447.53	229.68	1447.85	202.83	1445.24
240.35	1448.98	236.96	1448.61	240.00	1448.92	210.79	1446.16
249.80	1449.89	248.17	1449.80	252.48	1450.16	218.84	1446.87
259.79	1450.68	259.44	1450.77	264.42	1451.19	226.98	1447.71
268.35	1451.38	269.96	1451.51	276.53	1451.97	234.73	1448.63
279.74	1452.16	282.72	1452.42	288.79	1452.79	242.57	1449.51
291.30	1452.93	291.30	1452.99	300.64	1453.47	250.73	1450.23
300.30	1453.48	299.73	1453.45			258.75	1450.84
						266.50	1451.53
						274.34	1452.07
						282.04	1452.53
						289.93	1453.04
						297.23	1453.45

04-14-88 0700 CAST #36		04-14-88 2005 CAST #37		04-15-88 0930 CAST #38		04-16-88 0700 CAST #39	
d(m)	sv(m/s)	d(m)	sv(m/s)	d(m)	sv(m/s)	d(m)	sv(m/s)
3.68	1436.61	19.53	1436.88	6.67	1436.63	5.50	1436.71
9.54	1436.73	27.42	1437.01	13.05	1436.78	14.86	1436.87
17.98	1436.87	35.02	1437.14	20.18	1436.90	24.96	1437.04
28.71	1437.05	43.11	1437.28	28.06	1437.03	34.63	1437.21
37.97	1437.18	50.91	1437.41	36.05	1437.16	44.13	1437.37
47.08	1437.37	54.61	1437.63	44.64	1437.32	52.06	1437.50
52.95	1437.53	56.52	1438.20	49.25	1437.48	55.50	1437.69
55.37	1437.91	58.43	1438.79	51.29	1437.70	57.67	1438.23
57.54	1438.45	60.21	1439.00	53.59	1438.63	59.45	1439.12
59.07	1438.97	62.25	1439.35	54.48	1438.92	61.10	1439.55
60.34	1439.45	63.90	1439.58	56.65	1439.29	62.50	1439.68
61.36	1439.57	65.67	1439.93	59.32	1439.51	66.18	1439.96
70.11	1440.04	67.32	1440.06	63.52	1439.80	68.21	1440.19
78.95	1440.36	69.35	1440.04	68.21	1439.98	72.13	1440.37
88.39	1440.57	72.89	1440.18	77.31	1440.26	79.83	1440.57
98.78	1440.84	80.46	1440.37	88.26	1440.57	85.25	1440.64
109.88	1441.02	88.01	1440.59	99.28	1440.81	92.78	1440.79
118.69	1441.19	94.91	1440.72	108.01	1441.01	101.03	1441.04
128.20	1441.50	104.90	1440.96	121.16	1441.30	109.50	1441.14
136.93	1441.73	111.99	1441.09	129.80	1441.47	118.31	1441.28
148.69	1441.93	118.69	1441.18	138.65	1441.68	126.84	1441.45
159.53	1442.27	125.61	1441.41	147.22	1441.99	135.34	1441.65
170.56	1442.74	132.26	1441.55	155.88	1442.26	143.80	1441.81
181.17	1443.20	139.02	1441.72	164.63	1442.51	152.96	1442.11
189.93	1443.71	146.00	1441.88	173.33	1442.95	160.86	1442.40
198.77	1444.74	152.59	1442.06	181.89	1443.59	169.59	1442.69
209.72	1446.49	159.29	1442.37	185.97	1444.06	178.40	1443.18
220.61	1447.83	165.72	1442.61	188.37	1444.26	187.29	1443.74
231.09	1449.10	172.25	1442.78	197.10	1444.56	195.79	1444.48
239.65	1450.20	178.76	1443.37	205.80	1445.31	204.02	1445.35
248.17	1451.09	185.85	1443.68	214.70	1446.68	212.57	1446.21
256.78	1451.93	192.44	1444.18	223.32	1448.06	221.32	1447.28
267.66	1452.78	198.66	1444.74	231.91	1448.99	229.09	1448.11
276.30	1453.24	208.18	1445.89	240.47	1449.93	237.07	1449.04
285.13	1453.66	214.58	1446.86	248.52	1450.59	245.26	1449.88
293.58	1453.98	221.08	1447.61	256.78	1451.19	253.29	1450.62
300.75	1454.22	227.33	1448.31	264.88	1451.80	260.83	1451.25
		233.79	1449.00	273.08	1452.25	268.12	1451.71
		240.23	1449.77	281.46	1452.71	275.61	1452.20
		246.42	1450.51	290.05	1453.26	283.30	1452.66
		252.71	1451.13	298.59	1453.75	290.96	1453.10
		259.21	1451.75			298.14	1453.43
		265.58	1452.11				
		272.04	1452.62				
		278.13	1452.94				
		284.33	1453.22				
		290.73	1453.51				
		297.11	1453.83				

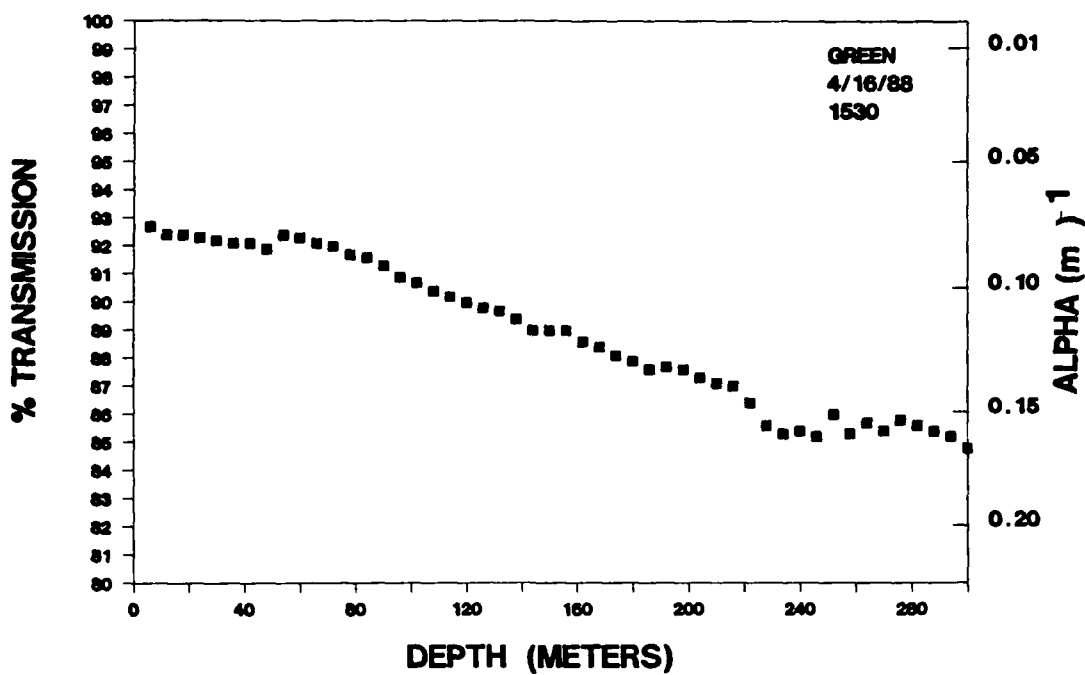
04-17-88 0830		04-18-88 0830		04-19-88 0745	
CAST #40		CAST #41		CAST #42	
d(m)	sv(m/s)	d(m)	sv(m/s)	d(m)	sv(m/s)
4.33	1436.59	6.02	1436.62	3.68	1436.70
8.76	1436.64	11.36	1436.77	7.98	1436.77
17.72	1436.90	21.21	1436.97	16.94	1436.93
26.64	1437.06	31.16	1437.12	25.74	1437.10
35.66	1437.22	40.93	1437.28	28.58	1437.45
44.90	1437.38	48.61	1437.47	30.90	1438.30
49.76	1437.65	50.65	1438.45	32.96	1439.13
52.06	1438.42	52.95	1439.32	35.66	1439.40
54.35	1439.44	53.46	1439.51	38.10	1439.67
55.37	1439.55	54.48	1439.71	40.41	1439.82
57.67	1439.73	56.90	1439.92	45.16	1440.03
59.70	1439.94	66.81	1440.28	54.10	1440.21
64.53	1440.21	76.43	1440.48	62.88	1440.37
68.84	1440.30	86.00	1440.66	71.88	1440.53
73.27	1440.44	95.41	1440.82	80.84	1440.69
82.48	1440.59	104.52	1441.04	89.64	1440.88
91.15	1440.75	113.48	1441.22	98.91	1441.07
100.03	1440.95	122.64	1441.41	108.01	1441.22
109.01	1441.12	131.77	1441.54	117.32	1441.41
118.07	1441.30	140.74	1441.74	126.35	1441.56
126.72	1441.50	149.79	1441.96	135.34	1441.74
135.21	1441.63	158.80	1442.19	144.53	1441.91
142.57	1441.82	167.41	1442.48	153.93	1442.10
151.13	1442.01	176.11	1442.86	162.69	1442.23
159.29	1442.23	185.01	1443.34	171.52	1442.34
167.05	1442.51	193.64	1444.29	180.08	1442.66
175.63	1442.78	201.99	1445.08	188.61	1443.04
184.29	1443.17	210.79	1445.95	197.34	1443.75
192.68	1443.79	219.67	1446.84	205.68	1444.56
200.68	1444.74	228.15	1447.68	214.23	1445.35
209.01	1445.64	236.25	1448.54	222.85	1446.40
217.66	1446.64	244.32	1449.31	230.74	1447.61
226.15	1447.38	252.18	1450.03	238.83	1448.69
234.50	1448.63	260.49	1450.68	247.36	1449.61
242.92	1449.40	268.23	1451.28	255.50	1450.42
251.32	1450.25	276.30	1451.93	263.61	1450.99
259.44	1450.88	284.56	1452.44	271.69	1451.77
268.35	1451.52	292.67	1452.89	279.74	1452.41
276.41	1451.99	300.52	1453.39	287.99	1452.91
284.56	1452.51			295.63	1453.29
292.10	1452.98			299.39	1453.45
300.64	1453.47				

APPENDIX E

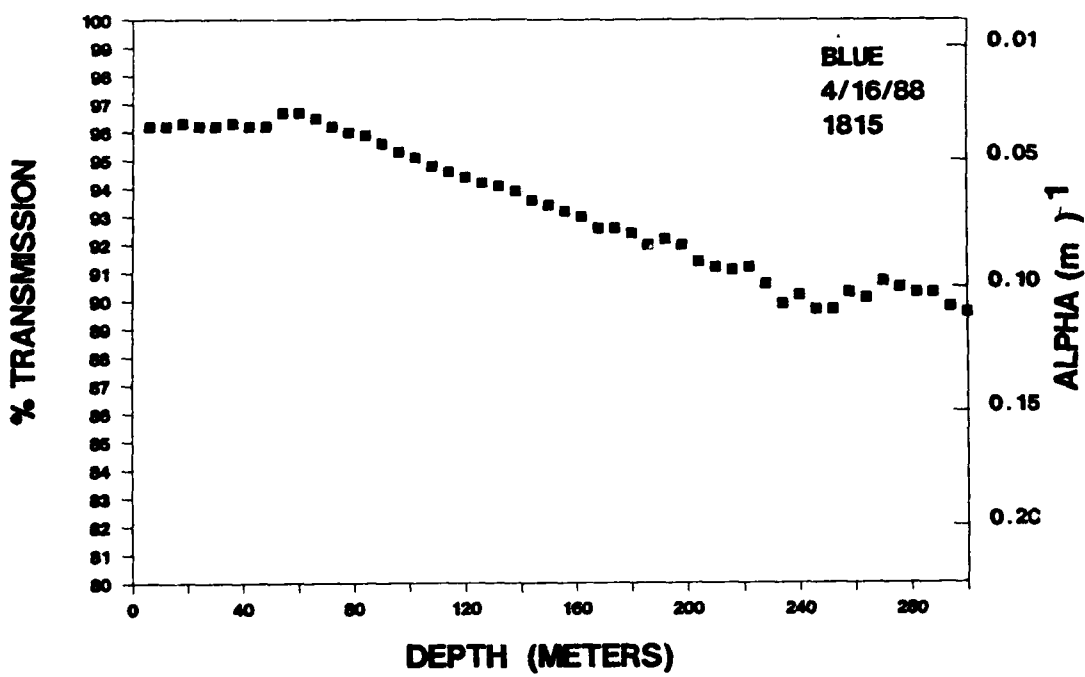
Water Clarity Measurements by Naval Surface Weapons Center

Color designations on graphs refer to wavelength in the optical spectrum.

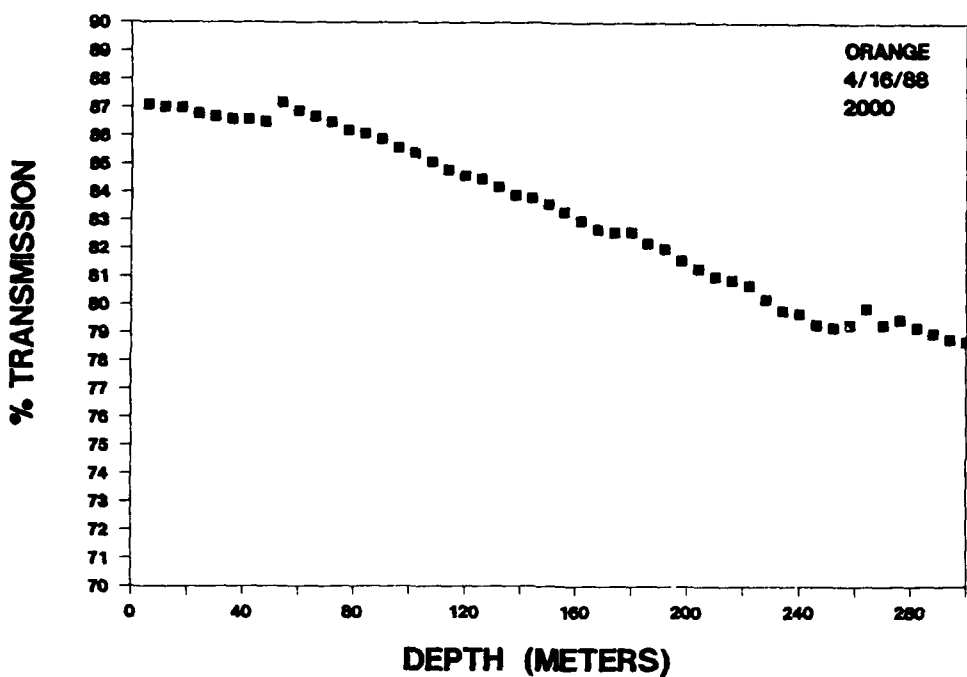
WATER CLARITY TEST



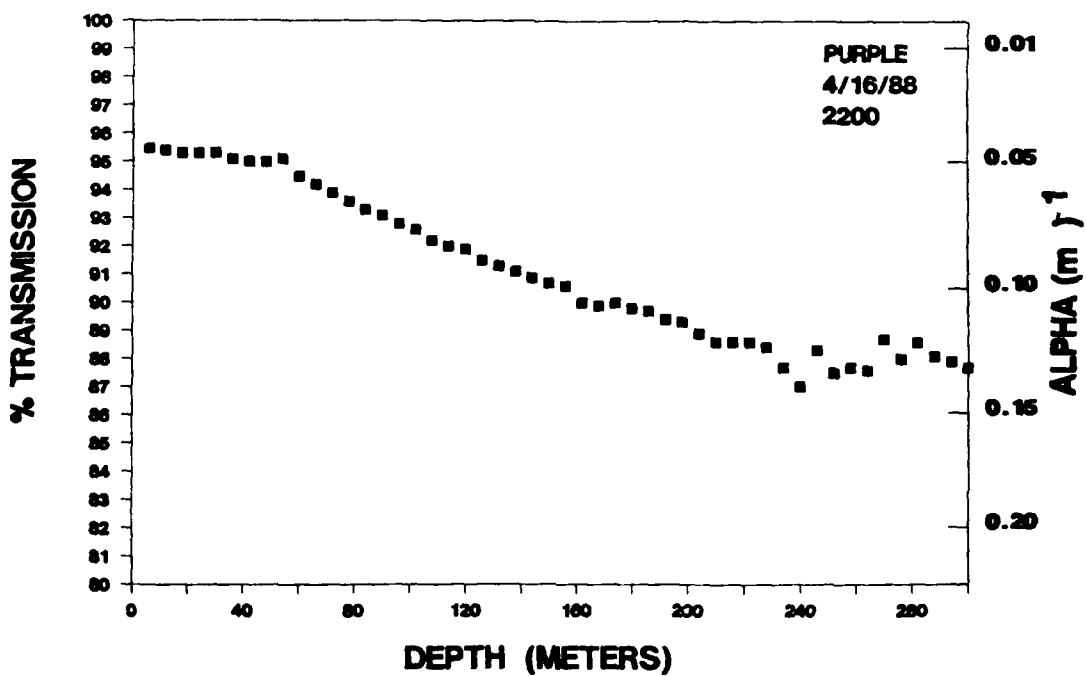
WATER CLARITY TEST



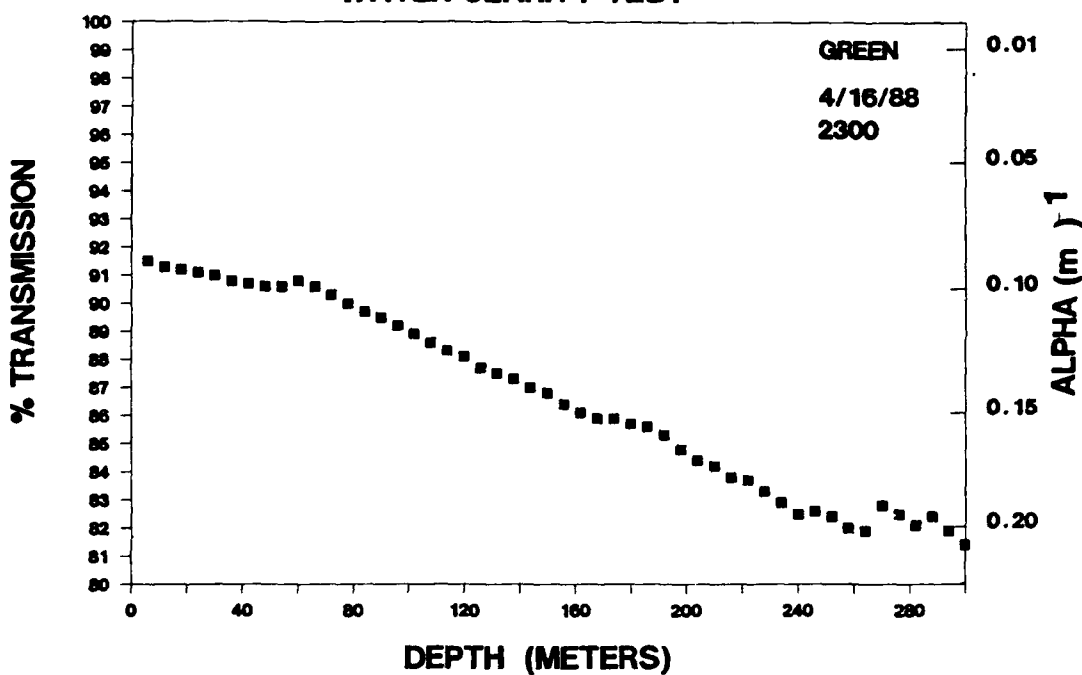
WATER CLARITY TEST



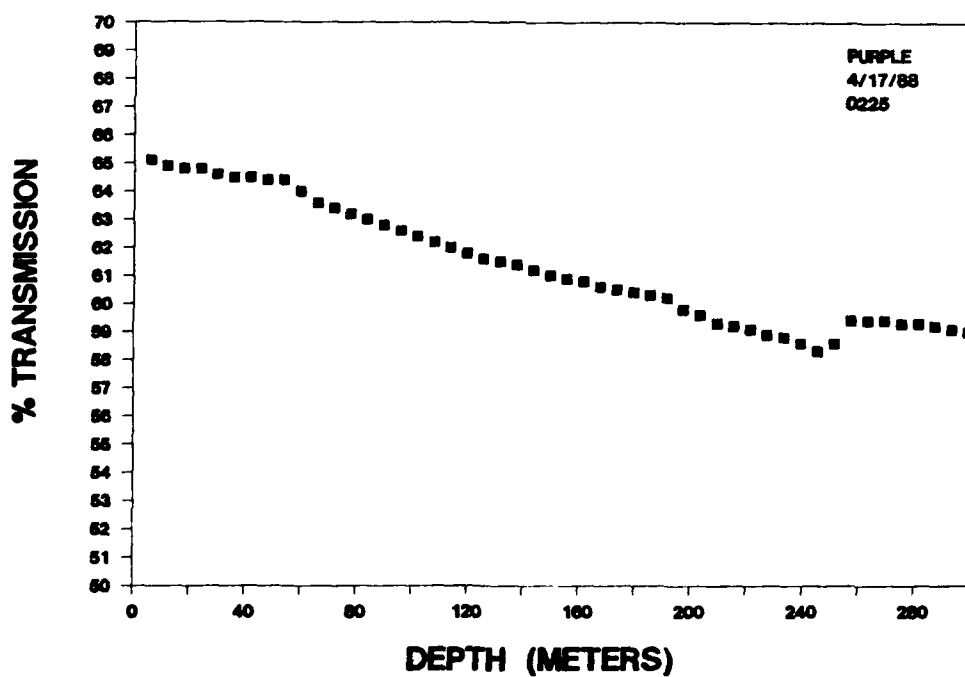
WATER CLARITY TEST



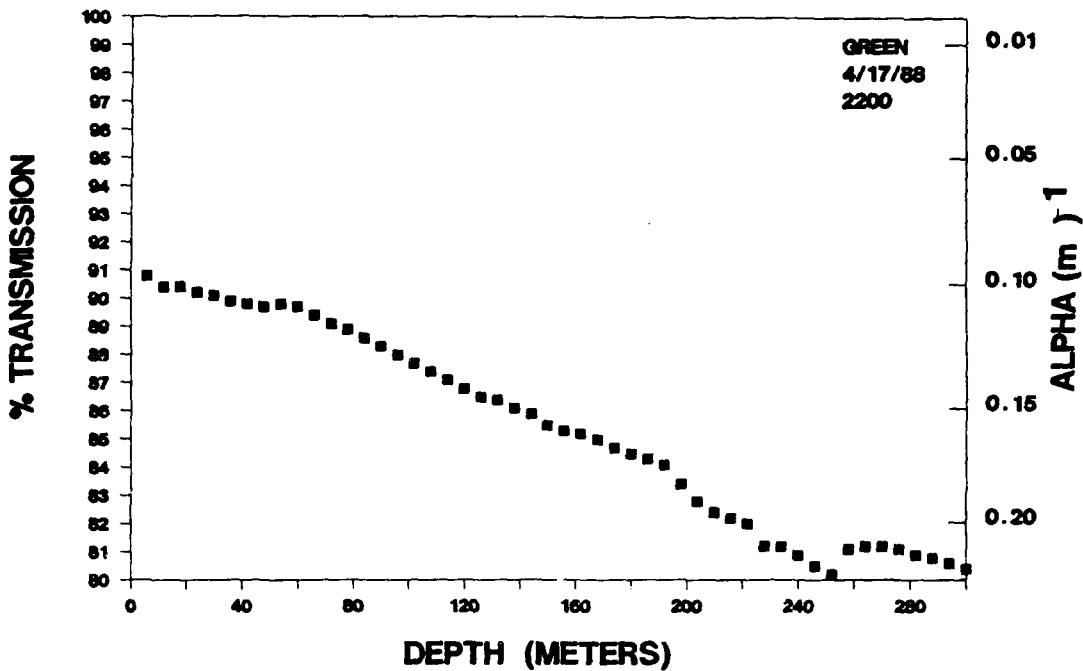
WATER CLARITY TEST



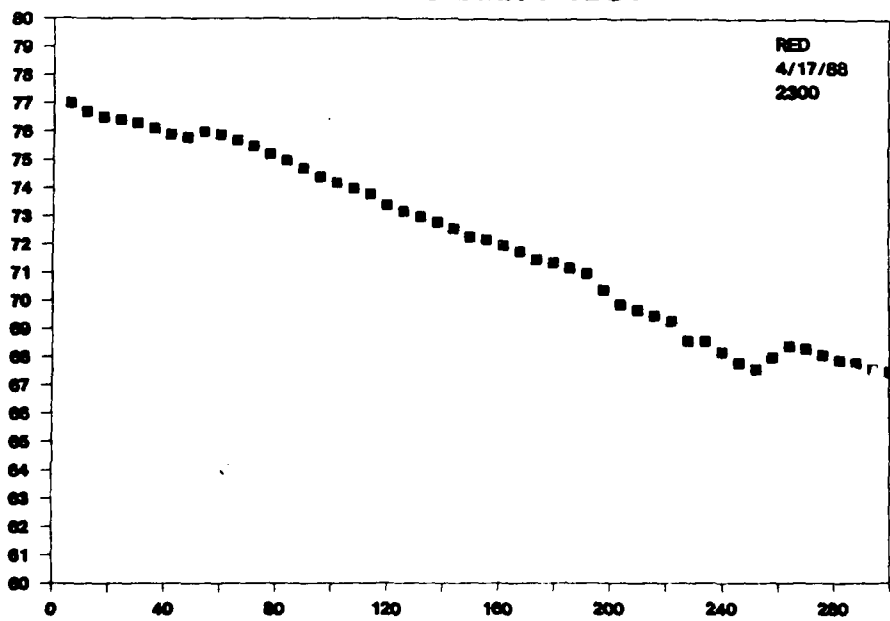
WATER CLARITY TEST



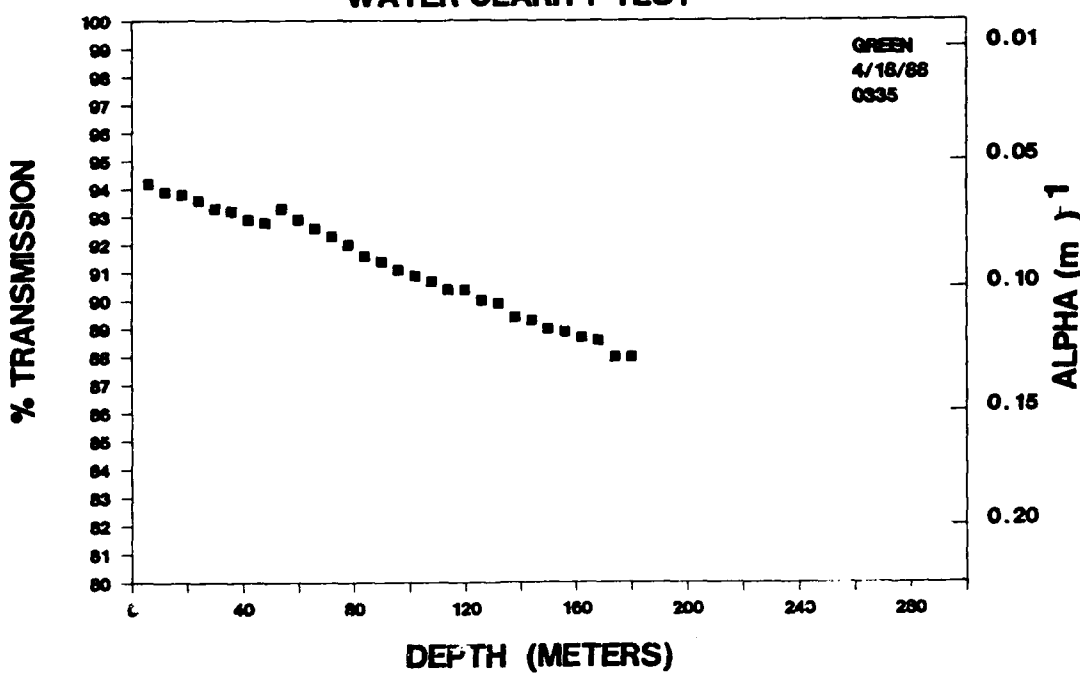
WATER CLARITY TEST



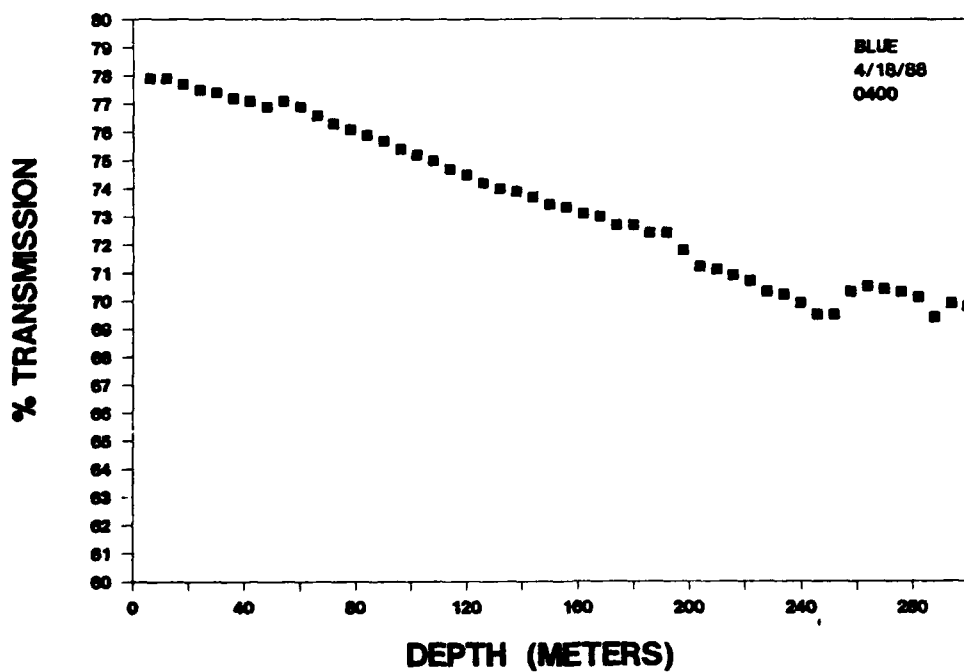
WATER CLARITY TEST



WATER CLARITY TEST



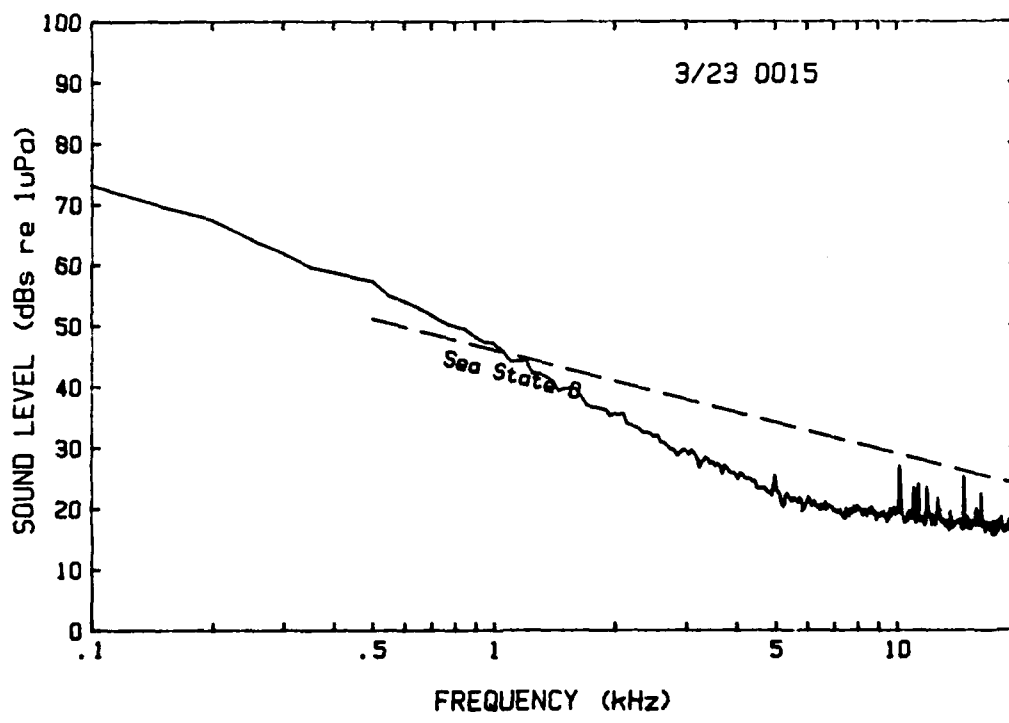
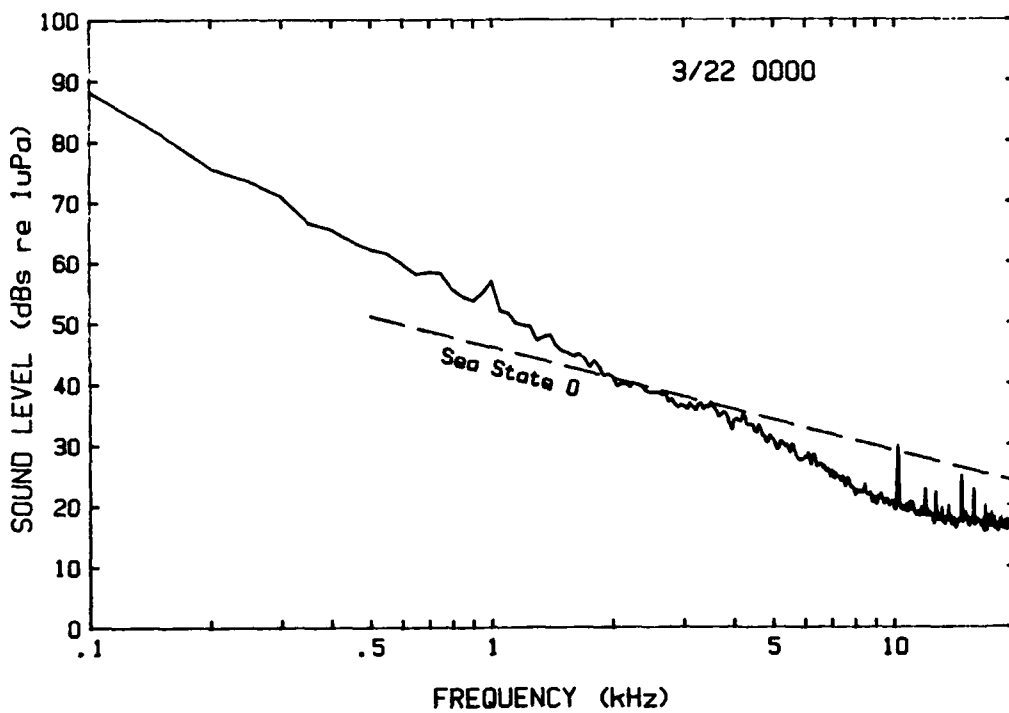
WATER CLARITY TEST



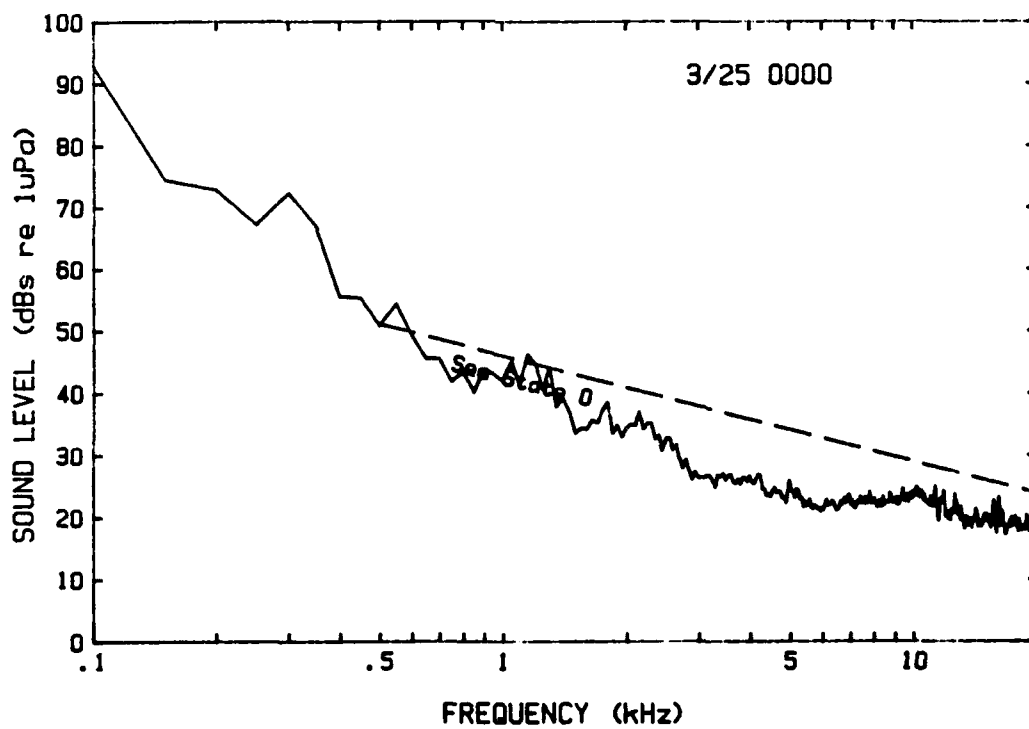
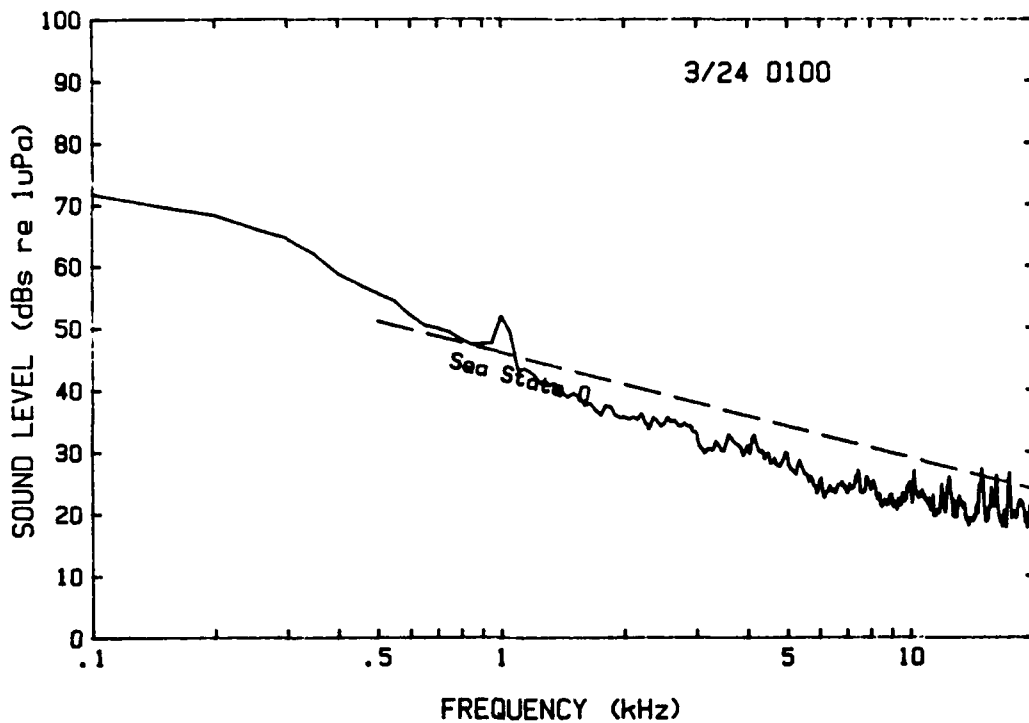
APPENDIX F

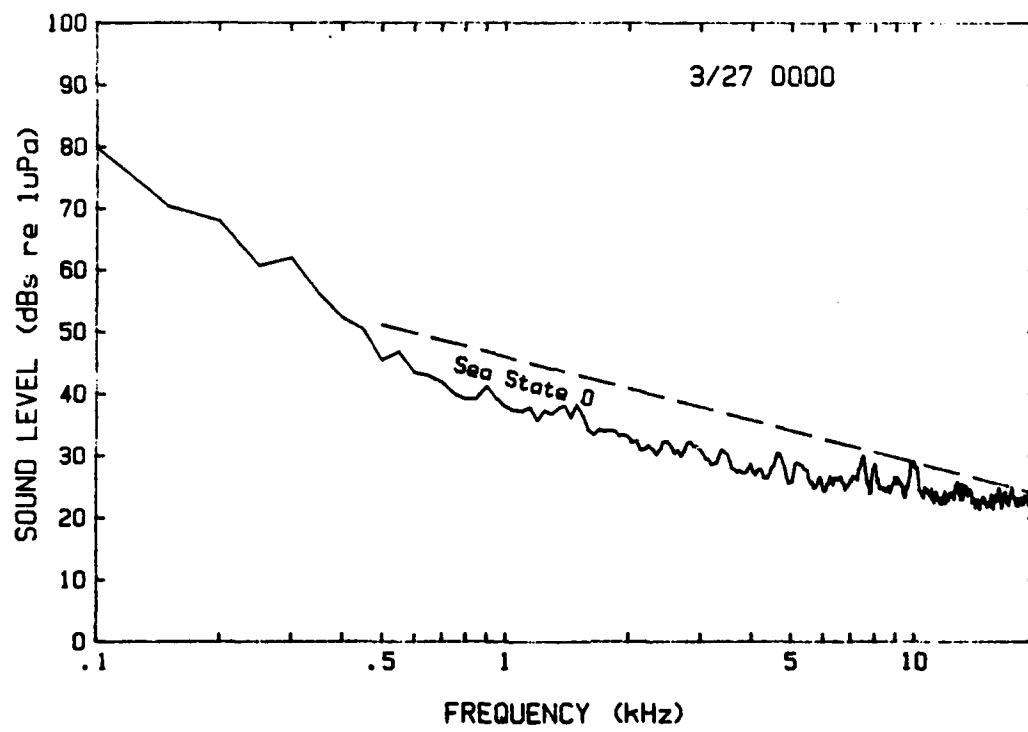
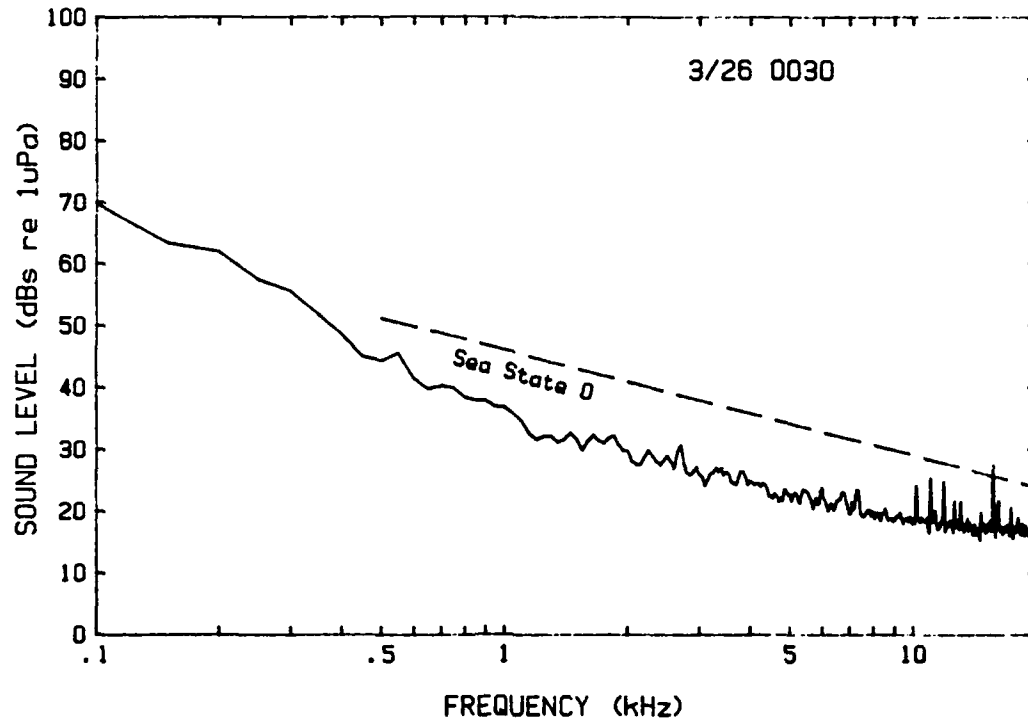
Plots of Under-Ice Ambient Noise Spectra

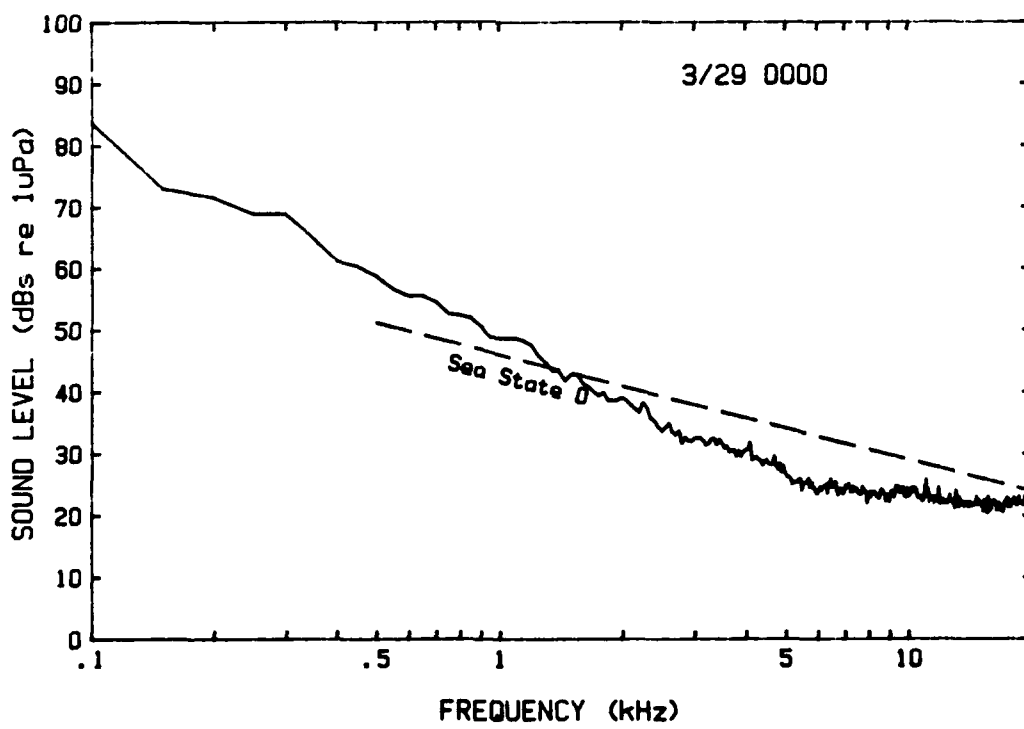
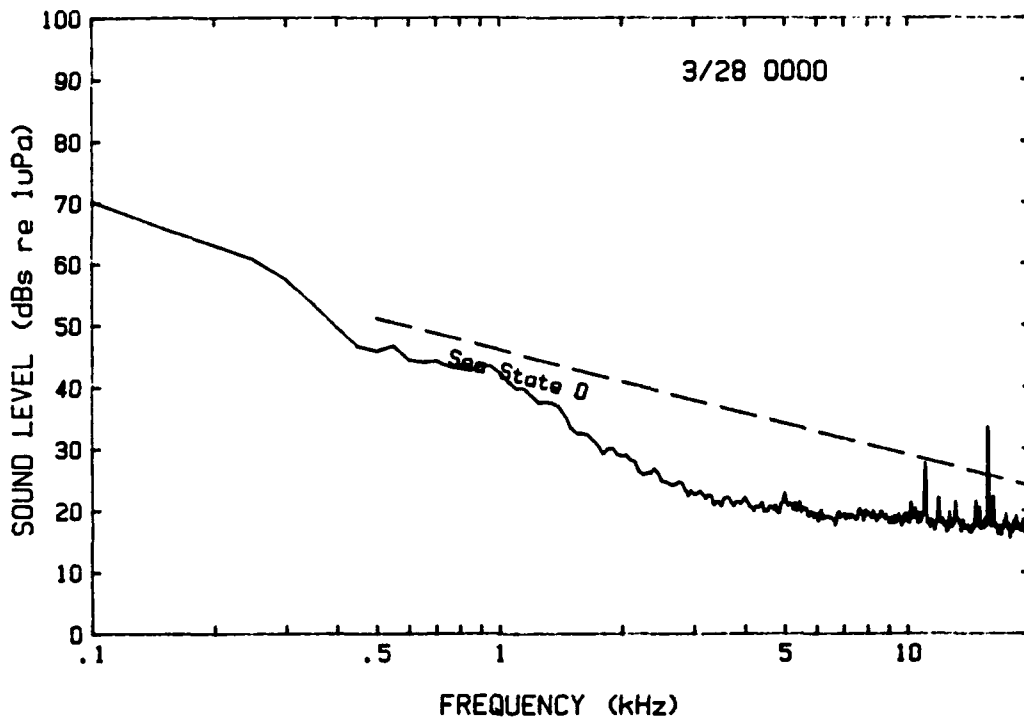
All times are local. Knudsen noise level at sea state 0 for open ocean is shown for comparison

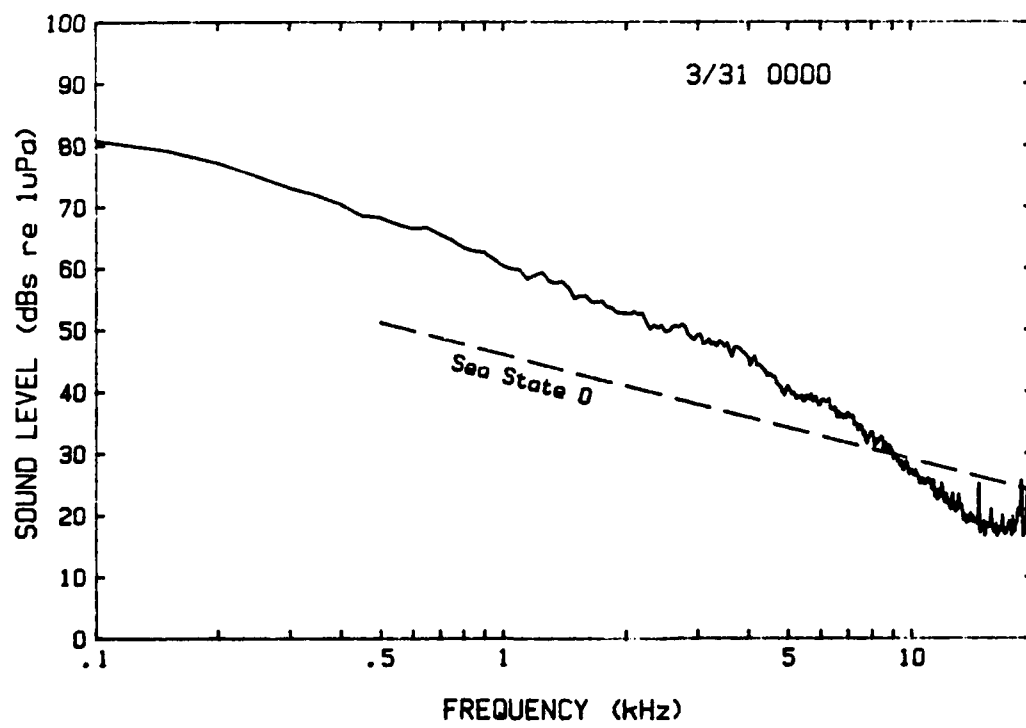
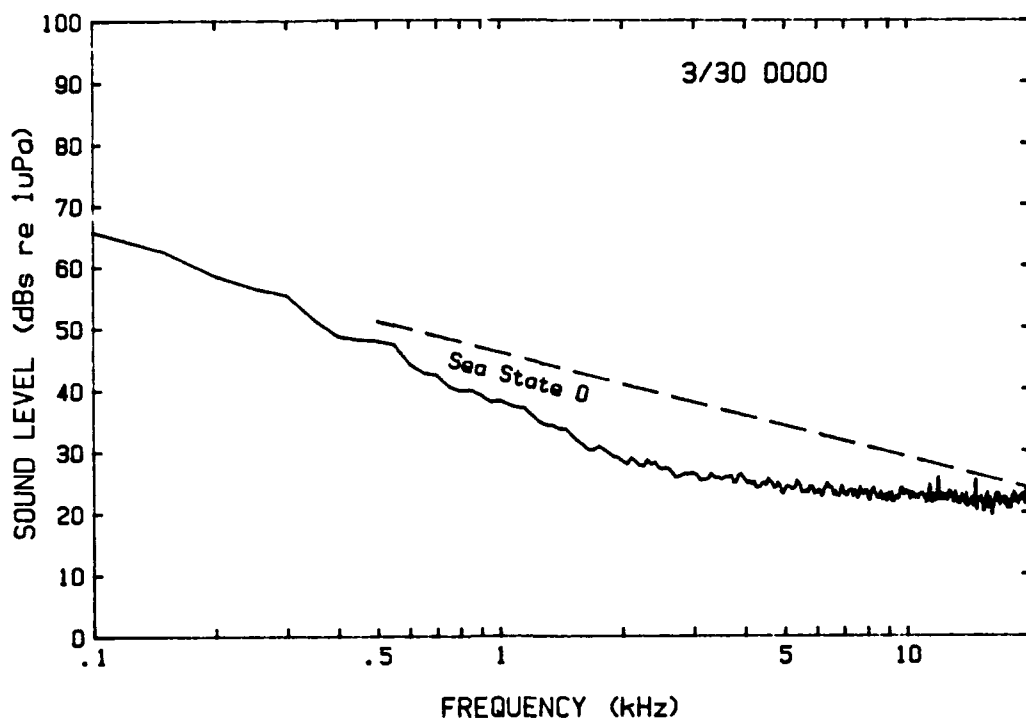


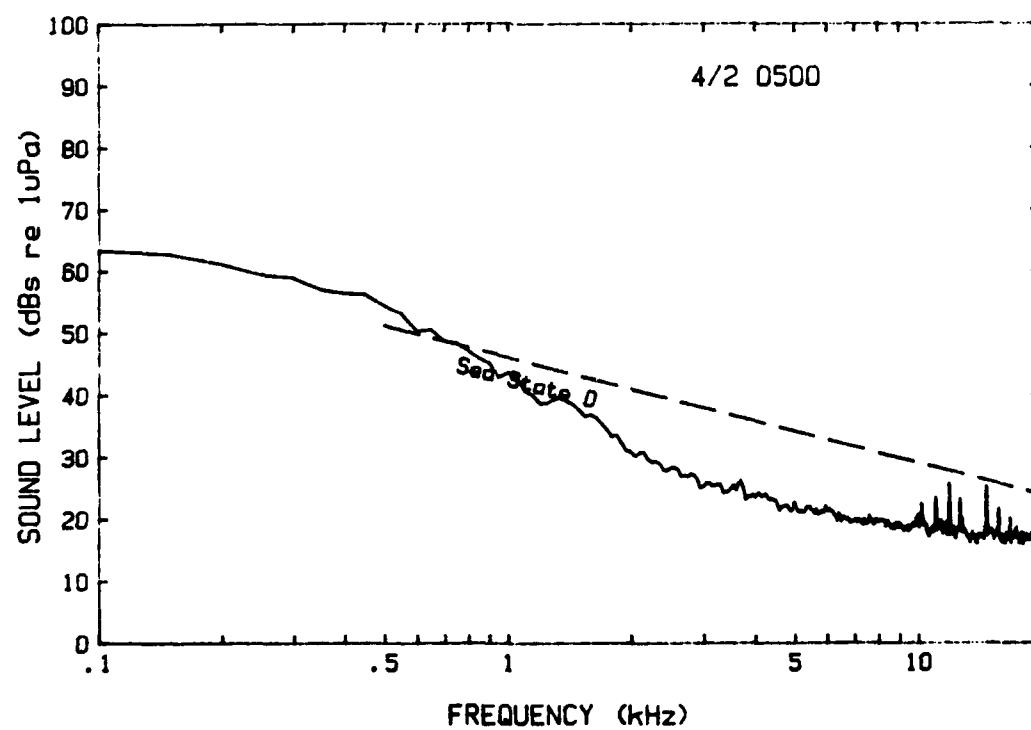
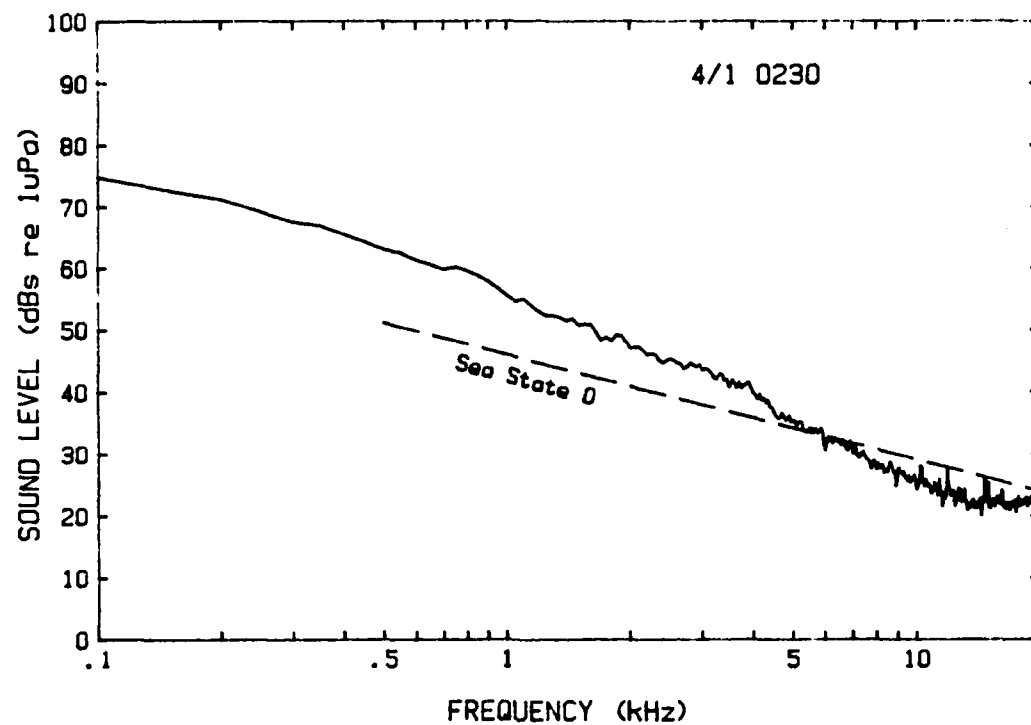
TR 8822 F-1

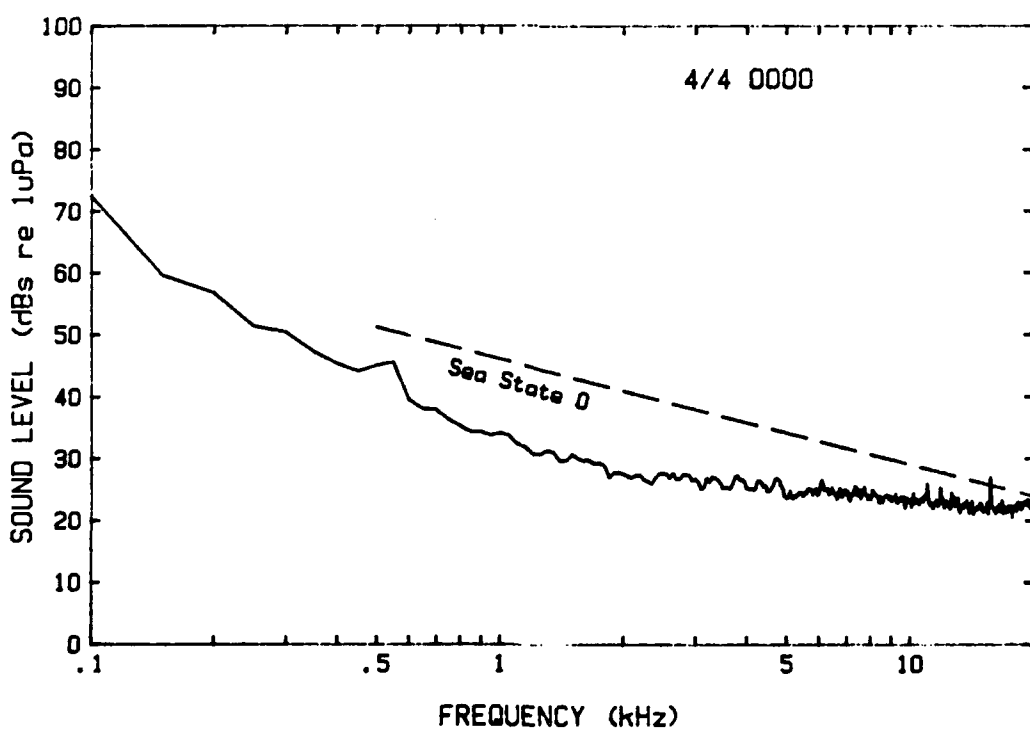
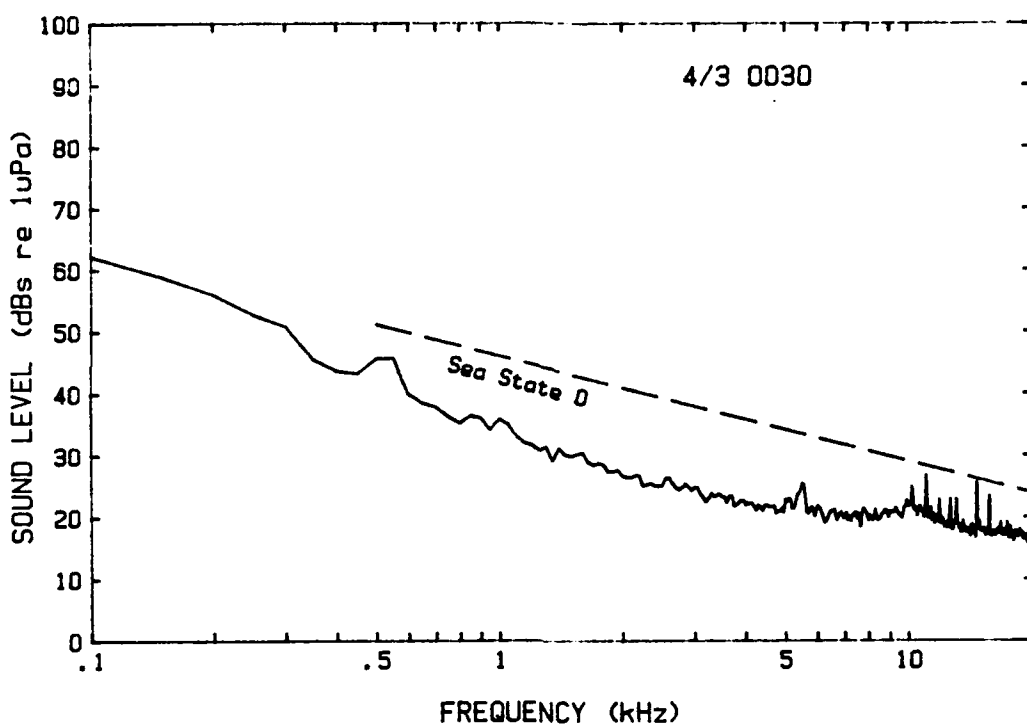


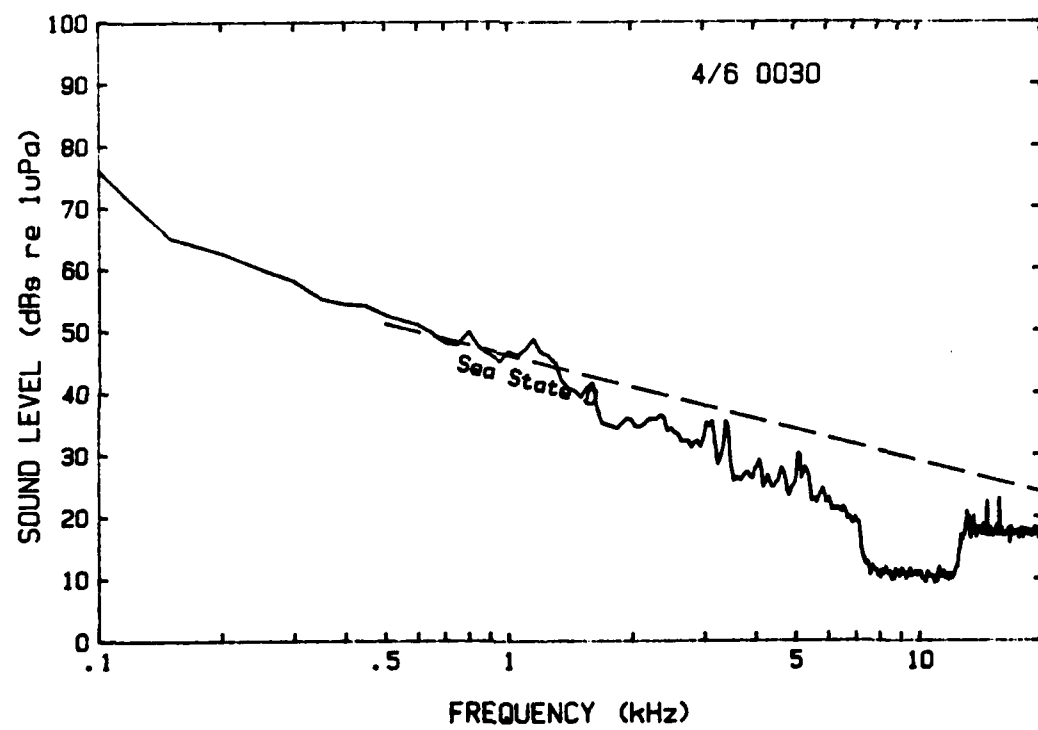
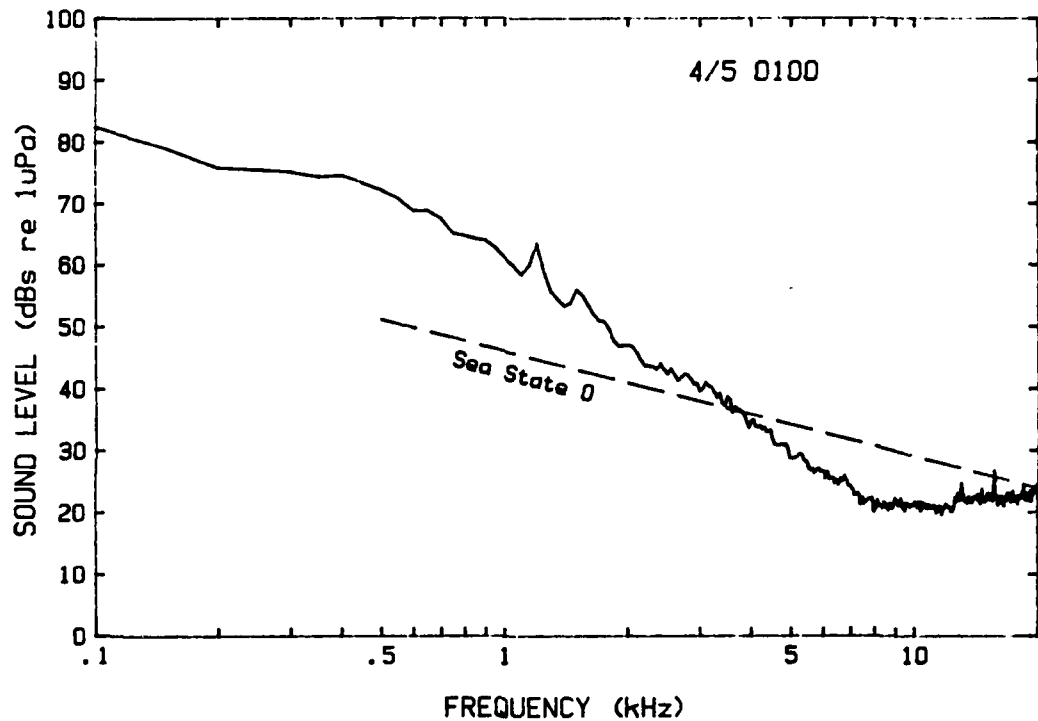


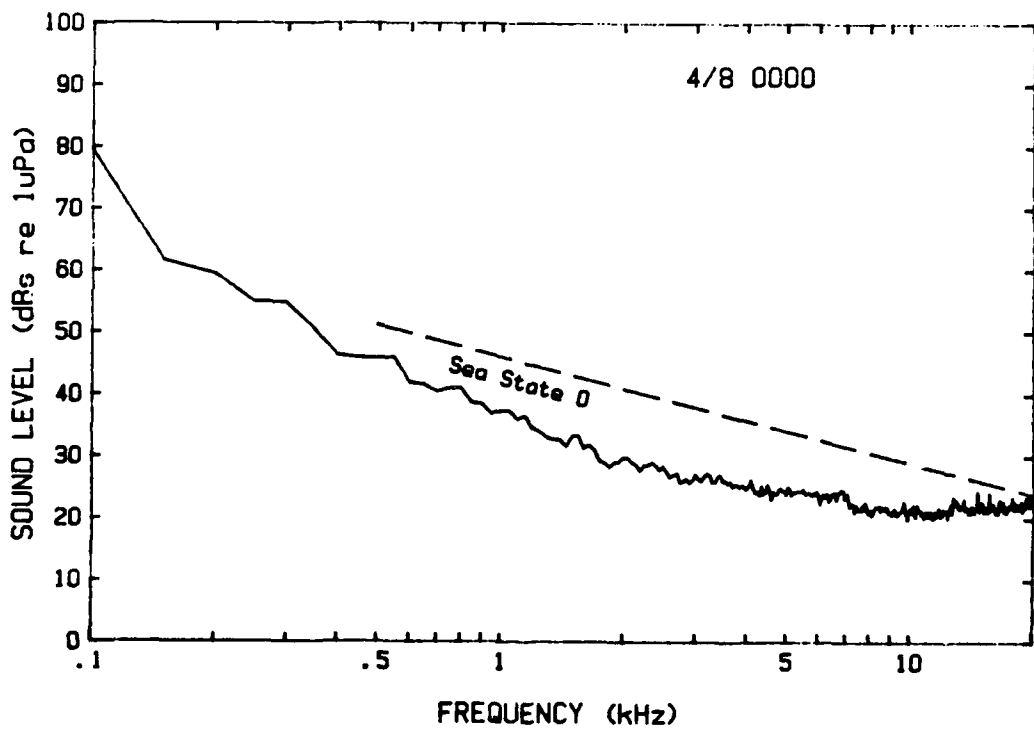
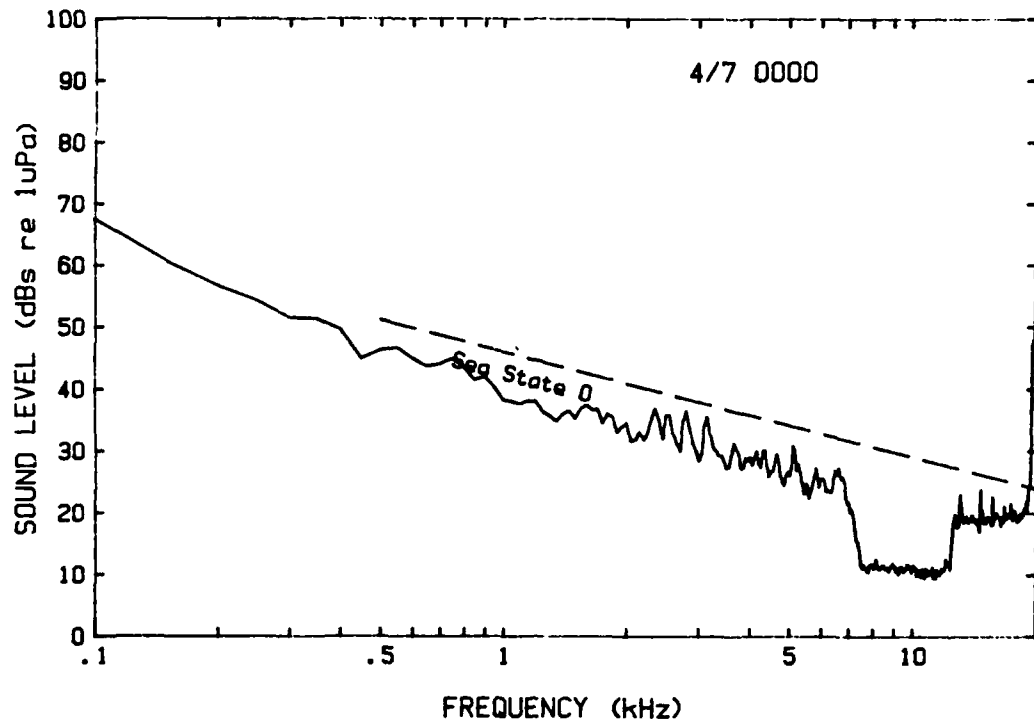


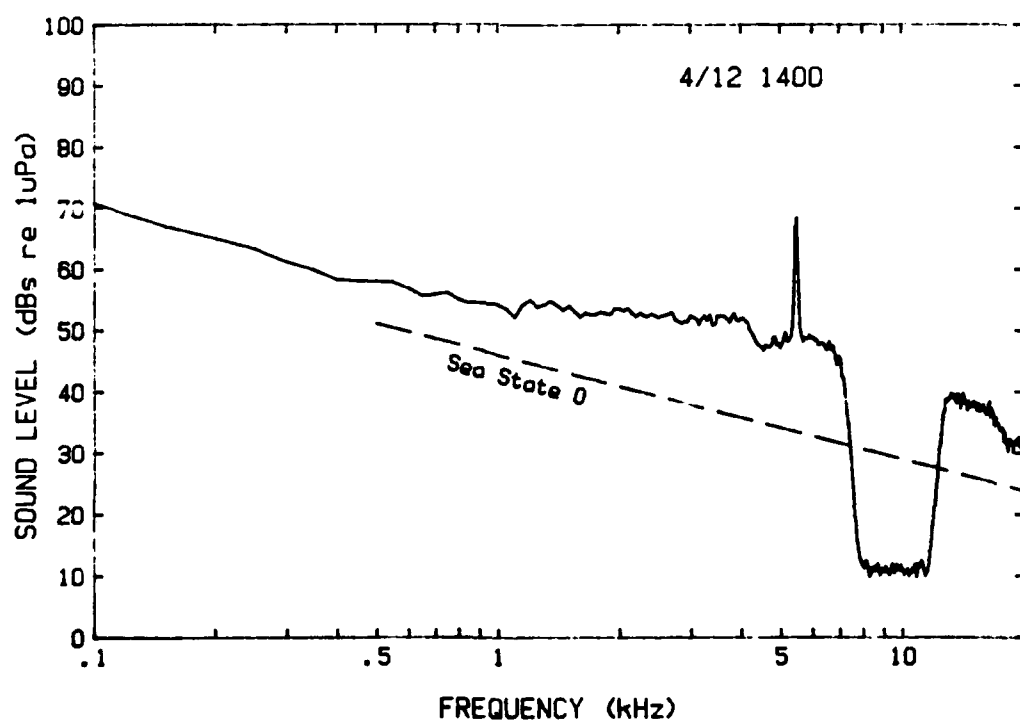
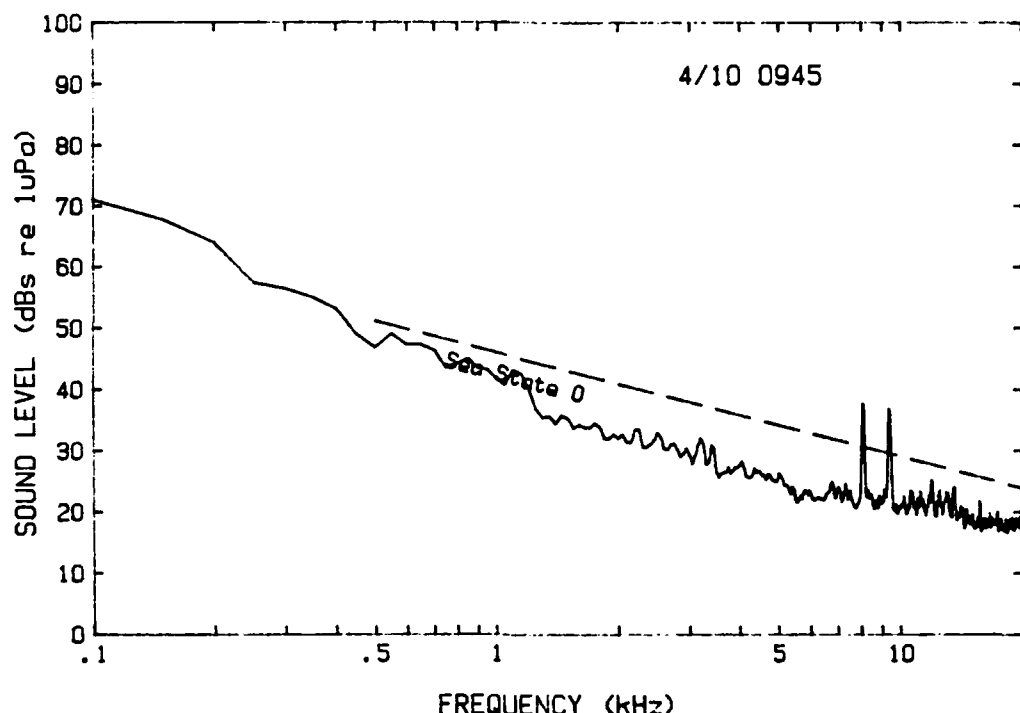


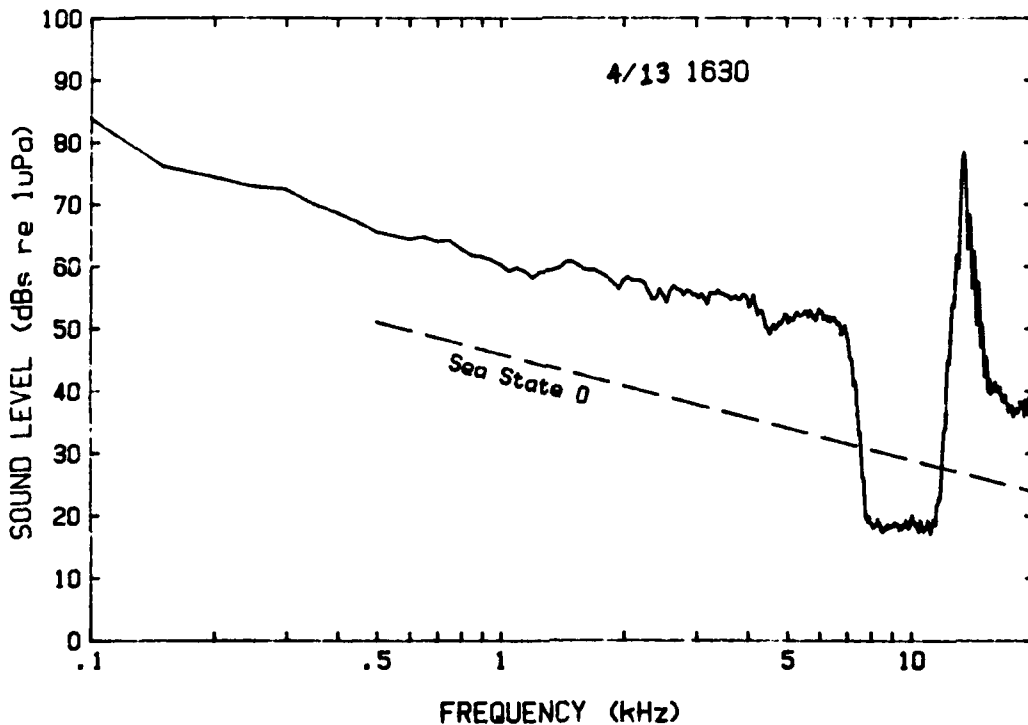
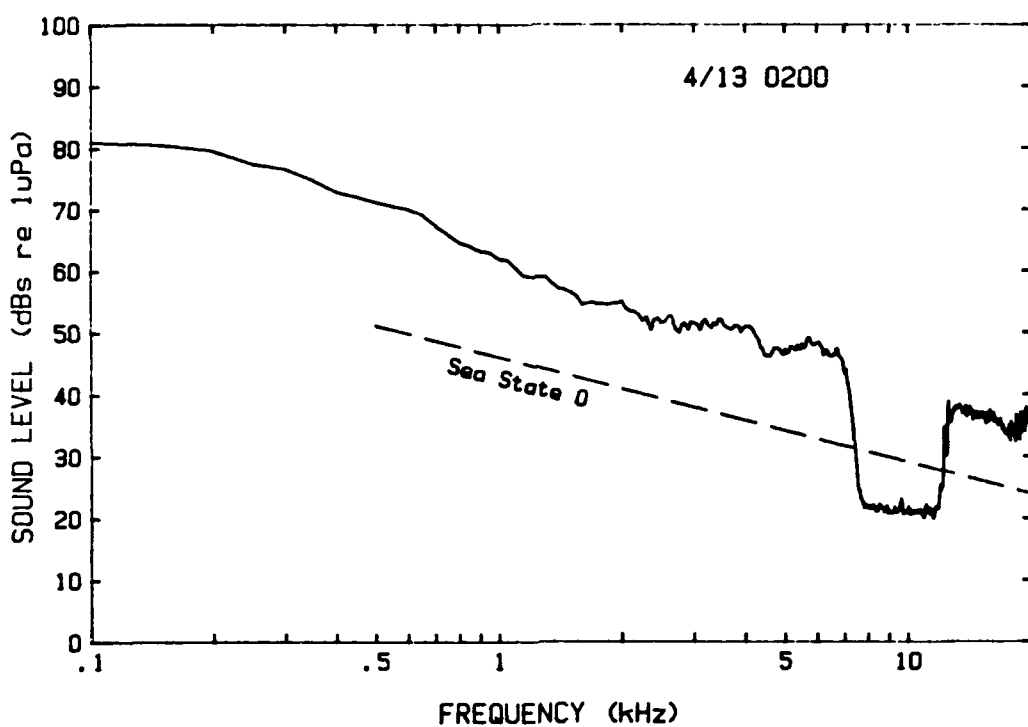




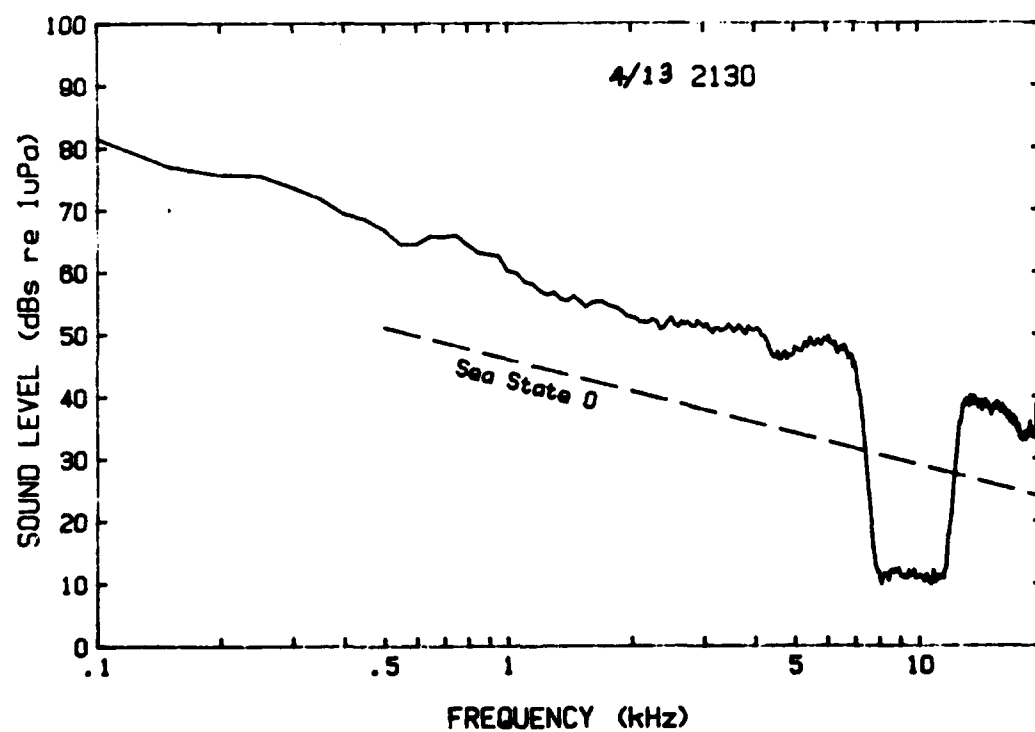
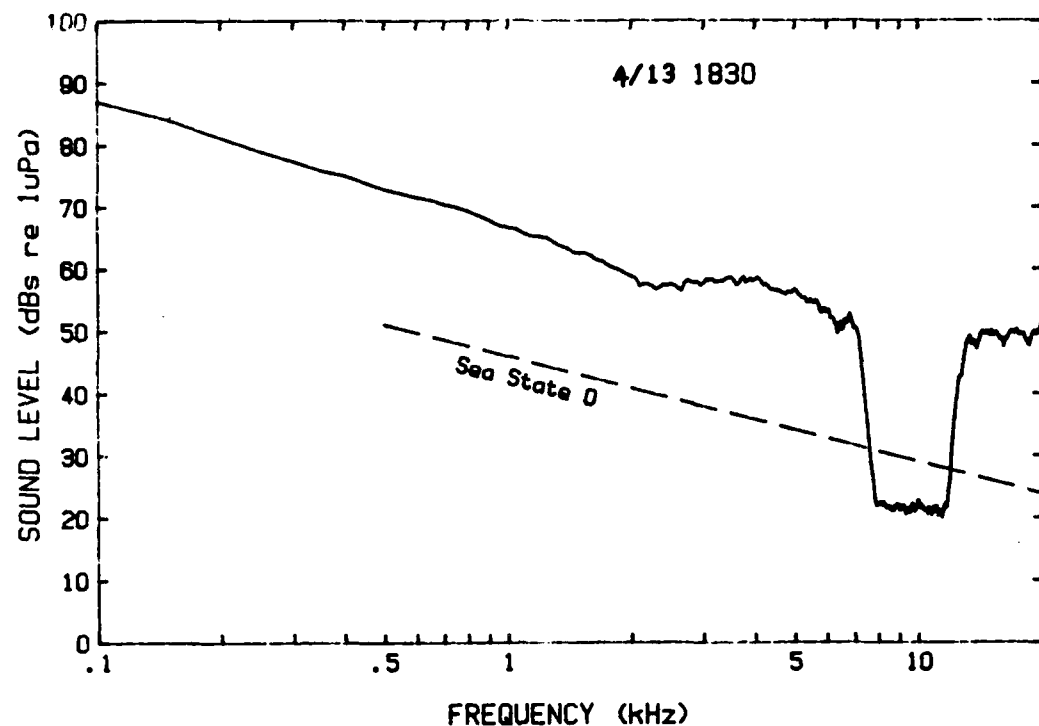




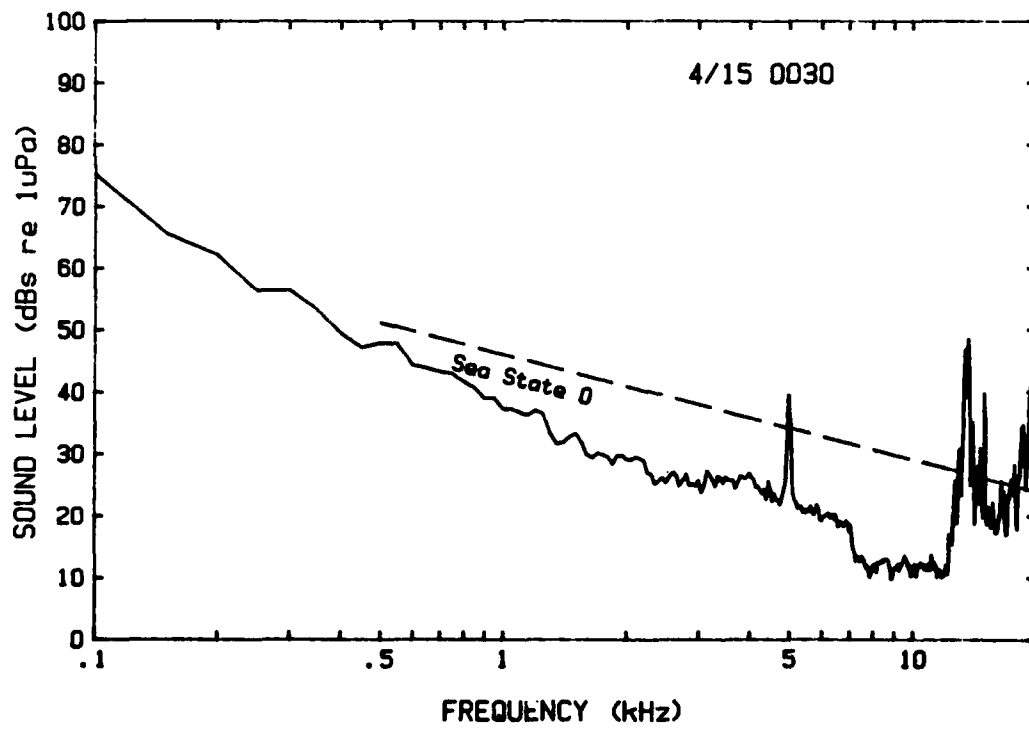
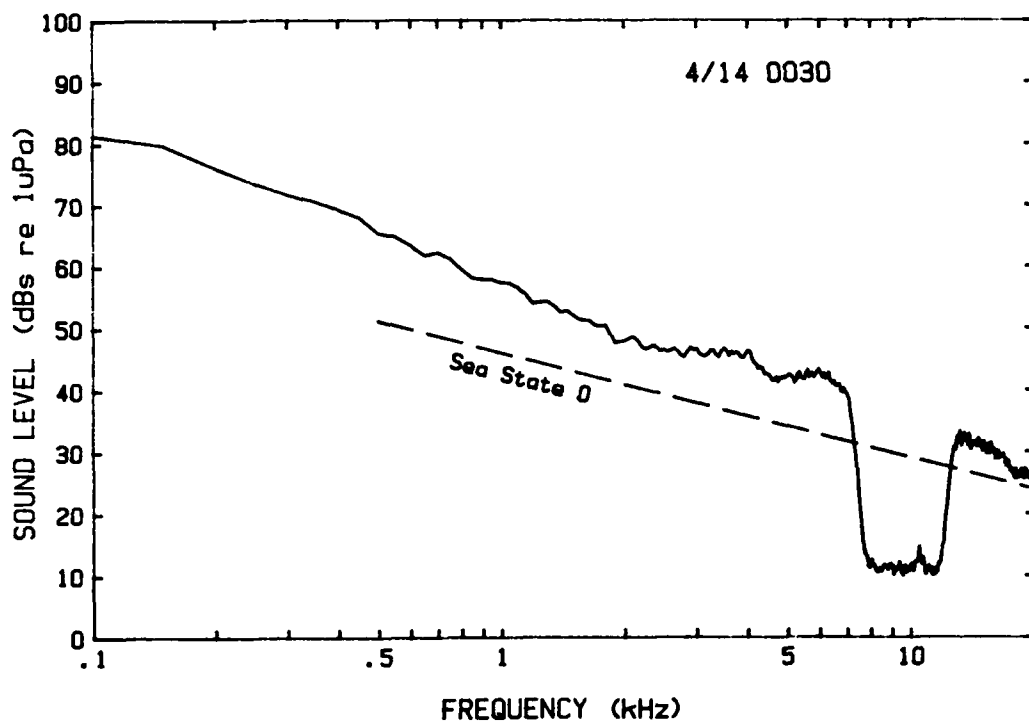


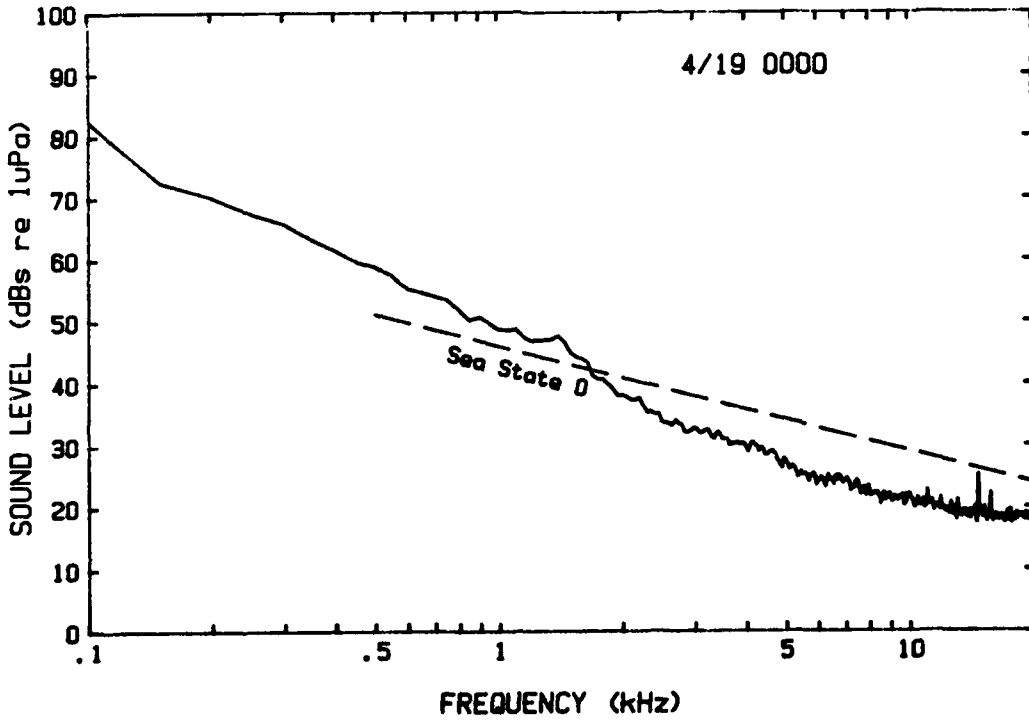
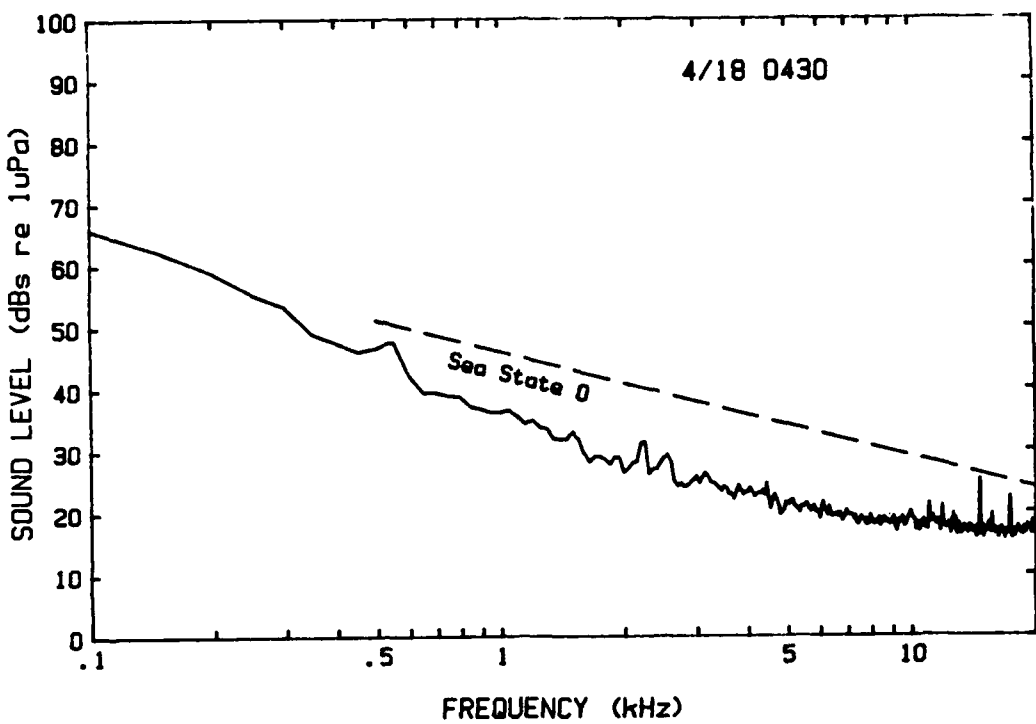


TR 8822 F-11

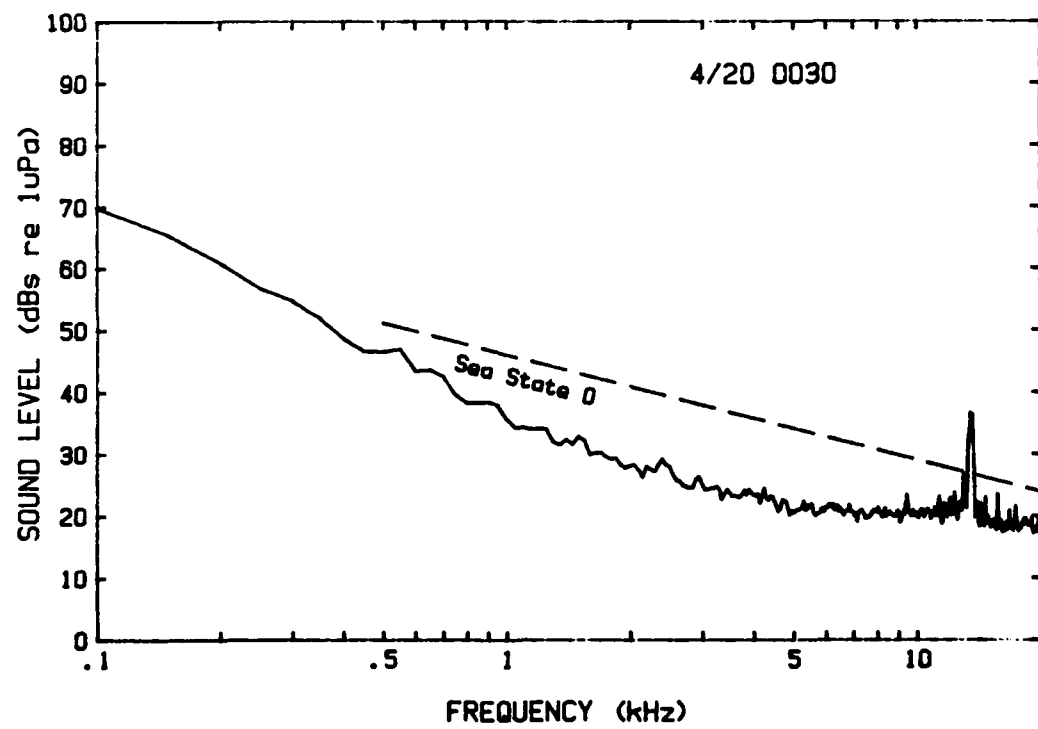
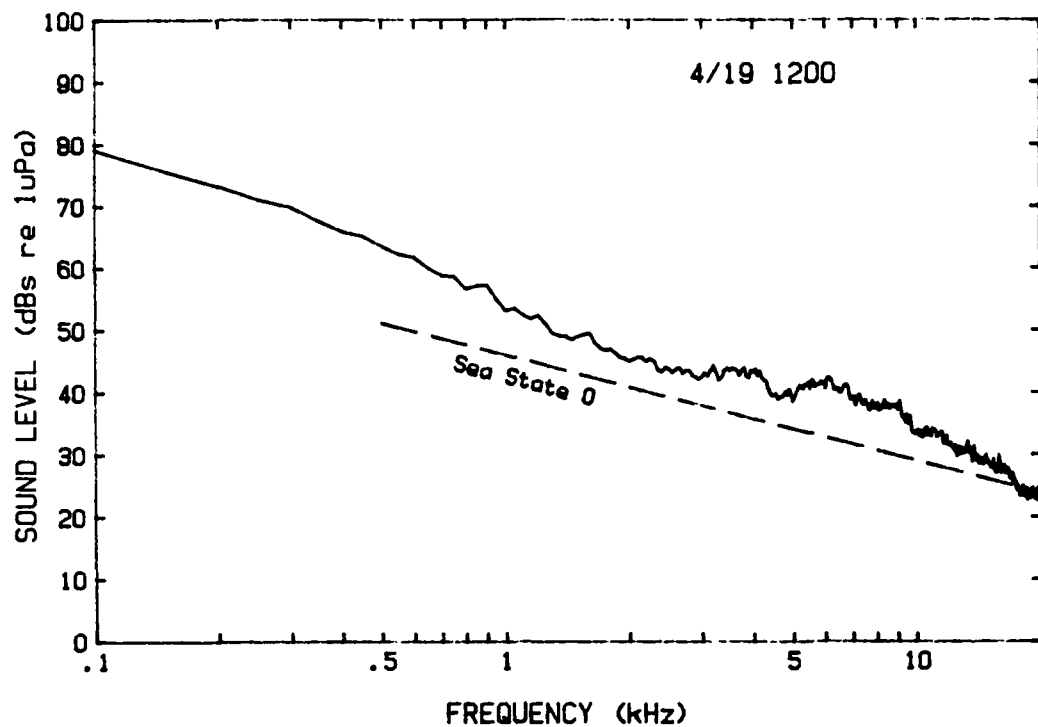


F-12 TR 8822





F-14 TR 8822



APPENDIX G

Analysis of Noise Level vs Distance from the Camp

APPENDIX G: Noise Level vs Distance from the Camp

It is obvious that the farther away from the camp the more attenuated the camp noise will be, hence the logic for deploying the hydrophone array 700 m from the camp. An interesting question is how far, for a given frequency, is far enough for the camp noise to be negligible? This has practical implications for a hard-wired system such as the one used, in that the time required to deploy the hydrophones and the cost of the cable are proportional to the distance. The shortest possible distance providing adequate camp noise attenuation is therefore desirable. To answer this question, on several occasions real-time spectral measurements were made sequentially with three omnidirectional hydrophones at different ranges along a radial line from the camp: one hydrophone of the orthogonal array at 700 m, a second (ITC 6050) at 274 m, and a third (B & K 8101) at the (0,0) hydrohole in camp, all at 30.5 m depth. Assuming spherical spreading, noise generated on the surface at the camp would have been attenuated at the three ranges by 57, 49, and 30 dB, respectively. The signal from each hydrophone was amplified and then analyzed on an HP 3561 spectrum analyzer in real time to obtain ensemble averages. Care was taken to avoid the 9.5 kHz tracking pulses during spectrum averaging since the notch filter was not used. The spectrum was then transferred to an HP85 via a GPIB bus and stored on disks.

Figures G-1a-f show the spectra obtained at the three ranges at different local times. The measured noise levels have been corrected for individual hydrophone calibration and are in spectral density units of dBs re 1 μ Pa // 1 Hz. The number of ensemble averages ranged from 35 to 100, with no noticeable improvement in the smoothness of the spectral shape using the higher number of averages. The spectra at frequencies above 10 kHz generally level out, approaching the self-noise level of the hydrophones, which were 30 dBs for the B & K 8101 (camp) and approximately 17 dBs for the ITC 6050s.

When the ambient noise level was quiet, comparable to that at sea state 0, comparison at high frequencies among the three ranges was impossible because of the higher self-noise level of the B & K hydrophone at camp. Comparisons were therefore made at frequencies below 5 kHz where self-noise was not a limiting factor and showed that the ambient noise measured at the camp was sometimes dominated by the camp noise. The spectra for the two far-range hydrophones (274 m and 700 m) generally showed close agreement, indicating no camp noise contamination, at least for frequencies above 1000 Hz; therefore using the shorter range (274 m) for noise measurement would have been satisfactory. It is puzzling that in the case of Figure G-1c, where the overall noise level was ~10 dB above that of sea state 0, the camp hydrophone registered a level slightly lower than the far ones. No reason could be found for this anomaly other than a sudden change in the wind between measurements.

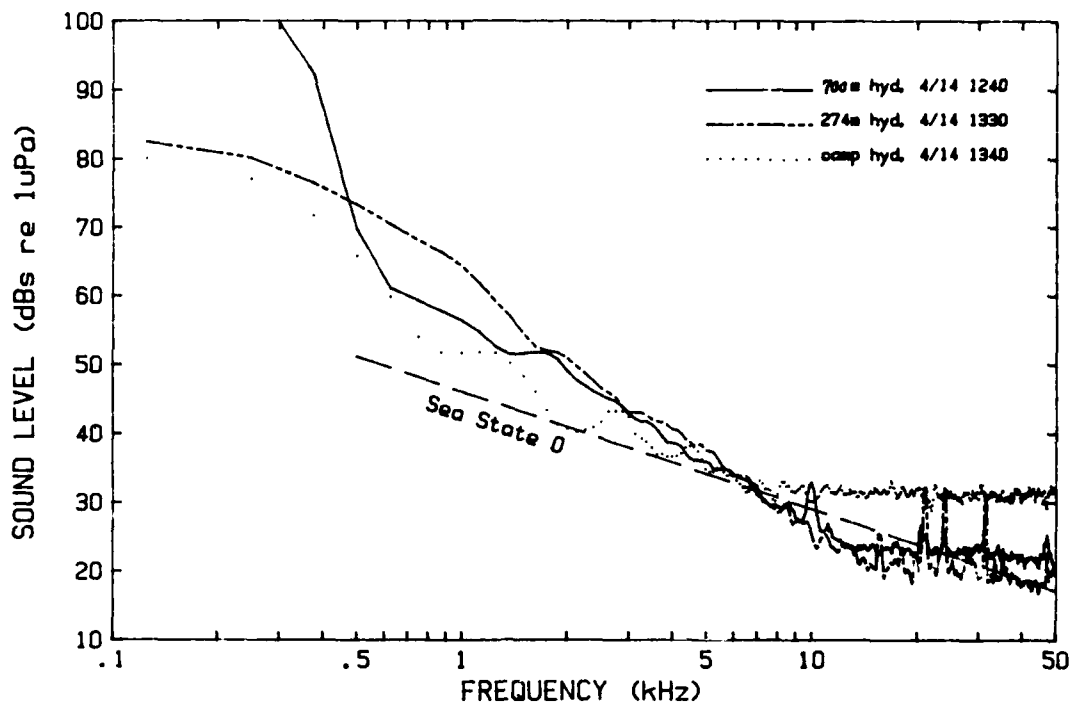


Figure G-1a. Ambient noise measured at three ranges from the camp on 14 April at approximately 1240 hours.

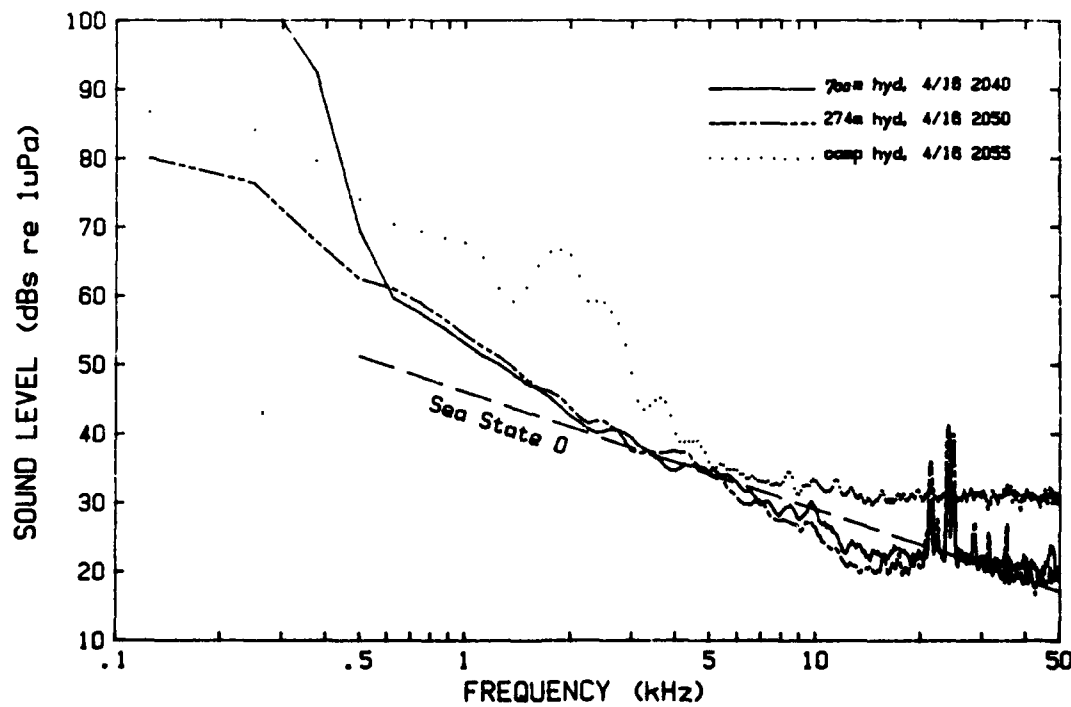


Figure G-1b. Ambient noise measured at three ranges from the camp on 16 April at approximately 2040 hours.

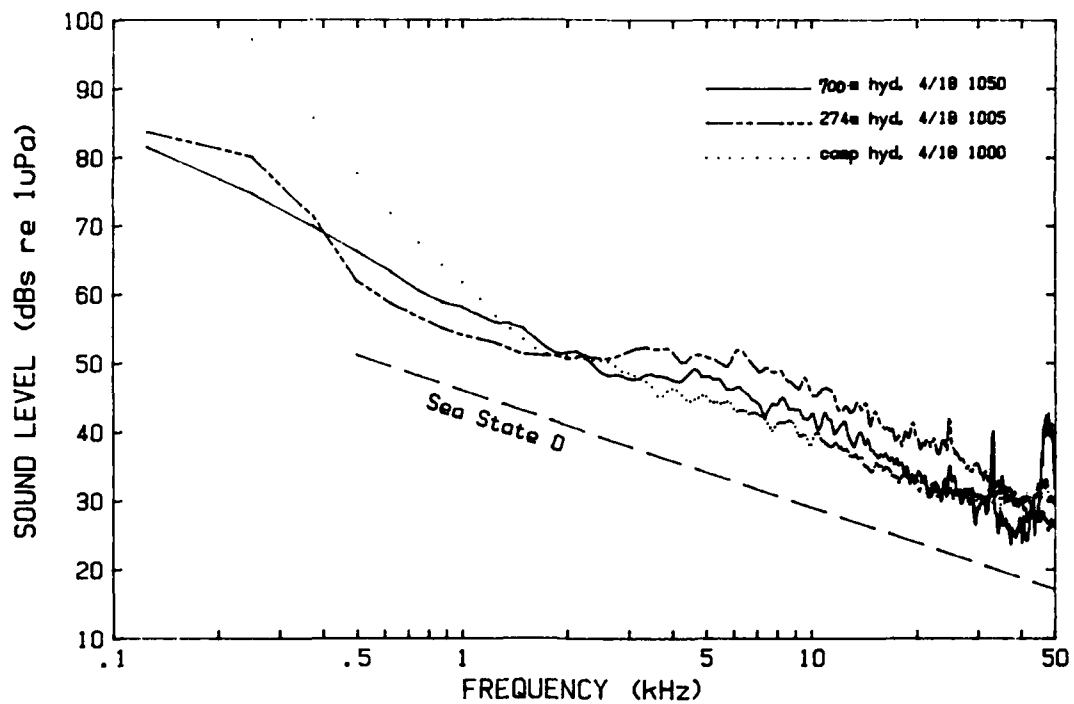


Figure G-1c. Ambient noise measured at three ranges from the camp on 18 April at approximately 1000 hours.

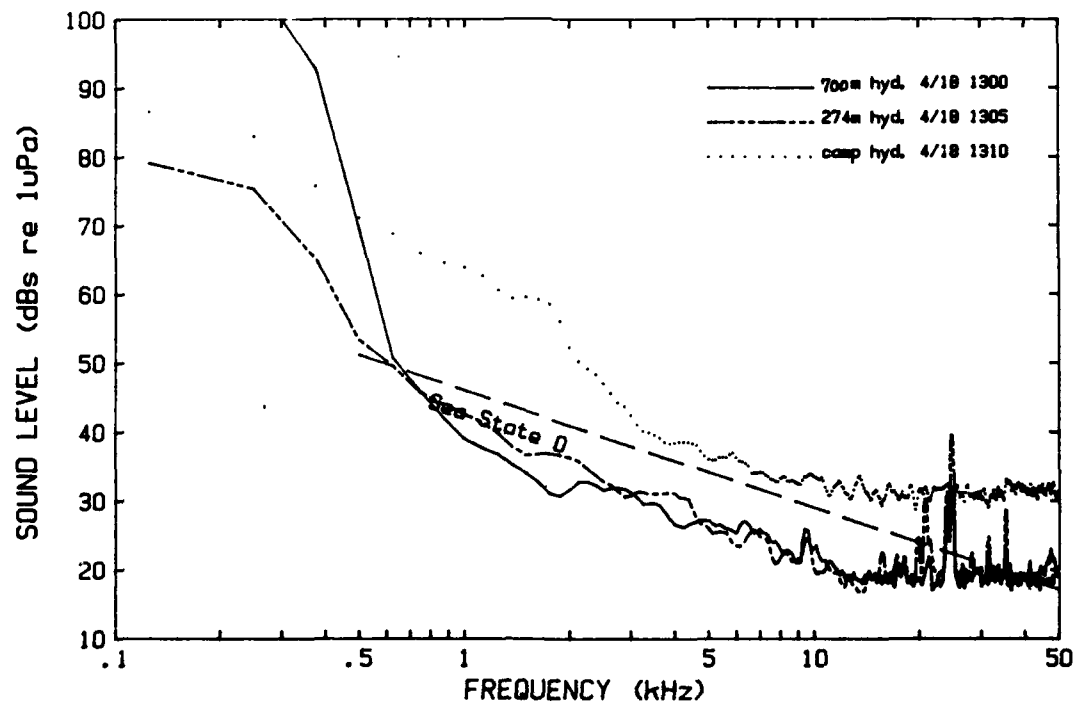


Figure G-1d. Ambient noise measured at three ranges from the camp on 18 April at approximately 1300 hours.

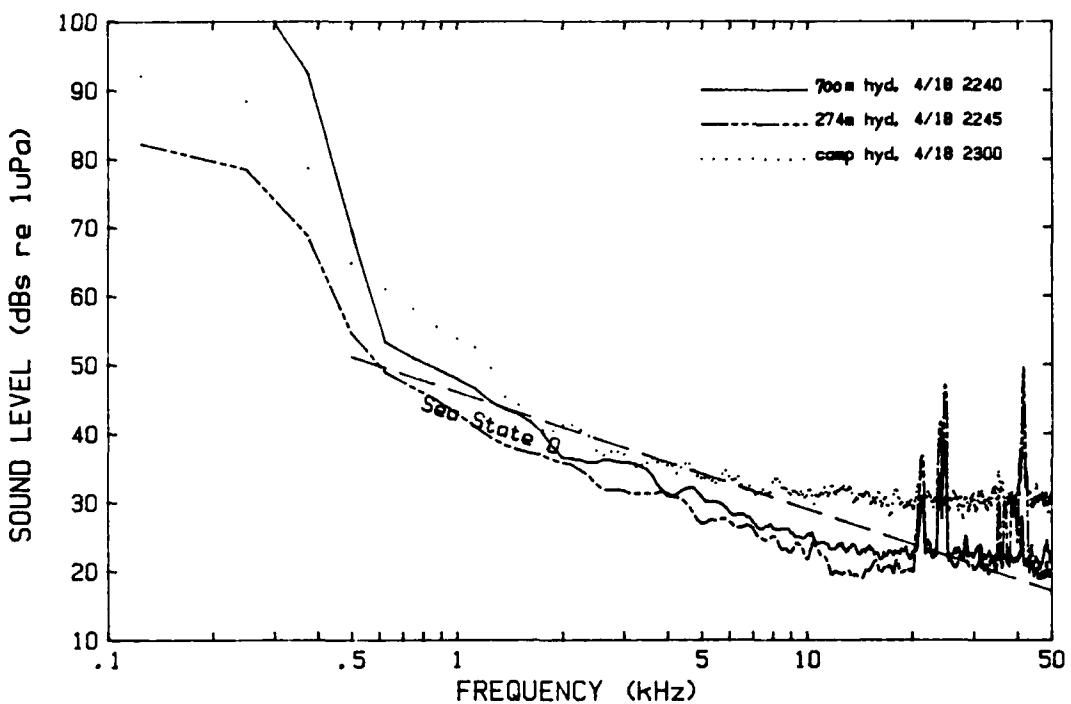


Figure G-1e. Ambient noise measured at three ranges from the camp on 18 April at approximately 2240 hours.

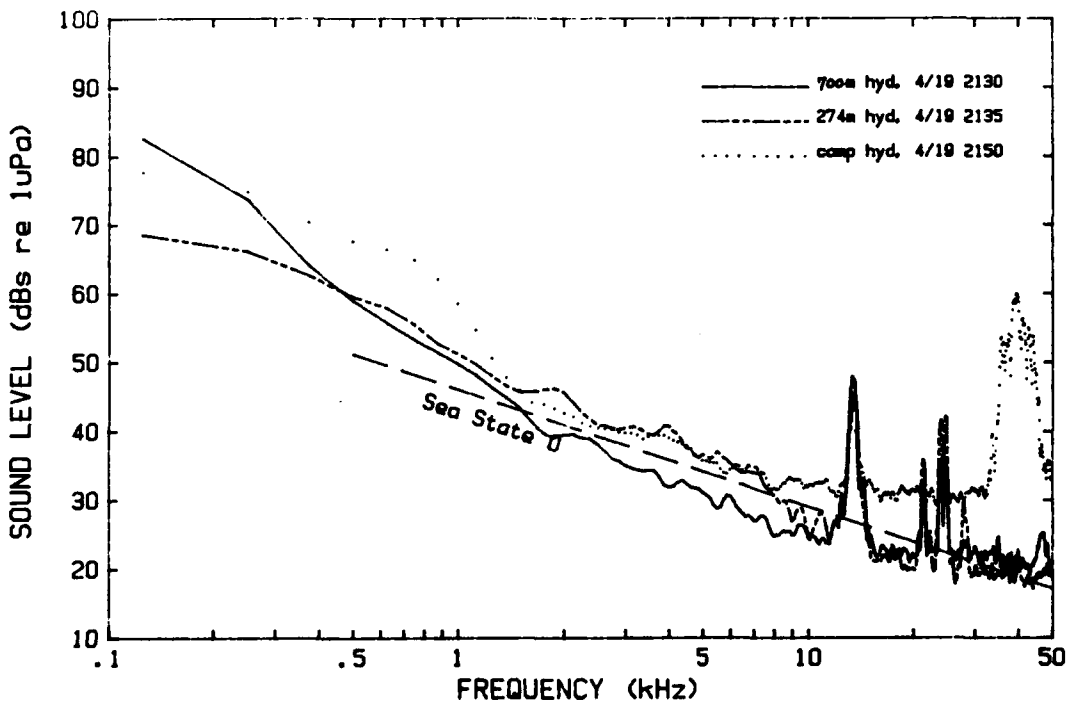


Figure G-1f. Ambient noise measured at three ranges from the camp on 19 April at approximately 2130 hours.

UNCLASSIFIED

SECURITY CLASSIFICATION OF THIS PAGE

REPORT DOCUMENTATION PAGE

Form Approved
OMB No. 0704-0188

1a REPORT SECURITY CLASSIFICATION Unclassified		1b RESTRICTIVE MARKINGS										
2a SECURITY CLASSIFICATION AUTHORITY NAVINST 5513.5A Encl. 73		3. DISTRIBUTION/AVAILABILITY OF REPORT Approved for Public Release: Distribution is Unlimited.										
2b. DECLASSIFICATION/DOWNGRADING SCHEDULE OADR												
4. PERFORMING ORGANIZATION REPORT NUMBER(S) APL-UW TR8822		5. MONITORING ORGANIZATION REPORT NUMBER(S)										
6a. NAME OF PERFORMING ORGANIZATION Applied Physics Laboratory University of Washington	6b OFFICE SYMBOL (If applicable)	7a. NAME OF MONITORING ORGANIZATION Naval Ocean Research & Development Activity Code 242										
6c. ADDRESS (City, State, and ZIP Code) 1013 NE 40th Seattle, WA 98105-6698		7b ADDRESS (City, State, and ZIP Code) Stennis Space Center, MS 39529-5004										
8a. NAME OF FUNDING /SPONSORING ORGANIZATION	8b. OFFICE SYMBOL (If applicable)	9 PROCUREMENT INSTRUMENT IDENTIFICATION NUMBER SPAWAR Contract N00039-88-C-0054										
8c. ADDRESS (City, State, and ZIP Code)		10 SOURCE OF FUNDING NUMBERS PROGRAM ELEMENT NO 62435N PROJECT NO WORK UNIT ACCESSION NO										
11 TITLE (Include Security Classification) Environmental Measurements in the Beaufort Sea, Spring 1988												
12 PERSONAL AUTHOR(S) T. Wen, W.J. Felton, J.C. Luby, W.L.J. Fox, and K.L. Kientz												
13a TYPE OF REPORT technical	13b TIME COVERED FROM 3/1/88 TO 4/25/88	14 DATE OF REPORT (Year, Month, Day) March 1989	15 PAGE COUNT 109									
16 SUPPLEMENTARY NOTATION												
17 COSATI CODES <table border="1"><tr><th>FIELD</th><th>GROUP</th><th>SUB-GROUP</th></tr><tr><td>08</td><td>03</td><td></td></tr><tr><td>20</td><td>01</td><td></td></tr></table>		FIELD	GROUP	SUB-GROUP	08	03		20	01		18 SUBJECT TERMS (Continue on reverse if necessary and identify by block number) arctic currents ice properties Beaufort Sea floe drift CTD profiles weather	
FIELD	GROUP	SUB-GROUP										
08	03											
20	01											
19 ABSTRACT (Continue on reverse if necessary and identify by block number) This report summarizes environmental data obtained in March and April 1988 at an ice camp in the Beaufort Sea 350 km north of Prudhoe Bay, Alaska. The measurements include weather, floe drift, CTD profiles, ice properties, and underwater noise.												
20 DISTRIBUTION/AVAILABILITY OF ABSTRACT <input checked="" type="checkbox"/> UNCLASSIFIED/UNLIMITED <input type="checkbox"/> SAME AS RPT <input type="checkbox"/> DTIC USERS		21 ABSTRACT SECURITY CLASSIFICATION Unclassified										
22a NAME OF RESPONSIBLE INDIVIDUAL D. Ramsdale, NORDA		22b TELEPHONE (Include Area Code) (601) 688-5230	22c OFFICE SYMBOL Code 242									

Distribution List for APL-UW TR8822

Assistant Secretary of the Navy
(Research, Engineering and Systems)
Department of the Navy
Washington, DC 20350 [2 cp]

Chief of Naval Operations
Department of the Navy
Washington, DC 20350-2000

OP 02
OP 22
OP 223
OP 225
OP 07
OP 071
OP 095
OP 96T
OP 0962E
OP 0962X
OP 098

Director of Defense Research
Office of Assistant Director (Ocean Control)
The Pentagon
Washington, DC 20301-5000

Defense Technical Information Center
Cameron Building #5
Alexandria, VA 22304-6145 [10 cp]

Office Chief of Naval Research
Department of the Navy
800 N. Quincy Street
Arlington, VA 22217-5000

OCNR 00
OCNR 000A
OCNR 112
OCNR 1125
OCNR 1125AR
OCNR 1125OA
OCNR 1222T
OCNR 125 [2 cp]

Office of Naval Research
R. Silverman, Resident Representative
315 University District Bldg., JD-16
1107 N.E. 45th Street
Seattle, WA 98195

Office of Naval Technology
Department of the Navy
Ballston Center Tower #1
800 N. Quincy Street
Arlington, VA 22217-5000

Code 22
Code 23
Code 23D
Code 232
Code 234

Director
Defense Advanced Research Project Agency
1400 Wilson Boulevard
Arlington, VA 22209

Commanding Officer
Naval Intelligence Support Center
4301 Suitland Road
Washington, DC 20390

Commanding Officer
Naval Polar Oceanographic Center
4301 Suitland Road
Washington, DC 20390-5140

Library

Center for Naval Analyses
4401 Ford Avenue
P.O. Box 16268
Alexandria, VA 22302-0268

Attn: Technical Information Center

Commander
Naval Air Systems Command Hq.
Department of the Navy
Washington, DC 20361

AIR 340L

Commander
Space and Naval Warfare Systems Command (NC1)
(SPAWAR)
Department of the Navy
Washington, DC 20363-5100

SPAWAR 005
PMW-180
PMW-181
PMW-182
PMW-182-2

Commander
Naval Sea Systems Command
Department of the Navy
Washington, DC 20362

NSEA 05R
NSEA 06
NSEA 06U2
NSEA 63
NSEA 63D [2 cp]
NSEA 63D4
Code PMS-402
Code PMS-406
Code PMS-407 [2 cp]

Commanding Officer
Naval Underwater Systems Center
Newport, RI 02840

Library [2 cp]
Code 00
Code 22202
Code 3824
Code 801
Code 81
Code 8211 [2 cp]
Code 8212

Officer-in-Charge
New London Laboratory
Naval Underwater Systems Center
New London, CT 06320

Library
Code 01Y [2 cp]
Code 2111
Code 3423

Commander
Naval Weapons Center
China Lake, CA 93555

Library

Commander
Naval Surface Warfare Center
White Oak
Silver Spring, MD 20903-5000

Library [2 cp]
Code R-01
Code R-43 [2 cp]
Code U-04
Code U-06
Code U-42 [2 cp]

Commander
Naval Ocean Systems Center
San Diego, CA 92152-5000

Library
Code 00
Code 19 [3 cp]
Code 541
Code 844 [3 cp]

Commanding Officer
Naval Civil Engineering Laboratory
Port Hueneme, CA 93043-5003

Library
Code L14
Code L43 [2 cp]

Director
Naval Research Laboratory
Washington, DC 20375

Library
Code 5100
Code 5123

Commanding Officer
Naval Coastal Systems Center
Panama City, FL 32407

Library

Commanding Officer
Naval Ocean Research and
Development Activity
Stennis Space Center, MS 39529-5004

Library [2 cp]
Code 113
Code 200
Code 240
Code 242 [3 cp]
Code 252

Commanding Officer
Naval Oceanographic Office
Stennis Space Center, MS 39522-5001

Code OA
Code OAR
Code OARU

Commander
Naval Air Development Center
Warminster, PA 18974

Library
Code 3031 (A. Horbach)

Commander
David Taylor Research Center
Bethesda, MD 20084

Library
Code 1720 [2 cp]
Code 1908

Commanding Officer
Naval Submarine School
Box 70
Naval Submarine Base New London
Groton, CT 06340

Superintendent
Naval Postgraduate School
Monterey, CA 93943-5100

Library [2 cp]
Code 68

Commander, SECOND Fleet
Fleet Post Office
New York, NY 09501

Commander, THIRD Fleet
Fleet Post Office
San Francisco, CA 96601

Commander Submarine Force
U.S. Atlantic Fleet
Norfolk, VA 23511

Code 00
Code 019
Code 22
Code N311

Commander Submarine Force
U.S. Pacific Fleet
Pearl Harbor, HI 96860

Code 00
Code N2
Code N21

Commander
Submarine Squadron THREE
Fleet Station Post Office
San Diego, CA 92132

Commander
Submarine Group FIVE
Fleet Station Post Office
San Diego, CA 92132

Commander
Submarine Development Squadron TWELVE
Box 70
Naval Submarine Base New London
Groton, CT 06340

Code 20

Knut Aagaard
Pacific Marine Environmental Laboratory
NOAA
7600 Sand Point Way NE, Building 3
Bin C15700
Seattle, WA 98115-0070

Director
Applied Research Laboratories
The University of Texas at Austin
P.O. Box 8029
Austin, TX 78713-8029

Library

Director
Applied Research Laboratory
The Pennsylvania State University
State College, PA 16801

C. Ackerman
R. Ingram [2 cp]
E. Liszka
S. McDaniel
F. Symons, Jr.
D. Upshaw
F. Reeser

Polar Research Laboratory, Inc.
6309 Carpenteria Avenue
Carpenteria, CA 90813

Sandia National Laboratories
Kirtland Air Force Base
P.O. Box 5800
Albuquerque, NM 87185

CBNS
P.O. Box 4855
Washington, D.C. 20008
Attn: CDR A.M. Poulter [2 cp]

Library